National Library of Canada

Acquisitions and Bibliographic Services Branch

395 Wellington Street
Ottawa, Ontario
K1A 0N4

Bibliothèque nationale du Canada

Direction des acquisitions et des services bibliographiques

395, rue Wellington
Ottawa (Ontario)
K1A 0N4

Your file Votre référence

Our file Notre référence

NOTICE

The quality of this microform is heavily dependent upon the quality of the original thesis submitted for microfilming. Every effort has been made to ensure the highest quality of reproduction possible.

If pages are missing, contact the university which granted the degree.

Some pages may have indistinct print especially if the original pages were typed with a poor typewriter ribbon or if the university sent us an inferior photocopy.

Reproduction in full or in part of this microform is governed by the Canadian Copyright Act, R.S.C. 1970, c. C-30, and subsequent amendments.

AVIS

La qualité de cette microforme dépend grandement de la qualité de la thèse soumise au microfilmage. Nous avons tout fait pour assurer une qualité supérieure de reproduction.

S'il manque des pages, veuillez communiquer avec l'université qui a conféré le grade.

La qualité d'impression de certaines pages peut laisser à désirer, surtout si les pages originales ont été dactylographiées à l'aide d'un ruban usé ou si l'université nous a fait parvenir une photocopie de qualité inférieure.

La reproduction, même partielle, de cette microforme est soumise à la Loi canadienne sur le droit d'auteur, SRC 1970, c. C-30, et ses amendements subséquents.

Canada

Brain Stimulation Reward in the Lateral Preoptic Area: An Examination of Its Substrate and Functional Connectivity to the Ventral Tegmental Area

Tamara L. BUSHNIK HARRIS

A thesis submitted to the School of Graduate Studies of the University of Ottawa as partial fulfillment of the requirements for the degree of Doctor of Philosophy

ISBN 0-315-83818-3

Canada

UNIVERSITÉ D'OTTAWA
UNIVERSITY OF OTTAWA

Abstract

Studies have shown that the medial forebrain bundle, extending from the lateral hypothalamus to the ventral tegmental area, is an important component of the circuit for brain stimulation reward. Many extra-medial forebrain bundle regions also support vigorous self-stimulation; the anatomical relationship between these sites and the medial forebrain bundle has been a principal focus of work in this area. The lateral preoptic area, situated rostral to the lateral hypothalamus, is of specific interest. In order to determine the nature of the hypothesized connection between the lateral preoptic and the ventral tegmental areas, two major experiments were conducted - a mapping of the reward substrate in the lateral preoptic area and a direct examination of the functional connectivity between the lateral preoptic and ventral tegmental areas using the behavioural adaptation of the collision test.

Due to the induction and potentiation of motor seizures as testing progressed in the lateral preoptic area, the viability of seizure suppression via pharmacological interventions without compromise of the refractory periods of the reward neurons was investigated (Experiment 1). It was found that the novel benzodiazepine, brotizolam, suppressed the motor seizures for up to six hours post-injection without altering the time

course of recovery from refractoriness of the reward neurons in the lateral preoptic area. As a result, brotizolam was used in the principal experiments whenever a subject showed overt signs of motor seizures.

The first major study (Experiment 2) consisted of an in depth mapping of the substrate for self-stimulation in the lateral preoptic area using dorsoventrally moveable electrodes which permitted the testing and characterization of multiple stimulation sites in each subject. A total of twenty-two rats were included in this study with electrode placements ranging from just rostral to the midline convergence of the anterior commissure back to the transition zone between the lateral preoptic area and the lateral hypothalamus. Self-stimulation was obtained throughout the lateral preoptic area and compartments 'a' and 'b' of the medial forebrain bundle; the pattern of positive sites was consistent with anatomical descriptions of the trajectory of the medial forebrain bundle. An examination of the period/current tradeoff functions generated at positive self-stimulation sites suggested that the substrate in the lateral preoptic area has a homogeneous distribution that is less dense than that found in the lateral hypothalamus.

The third experiment investigated the existence of a direct anatomical connection between the lateral preoptic area and the ventral tegmental area reward neurons using the behavioural

adaptation of the collision test. The collision test is a double pulse, two electrode technique based on the axonal conduction failure that occurs when two separate sites in the same axon bundle are electrically stimulated. Collision is interpreted when an increase in the double pulse stimulation effectiveness at interpulse intervals exceeding the sum of the interelectrode conduction time and the neural refractory period is observed and is considered as strong evidence for direct axonal linkage between the sites in question. In this study, nine rats with a total of forty-four pairs of sites were examined; in only one case was there a profile suggestive of an axonal collision effect. However, in seven sites, the double-pulse effectiveness curves were consistent with the characteristics of transynaptic collision. The unique shapes of collision curves predicted by the transynaptic collision model permit the direction of conduction to be inferred from the matching collision profiles; six of the seven curves were suggestive of a caudorostral direction of conduction, that is, ventral tegmental area to lateral preoptic area. These results do not support the hypothesis that the lateral preoptic area is the location of the cell bodies of origin for the descending reward pathway that courses between the lateral hypothalamus and ventral tegmental area. However, the absence of axonal collision effects or transynaptic collision profiles consistent with a rostrocaudal direction of conduction can not be

interpreted to suggest that other patterns of connectivity between the reward neurons in the lateral preoptic and ventral tegmental areas do not exist.

Acknowledgements

The debt of gratitude that I owe to my supervisor, Dr. Catherine Bielajew, cannot begin to be acknowledged by these few words. Her guidance, thoughtfulness, and humour made the potentially long years of this program thoroughly enjoyable, while her example helped me realize that a career in academia could indeed be a viable and rewarding choice. I will also always remember the last few months of concentrated writing when her door was always open to discuss the most recent 'minor' crisis (plus a few major ones) and the umpteenth revision of the introductory paragraph - if I ever have the opportunity to supervise students, I hope I will do so with at least half of her 'grace under pressure'.

For the members of the lab - Janet, Monika, and Lisa - we started off just sharing lab space but have now progressed to sharing our hopes, dreams, and fears; it's hard to believe that this stage is over. You had all better be at the next Neurosciences conference! To the honorary members of the lab - Tom and Claude - the laughter and impromptu coffee breaks sitting in the hall won't be forgotten.

There are other people in the department who can't be omitted: Dr. George Fouriezos who gave me a rudimentary grounding in electronics, Dr. Zulfiquar Merali who always asked questions in just such a way as to tap knowledge I didn't know

I had, and Dr. Robert Leclerc who allowed me the use of his lab containing the huge table at which I wrote both my comprehensive document and dissertation.

Last, but definitely not least, I want to thank my family: my father who unquestioningly supported me in all my endeavors, my sister who almost made it out of university before me, Pauline who showed me that shopping is a terrific stress-reducing activity, and my husband who constantly had to listen to my diatribes about computer glitches and then strive to fix them. I have finally finished!

Table of Contents

List of Figures

List of Tables

General Introduction

An important paradigm today for studying the physiological basis of motivation has its origin in the 1954 observation by Olds and Milner, who discovered the reinforcing effects of electrical brain stimulation in the rat while studying the role of the reticular formation in learning (Olds and Milner, 1954). Although the first indications of this phenomenon came from non-contingent administration of the stimulation, they soon found that rats would acquire a task in order to self-administer stimulation. From this inauspicious beginning, the field of brain stimulation reward (BSR) was born and the study of its behaviour, intracranial self-stimulation, begun.

One of the compelling features of BSR is its pervasiveness across species and brain sites. It has been reported in a variety of animals, from fish (Boyd and Gardner, 1962) to squirrel monkeys (Rolls, 1974) and even in humans (Bishop, Elder and Heath, 1963). The medial forebrain bundle (MFB), which courses through the lateral hypothalamus (LH) to the ventral tegmental area (VTA), is the best documented region with respect to BSR (see Stellar and Stellar, 1985 for review); however, the behaviour has also been observed from stimulation of the cerebellum (Corbett, Fox and Milner, 1982), the dorsal raphe nucleus (Miliaressis and Malette, 1987; Rompre and Miliaressis, 1985), the rostral pons (Rompre and Boye, 1989), the periaqueductal gray (Bielajew, Jordan, Ferme-Enright, and

Shizgal, 1981), the thalamic nuclei (Bielajew and Fouriezos, 1985; Clavier and Gerfen, 1982), the stria medullaris (Blander and Wise, 1989), the preoptic and anterior hypothalamic areas (Bielajew, Thrasher, and Fouriezos, 1987; Fouriezos, Walker, Rick, and Bielajew, 1987), and the prefrontal and sulcal cortices (Corbett, Laferriere, and Milner, 1982; Robertson, Laferriere and Milner, 1982; McGregor and Atrens, 1991; Schenk and Shizgal, 1982; Trzcinska and Bielajew, 1992).

One of the goals in studying BSR is to understand its relationship to natural reinforcers and ultimately, the mechanisms underlying motivation. In this vein, an interest of BSR researchers has been to identify and characterize the neurons responsible for self-stimulation and stimulation-induced behaviours that are linked to other motivational states. Many behaviours can be elicited from the same sites that support self-stimulation; these include circling (Miliaressis and Rompre, 1980), analgesia (Cooper and Taylor, 1967), and general motor activity (Rompre and Miliaressis, 1980), as well as such motivated behaviours as eating (Hoebel and Teitelbaum, 1962), drinking (Mendelson, 1967), copulation (Cagguila and Hoebel, 1966), and aversion (Bower and Miller, 1958).

One hypothesis is that a common set of fibers in the MFB underlie the variety of behaviours elicited by electrical stimulation (Valenstein, Cox, and Kakolewski, 1968). The

opposing view suggests that each behaviour is subserved by a unique set of MFB fibers (Wise, 1974). A resolution to this issue would help to answer some of the questions regarding the central organization of motivation. If self-stimulation neurons in the MFB are distinguishable from those of other motivated behaviours, then BSR research could be envisioned as a model for investigating specific "drives". On the other hand, if the same neurons are responsible for different motivated behaviours, BSR research would encompass the study of a general arousal system which becomes directed when appropriate stimuli are encountered, for example.

The use of psychophysical scaling techniques has had a significant influence on the study of BSR and has contributed to the resolution of these issues. The application of stimulus/response functions and their subsequent trade-off derivations has been fruitful in addressing methodological concerns and the resulting inconsistencies in earlier BSR work (Valenstein, 1964). The development of behaviourally derived tests for assessing the refractory period and connectivity of reward loci has succeeded in demonstrating that the elicitation of circling, general motor activity, and aversion are not due to the activation of reward neurons (Bielajew and Shizgal, 1980; Durivage and Miliaressis, 1987; Miliaressis and Rompre, 1980). In addition, these and other techniques have led to a preliminary characterization of the directly driven neurons

that underlie BSR. The portrait that has emerged has facilitated the identification of their rostral and caudal MFB extensions and challenged traditional views regarding the neurochemistry of BSR (Bielajew and Shizgal, 1986; Corbett, Skelton, and Wise, 1977).

The following sections describe the development and rationale behind the techniques used in this thesis and their contributions to the study of BSR.

Parametric Techniques

As early as 1964, Valenstein suggested that response rate contained both reward and performance components. He argued that this measure was influenced by a variety of factors unrelated to the rewarding effects of stimulation, such as the motoric consequences of electrical stimulation, the health of the animal, or the particular challenges under study. An alternative scaling method was proposed, and later refined by Yeomans' (1975), which attempts to control for the contribution of performance variables; it is based on a constant behavioural output and assumes that response rate is monotonically related to the total level of excitation rather than the assumption of linearity underlying earlier simple rate paradigms. Instead of obtaining one rate measure, the responses associated with several levels of stimulation are recorded, and a change in, for example, the frequency of stimulation associated with a constant level of performance is obtained. A widely used

stimulus/response function in BSR studies is the rate/frequency curve.

Rate/frequency curves. The rate/frequency curve is generated by systematically varying the frequency of electrical stimulation so that a full range of response rates, from minimum to maximum values, is obtained (see Figure 1A). A family of these curves is produced by varying the conditions, such as current or drug dose, under which the individual frequencies are tested.

These curves can be used in two ways. First, the relative position and asymptotic response rate illustrate the effect of an experimental manipulation on reward and performance (see Figure 1B). When the animal's ability to press the lever is altered, for example when task difficulty is significantly increased or the health of the animal is compromised, the asymptote of the rate/frequency curve is changed. Second, manipulations that influence the rewarding value of the stimulation, such as changes in current or administration of reward enhancing drugs, cause the rate/frequency curve to shift laterally (Edmonds and Gallistel, 1974, 1977; Miliaressis and Rompre, 1987; Miliaressis, Rompre, Laviolette, Philippe, and Coulombe, 1986).

Trade-off functions. A trade-off function can be derived from the family of rate/frequency curves. It represents a constant-output function which relates the change in the level

Figure 1. A) This figure shows the main features of a family of rate/frequency curves. The three curves are plotted with response rate per minute on the ordinate and frequency on the abscissa. What distinguishes the three curves is that each one has been obtained at a different current resulting in a progressive shift to the right as current is decreased (this is just one example of a variable parameter). On curve 1 are illustrated the main parts of the rate/frequency curve. Section A corresponds to a minimal response rate at a low frequency; section B is the dynamic interval over which small increases in frequency result in large increases in response rate; C indicates the asymptotic response rate which, despite increases in frequency, will show no further significant changes.

B) This figure illustrates how the rate/frequency curve changes as a function of reward or performance factors. Curve A represents the baseline condition (no experimental manipulation). In B, the curve has shifted, relative to A, to the left with no change in asymptotic response rate suggesting that the manipulation has increased the rewarding value of the stimulation without altering performance. Curve C has shifted to the right, relative to A, and has a decreased asymptote suggesting that the experimental manipulation has decreased the rewarding value of the stimulation and also affected the ability of the animal to perform the operant task.

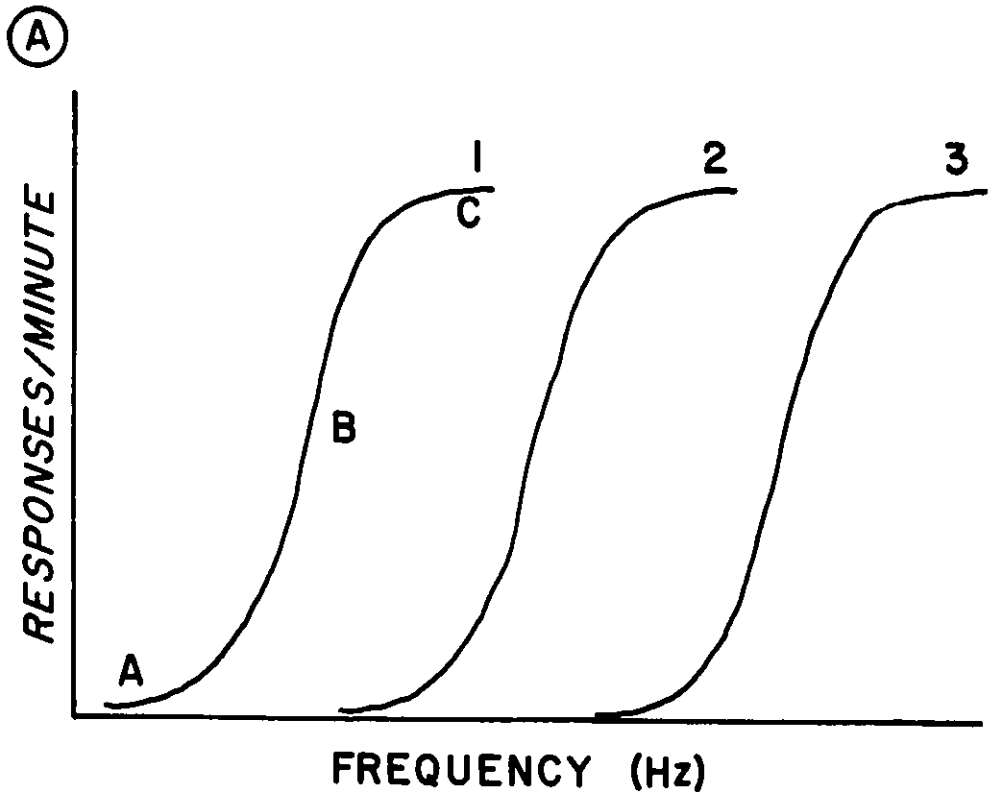
A
RESPONSES/MINUTE
1
2
3
C
B
A
FREQUENCY (Hz)

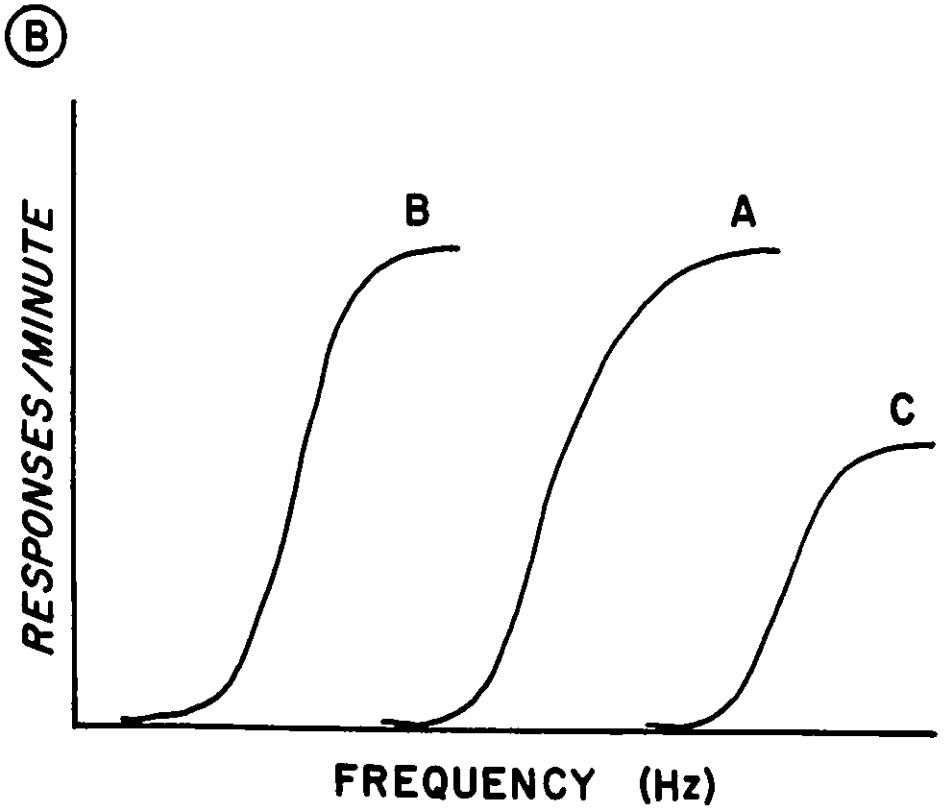
B
RESPONSES/MINUTE
B
A
C
FREQUENCY (Hz)

of one parameter required to compensate for a systematic change in the level of a second parameter and maintain a constant behavioural output.

To derive the trade-off function, a family of rate/frequency curves is generated with, for example, each curve representing a different current value. The frequency threshold, defined as the frequency required to attain a criterial response rate is interpolated from each curve (see Figure 2A). When frequency thresholds are plotted against current level (see Figure 2B), the trade-off function is generated (Edmonds and Gallistel, 1974). It is assumed, since behavioural output is kept constant, that performance contributions are also kept constant for all related rate/frequency curves. As a result, the rewarding effects of stimulation can be more clearly quantified (Edmonds, Stellar, and Gallistel, 1974).

The choice of the criterial response rate is an important factor in ensuring the reliability of the trade-off function. When near maximal response rates are chosen as criterion, ceiling effects can distort the derived trade-off functions (Edmonds et al, 1974). One approach is to select a response rate which is located within the rapidly rising portion of the rate/frequency curve; criterial rates such as the commonly used 50% of the maximal response rate (M_{50}) or some other like proportion of the maximal rate usually fall within this category (Edmonds and Gallistel, 1977). A second approach is

Figure 2. A) An illustration of how frequency thresholds are determined from a family of rate/frequency curves. In this example, current is the parameter of interest. A constant criterion of 35 responses/minute was used to evaluate frequency threshold as indicated by the horizontal dashed line. The corresponding frequency thresholds are shown by the downward arrows.

B) An example of a trade-off function generated from the frequency thresholds interpolated in part A. The manipulated parameter, in this case, current, is on the abscissa, which is plotted using a log scale, while frequency threshold is on the ordinate.

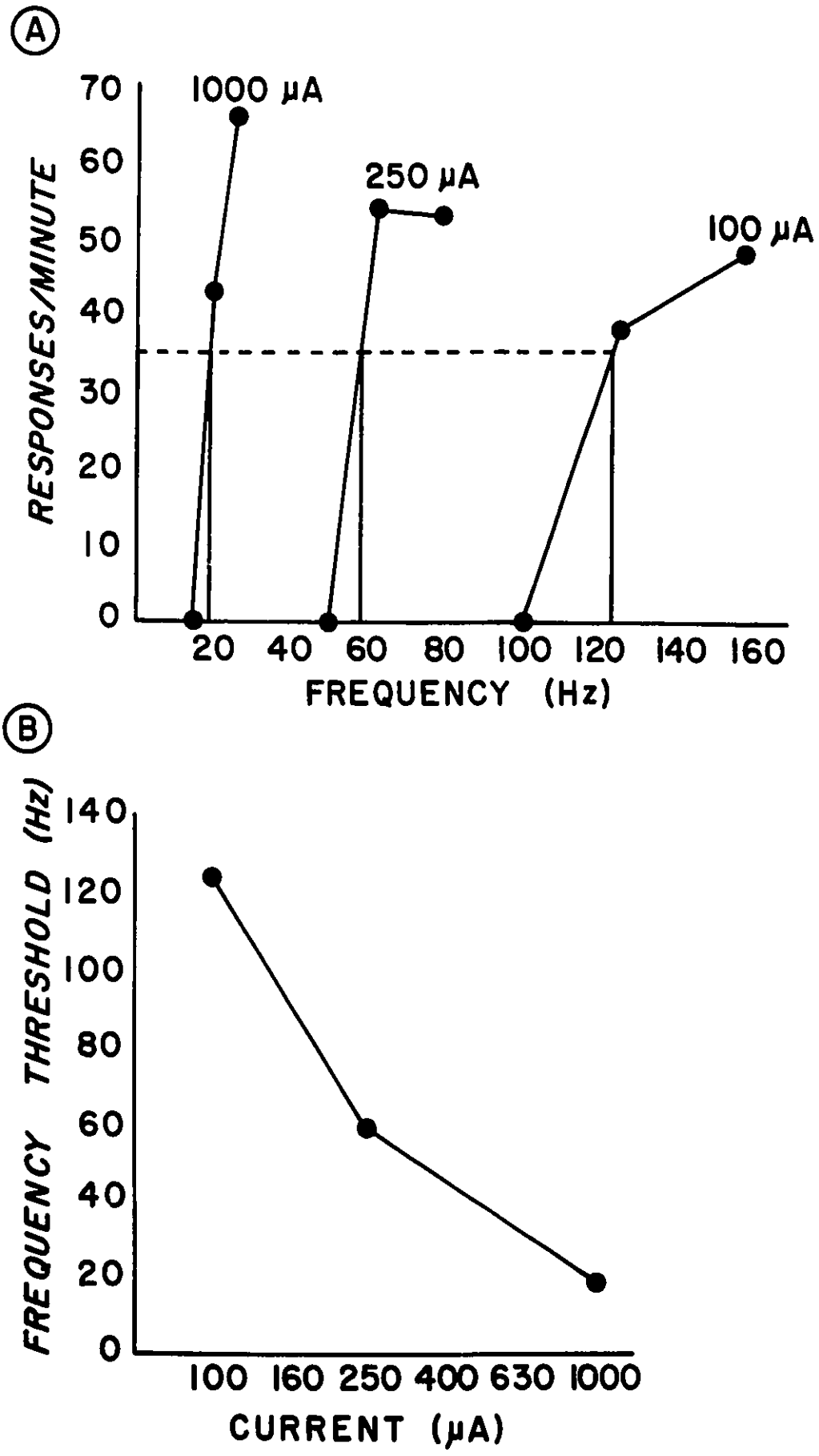
A
70
60
50
40
30
20
10
0
RESPONSES/MINUTE
1000 µA
250 µA
100 µA
20
40
60
80
100
120
140
160
FREQUENCY (Hz)
B
140
120
100
80
60
40
20
0
FREQUENCY THRESHOLD (Hz)
100
160
250
400
630
1000
CURRENT (µA)

to use zero responses/minute (θ_o) as a threshold criterion; this value should be unaffected by performance factors since it is determined at a zero performance level (Miliaressis et al., 1986). In this method, the problem of instability at low response levels is solved by using curve-fitting procedures to estimate θ_o. In fact, similar estimates of threshold result when either method, a low constant cut or a proportional cut, are used (Fouriezos, Bielajew, and Pagotto, 1990); thus, the most expedient criterion can be used. For more in depth explanations of the use of response/stimulus and trade-off functions, please see Stellar and Stellar (1985), Miliaressis et al., (1986), and Yeomans (1990).

Refractory Period Test. The refractory period test is a double-pulse, single electrode technique used to assess the time course for the return to excitability of the directly stimulated fibers which, in this case, are the reward relevant ones.

In the typical self-stimulation set-up, a lever press usually results in the delivery of a single stimulation train, often 500 ms long; the train consists of pulses, usually 100 us in duration. The interval of time which separates the individual pulses is called the period (see Figure 3A). Period, the reciprocal of frequency, is often scaled because this parameter can be discussed in more precise terms than frequency. The number of pulses and the period are co-varied

Figure 3. This figure illustrates the relevant relationship between single- and double-pulse stimulation

A) A train of single-pulse stimulation is shown. The train duration is always held constant; therefore, the number of pulses and the interval between pulses (C-C interval or period) covary. For example, when the number of pulses in the train is increased, there is a corresponding decrease in the period.

B) In the double-pulse condition, each C pulse is followed by a T pulse of the same amplitude.

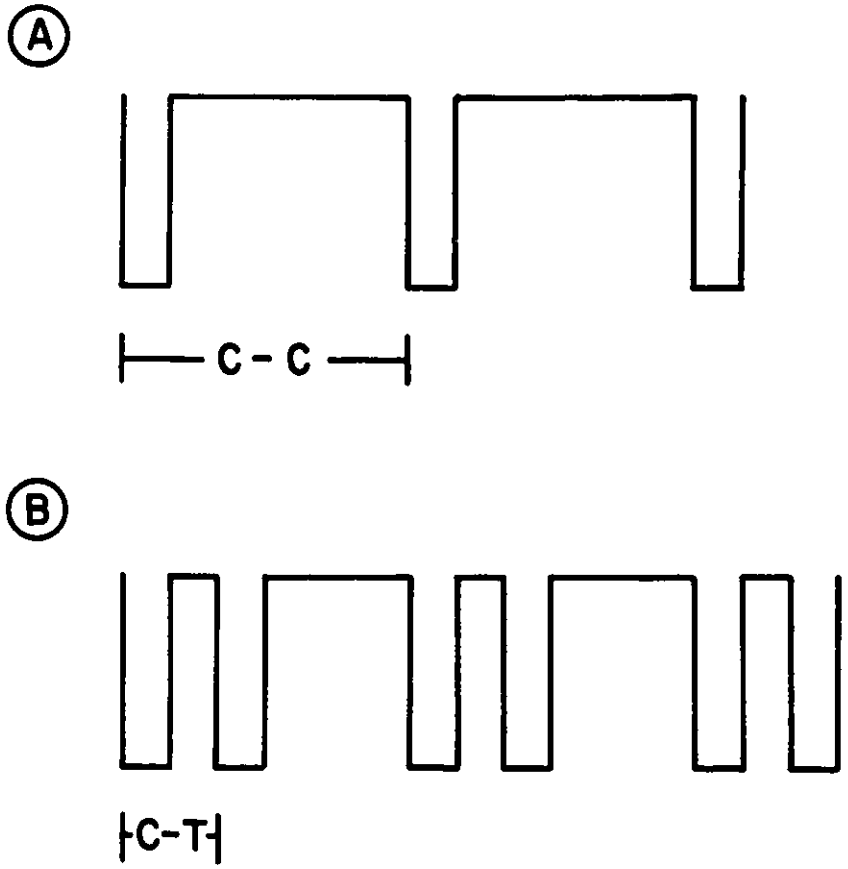
A
C - C
B
C-T

in order to maintain a constant train duration.

To determine the refractory period, a second set of pulses, with the same characteristics, is interdigitated in the stimulation train such that the pulses are paired (see Figure 3B). The first pulse of each pair is called the conditioning (C) pulse and the second pulse is called the test (T) pulse. The interval separating the C and T pulses of each pulse pair is the C-T interval.

The refractory period test evaluates the post-stimulation excitability of the behaviourally relevant elements by assessing their ability to re-fire to T-pulse stimulation following suprathreshold C pulse activation. In the behavioural paradigm, the rewarding effectiveness of the T pulse is determined by varying the C-T interval, typically from 0.2 msec to 10 msec; a rate/period curve is generated for each C-T interval and the period threshold associated with that interval is calculated. Then each double-pulse period threshold is compared to the period threshold obtained when only C pulses are administered using the equation (adapted from Yeomans, 1975):

$$E_T = (PT_{c-t}/PT_{sp})-1 \text{ where}$$

E_T = effectiveness of the T pulse

PT_{sp} = period threshold, C pulses only

PT_{c-t} = period threshold, at a given C-T interval

This equation is based on the assumption that the stimulated

neurons comprise a homogeneous population of uniformly distributed elements.

As an example, assume that PT_{sp} is 20 msec. When the C-T interval falls within the absolute refractory period, the T pulses will be unable to depolarize neurons a second time; thus, only C pulses will be effective, and PT_{c-t} will equal the PT_{sp} of 20 msec. Therefore, the equation will yield the minimum E_T value of 0. When the C-T interval exceeds the refractory period of the neurons, both C and T pulses will be effective; therefore, PT_{c-t} will be twice PT_{sp}, or 40 msec, since half the number of pulse pairs will be required to sustain criterion performance. When this occurs, the equation yields the maximum E_T value of 1.

The actual profile that is observed is more complex than the simple case just described. There are five major components of neural refractoriness which can be detected using slight modifications of the above paradigm: local potential summation, absolute refractory period (ARP), relative refractory period (RRP), and the supernormal and subnormal period (see Figure 4).

Local potential summation effects are observed at short C-T intervals, usually not more than 0.4 msec for self-stimulation neurons (Yeomans, Matthew, Hawkins, Bellman, and Doppelt, 1979). These effects are due to the summation of the partial depolarizations caused by C and T pulses to neurons just outside of the effective stimulation field. At C-T intervals

Figure 4. This figure illustrates the components of the behaviourally derived refractory period curve using Yeomans (1975) scaling method. The effectiveness of the T pulse is plotted as a function of C-T interval. Local potential summation effects are seen initially (A), followed by recovery from the absolute and relative refractory periods (B), with the supernormal period, when observed, obscuring the end of the relative refractory period by an overshoot of the theoretical maximum E value of 1 (C), followed by a subnormal period where the E value falls below 1.0 (D).

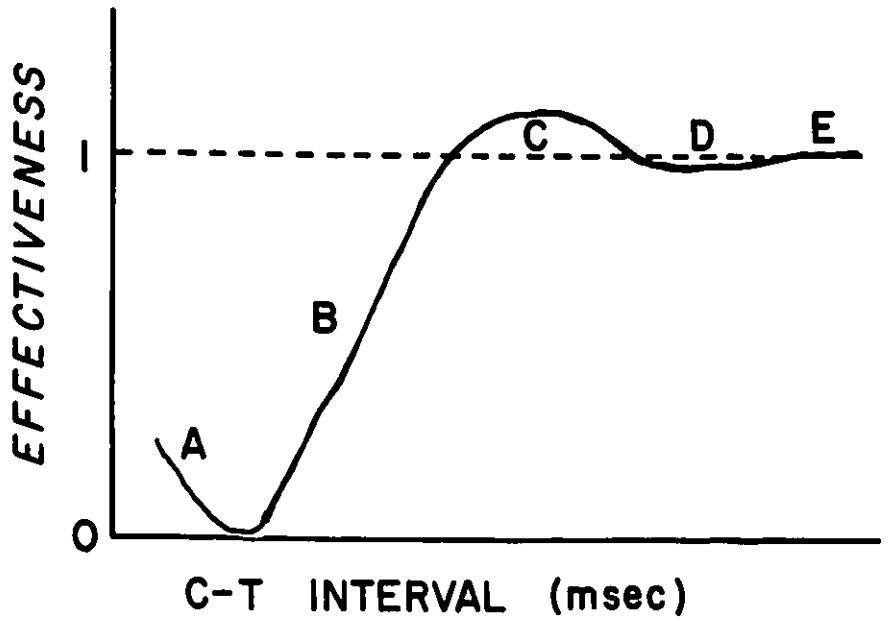
EFFECTIVENESS
1
0
A
B
C
D
E
C-T INTERVAL (msec)

greater than 0.4 msec, the partially depolarized neurons, due to C pulse excitation, have time to recover to baseline polarization levels before the T pulses are delivered; in this case, local potential summation effects are not observed.

The ARP phase becomes evident once local potential summation effects disappear. During this period, the neurons are completely refractory to any stimulation following the delivery of the C pulse; as a result, E_T should be zero but frequently is not. Two factors influence this value; first, local potential summation effects may still be present at C-T intervals greater than 0.4 msec and, second, some neurons may already be in the RRP phase during which T pulses can cause these neurons to fire again (Yeomans, 1975; 1979).

In the RRP phase, the neurons are hypoexcitable but will fire again if the T pulse current is sufficiently intense. For example, neurons closest to the electrode tip will experience a higher current density and may fire as soon as the T pulse falls within their RRP while neurons farther away from the electrode tip, and subject to lower current densities, will be excited only at some point further into their RRP.

The supernormal and subnormal periods are observed at long C-T intervals when RRP effects begin to dissipate. These components of the excitability cycle are variable since their presence depends greatly on the size of the neurons being stimulated and the repetitiveness of the stimulation (Yeomans,

1990). As a result, they have not been used extensively in self-stimulation studies.

The different components of the post-stimulation excitability cycle can be dissociated using equal and unequal current C and T pulses. When equal current C and T pulses (C=T) are used, local potential summation effects, ARP, and RRP all contribute to the refractory period profile. When larger C pulses are used (C>T), the ARP, RRP and supernormal phases of recovery are present. To estimate the contribution of the supernormal period, the C>T excitability curve is compared to the C=T curve; any increases in T pulse effectiveness once the RRP is complete are interpreted to be due to the supernormal period. When smaller current C pulses are used (C<T), the observable components of the excitability cycle are the local potential summation and the ARP phases. Thus, C<T allows for the determination of the ARP without contamination from the RRP (Yeomans, 1979).

However, the one component of the excitability cycle which appears to be relatively invariant to different current levels is the ARP. An important result of the unequal C and T pulse work has been the finding, for self-stimulation neurons in the MFB, that the RRP does not appear to make a significant contribution to the excitability cycle beyond the range of the ARP (Bielajew, Lapointe, Kiss, and Shizgal, 1982; Fouriezos et al, 1987; Yeomans, 1979). Therefore, the use of equal current

C and T pulses appears adequate to allow a reasonable estimate of the ARP.

The early components of the excitability cycle for MFB reward neurons have been well defined. Local potential summation effects are evident up to C-T intervals of 0.4 msec (Yeomans et al, 1979). The ARP phase, estimated from C=T and C<T studies, ranges from 0.4 to 1.2 msec (Bielajew et al, 1981; Bielajew et al., 1982; MacMillan, Simantirikis, and Shizgal, 1985; Schenk and Shizgal, 1982; Yeomans, 1979). The subnormal and supernormal periods have not been well characterized.

Collision Test. The basis of this test is the observation that two action potentials, approaching in opposite directions along the same axon, will collide and cancel each other without further propagation.

The behavioural collision test, analogous to the refractory period test, is a double pulse technique in which the C-T interval is varied; the distinction between the two methods is that, in the collision test, the C and T pulses are delivered to different electrodes (see Figure 5). When an axon is excited, an antidromic (toward the soma) and an orthodromic (toward the terminals) action potential are generated; this is in contrast to normal conduction which is in the orthodromic direction. When two points on the same axon bundle are stimulated, the set of orthodromic action potentials of the electrode closest to the soma will collide with the set of

Figure 5. In the upper portion of this figure, the C and T pulses are illustrated as 2 trains of pulses separated by an interval (C-T interval). The lower part of the figure shows a stylized drawing of 2 electrodes stimulating the same axon bundle. As indicated by the dashed lines, the C pulses are delivered to the electrode on the left and the T pulses to the right electrode. The 2 dashed circles directly below the electrode tips represent the effective stimulation fields through which the same fibers are coursing.

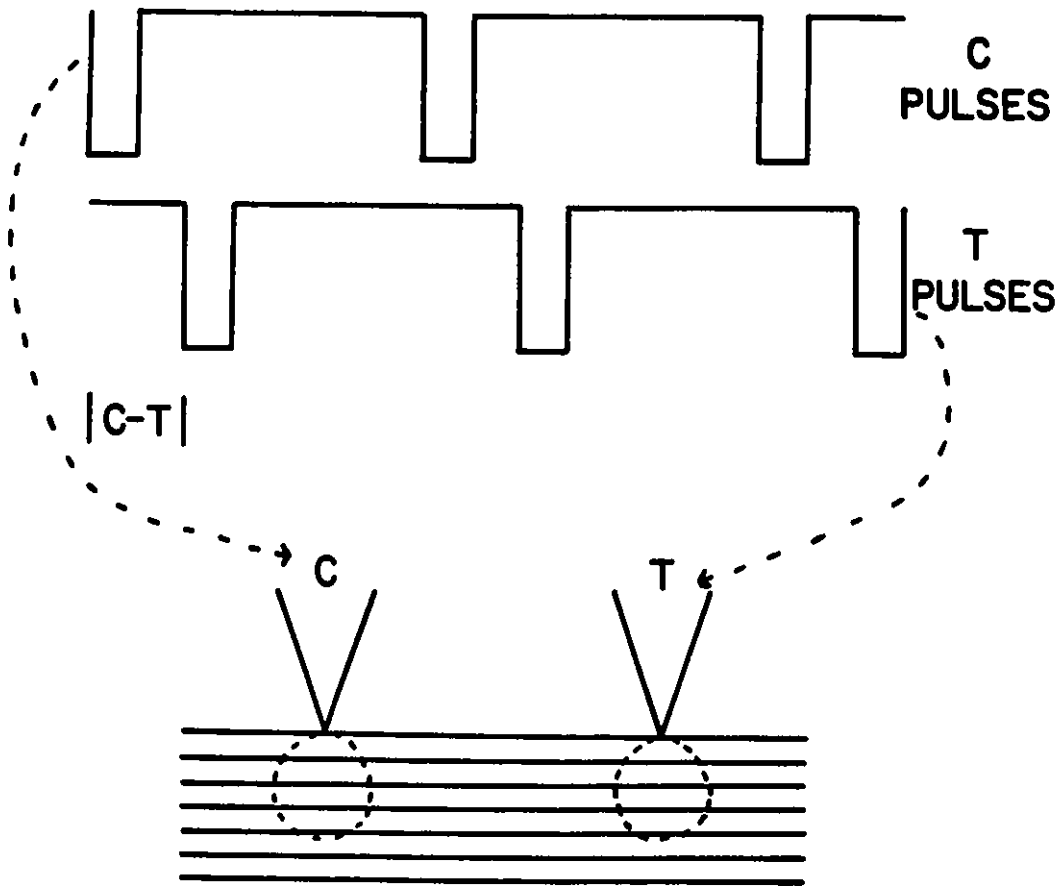
C
PULSES
T
PULSES
|C-T|
C
T

antidromic action potentials from the electrode nearer the terminals (downstream); this results in the arrival at the terminals of a single set of orthodromic action potentials, generated by the downstream electrode. Collision does not occur if the stimulation via the upstream electrode is delayed enough so that the set of antidromic action potentials generated at the downstream site has time to conduct past the upstream site and recover from refractoriness; thus, two sets of orthodromic action potentials will arrive at the synapses (Shizgal, Bielajew, Corbett, Skelton, and Yeomans, 1980).

The effectiveness of double-pulse stimulation is assessed using an equation similar to one employed by the refractory period test (see previous section). When the C-T interval is less than the collision interval, only a single set of orthodromic action potentials reaches the relevant terminals; as a result, double pulse stimulation is no different than single pulse stimulation, and the effectiveness of double pulse stimulation is zero. When the C-T interval exceeds the collision interval, defined as the sum of the inter-electrode conduction time and the refractory period, both sets of orthodromic action potentials reach the terminals; thus, double pulse stimulation is twice as effective as single pulse stimulation resulting in an effectiveness value of 1.

Under ideal conditions, the single pulse period thresholds are identical so that each electrode contributes the same

rewarding value to the double pulse stimulation. The following collision equation has been adjusted to correct for minor inequalities in the single pulse thresholds:

$$E=[(PT_{c-t}/PT_{sph})-1]/(PT_{spl}/PT_{sph})$$ where

E = effectiveness of the double pulse stimulation

PT_{spl} = lower value of the two single pulse period thresholds

PT_{sph} = higher value of the two single pulse period thresholds

PT_{c-t} = double pulse period threshold, at a given C-T interval

The denominator takes into account the difference between the two electrodes. If PT_{spl} and PT_{sph} are equal, the correction factor reduces to 1 and the equation closely resembles the refractory period one.

One assumption of the collision test is that the refractory period estimates at both sites are identical. If this assumption is met, one characteristic of the collision profile is that the estimated collision interval should be identical regardless of which electrode delivers the C pulse because of the bidirectional nature of axonal propagation.

The estimates of refractory period, collision interval, and interelectrode distance, allow one to compute the conduction velocity of the neurons that contribute to the collision effect by dividing the interelectrode distance by the difference

between the collision interval and the refractory period estimate. This calculation produces a low estimate of conduction velocity since it is assumed that the relevant axons course via the shortest route between the two stimulating electrodes.

When collision is observed, the suggestion that direct functional connections exist between the two sites can be confidently asserted. When collision is not observed, the interpretation is less clear. The absence of collision indicates that either different fibers are stimulated or that the electrodes are misaligned. Bielajew and Shizgal (1982) showed that an increase in current gave rise to a collision effect which had not been observed at low currents (see Figure 6 for an example), suggesting that the electrodes were misaligned.

The Specificity of Brain Stimulation Reward Fibers

The results of the refractory period and collision tests contributed to the identification of the electrophysiological characteristics of stimulation-induced behaviours in the MFB and other sites. The properties of reward elements can be compared to those of other stimulation-induced behaviours that are elicited at common loci, beginning the process of determining the nature of BSR.

In a study of LH and VTA sites that produced both self-stimulation and stimulation-escape, all subjects exhibited

Figure 6. An illustration of how low current can alter the outcome of a collision test when two electrodes, located in the same axon bundle, are misaligned. When lower currents are used (small circles), 2 different subsets of the same fiber bundle are stimulated; an absence of collision is observed. When the currents are increased (large, dashed circles), a subset of fibers, common to both fields, are stimulated and collision effects are observed.

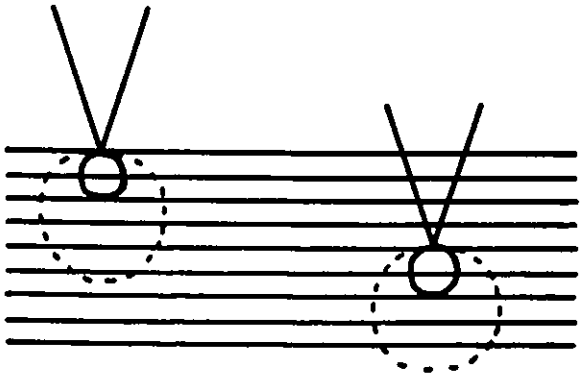

collision for self-stimulation but only 1 of the 3 subjects showed a small collision effect for stimulation-escape (Bielajew and Shizgal, 1980). This finding suggests that while the reward neurons appear to form a continuous axon bundle coursing from the LH to the VTA, the majority of the aversion-related neurons do not have this configuration at the tested sites (Bielajew and Shizgal, 1980).

Similarly, although the MFB substrate for self-stimulation and general motor activity has similar refractory periods (Rompre and Miliaressis, 1980), two different fiber bundles appear to mediate these behaviours, based on the observation of a collision effect for self-stimulation and its absence for general motor activity at the same stimulation sites (Durivage and Miliaressis, 1987).

Conversely, the observation of overlapping refractory period estimates and positive collision results at the same LH and VTA sites for self-stimulation and stimulation-induced feeding have led to the suggestion that the directly stimulated fibers underlying both behaviours are probably the same (Gratton and Wise, 1988a,b). A detailed study of the rate/frequency patterns for these two behaviours indicated that, unlike self-stimulation which exhibited a lateral shift in frequency threshold, the feeding curves showed a shift in asymptotic feeding rate when current was increased. These results suggest that different processes of integration characterize the two

behaviours downstream from the stimulation site (Waraczynski and Kaplan, 1990).

The Search for the Cell Bodies of Origin

Mapping studies. The LH has been shown to have efferent projections to many structures extending caudally to the VTA and the mamillary complex and, rostrally, from the medial-septal diagonal band complex through the lateral preoptic area (LPO) (Nieuwenhuys, Geeraedts, and Veening, 1982; Saper, Swanson, and Cowan, 1979; Veening, Lie, Posthuma, Geeraedts, and Nieuwenhuys, 1987). The LPO has reciprocal connections with both the LH and VTA (Phillipson, 1979; Swanson, 1976). Single cell recordings have shown that neurons in the LPO and the area between the preoptic and anterior hypothalamic nuclei respond antidromically to stimulation of the MFB (Perkins and Whitehead, 1978; Rompre and Shizgal, 1986).

The VTA, from which robust self-stimulation can be elicited, receives projections from many rostral reward sites including the prefrontal cortex, nucleus accumbens, bed nucleus of the stria terminalis, amygdala, medial and lateral preoptic areas, and the LH. The caudal afferents of the VTA include the superior colliculus, parabrachial nucleus, locus coeruleus, and dorsal raphe (Nieuwenhuys et al, 1982; Phillipson, 1979).

In recording studies, placing electrodes in MFB reward loci have resulted in more meaningful results. For example, cells responsive to self-stimulation electrodes in the MFB are

present in the lateral and medial preoptic areas, the ventral pallidum, and the parastrial nucleus, with a much larger region of antidromically driven neurons existing in and around the septal complex (Shizgal, Schindler, and Rompre, 1989).

Metabolic markers have been used to further define regions selectively activated by self-stimulation electrodes in the MFB. The compound, [^{14}C]-2-deoxyglucose, which is metabolically inert and is taken up by neurons in place of glucose, was employed to demonstrate that self-stimulation from the anterior VTA produced activation in the vertical limb of the diagonal band of Broca, compartment "c" of the MFB, the bed nucleus of the stria terminalis, the medial preoptic area, and throughout the midhypothalamic levels of the MFB with a bilateral suppression of activity in the lateral habenula. The activation extended caudally to about the level of the anterior VTA (Gallistel, Gomita, Yadin, and Campbell, 1985).

A different metabolic marker, cytochrome oxidase, was similarly exploited to examine the sites activated by LH self-stimulation. Short pulse durations resulted in increased metabolic activity of the lateral septal nucleus and the nucleus accumbens. When longer pulse durations were used, more widespread activation was observed in the frontal cortex, olfactory tubercle, lateral habenula, along with stronger activation of the septal nucleus (Bielajew, 1991), similar to that found using the [^{14}C]-2-deoxyglucose method (Gallistel et

al, 1985).

When brain regions exhibit excitation in response to stimulation of MFB self-stimulation loci, these areas become candidates for the location of the cell bodies of the pathway responsible for self-stimulation in the MFB. Interpretation difficulties result from the fact that the stimulation field contains many fibers, of which probably only a subset are reward relevant. Conversely, the absence of activation is strong evidence that the unaffected regions are not part of the MFB reward system.

Lesion Studies. Another approach used to determine if extra-MFB regions are functionally connected to the MFB reward system has been to study the effect of lesions or ablations of these areas on MFB self-stimulation. Bilateral ablations of brain regions rostral to the thalamus resulted in "thalamic" rats with severely limited behavioural output; nonetheless, the rats could still be trained to respond in order to obtain hypothalamic stimulation suggesting that the major forebrain regions were not required for self-stimulation (Huston and Borbely, 1973; 1974). However, once acquired, this "operant" behaviour could not be extinguished producing doubts as to whether operant conditioning for rewarding stimulation had actually been established.

The destruction of LH neurons by kainic or ibotenic acid or of MFB neurons at the level of the sub-thalamic nuclei by

electrolytic lesion had no effect on response rates for LH self-stimulation in some studies (Sprick, Munoz, and Huston, 1985; Umemoto, 1968), although rate decreases have been reported (Velley, 1986a). Similar ibotenic acid lesions of the LH have been reported to decrease self-stimulation rates in the parabrachial nucleus (Ferssiwi, Cardo, and Velley, 1987). Damage to fibers rostral to the LH, at the level of the septal region and preoptic areas, were ineffective, transiently effective, or permanently effective in decreasing LH self-stimulation rates (Huston, Kiefer, Buscher, and Munoz, 1987; Munoz, Keller, and Huston, 1985; Umemoto, 1968; Velley, 1986b).

The contradictory findings obtained from the early lesion work are the result of a number of factors. One important characteristic of this research was the widespread damage inflicted by the lesioning methods in which, not only the structure of interest, but frequently neighbouring regions were severely compromised. Thus, there was a poor containment of the lesion damage which weakens the interpretation. A second consideration was the use of response rate as the measure from which changes in the rewarding value of the stimulation was inferred.

When psychophysical scaling techniques were combined with lesion methods, the results were more consistent. Large post-lesion increases in LH frequency thresholds were observed following small electrolytic lesions of the VTA (Glimcher and

Gallistel, 1988; Janas and Stellar, 1987) providing support for the suggestion that the direction of conduction for the rewarding signal was rostrocaudal (Bielajew and Shizgal, 1986).

Frequency thresholds associated with LH self-stimulation were unaffected by unilateral forebrain ablations above the level of the thalamus; however, the authors suggest that this result was due to the incomplete destruction of the preoptic and septal regions (Stellar, Illes, and Mills, 1982). This idea has been supported by the moderate success of ipsilateral electrolytic lesions and knife-cuts of the anterolateral portion of the MFB at the level of the preoptic area in disrupting both LH and VTA self-stimulation (Janas and Stellar, 1987; Murray and Shizgal, 1991; Waraczynski, 1988). Thus, the preoptic region, anterior to the MFB, seems to be important for the integrity of MFB self-stimulation.

The problem with lesion studies is that effective and ineffective lesions can be localized at virtually the same site (Janas and Stellar, 1987). Due to such factors as the local trauma that is produced at the lesion site or the possibility of regeneration some time after the lesion, it is difficult to make strong inferences based on studies of this kind. In addition, regardless of whether the lesion is effective or not, it is not possible to make unambiguous conclusions about the reward circuitry based on lesion results. Many different functional arrangements can exist to account for positive or

negative lesion results (for further discussion, see Bielajew, 1983). Thus, lesion studies have a limited utility in mapping the circuitry for BSR.

Refractory period studies. Comparisons between the refractory periods of self-stimulation neurons within and outside of the MFB have resulted in the classification of extra-MFB regions as feasible candidates for the first stage extension of the MFB reward pathway. Outside of the MFB, the ARP for self-stimulation neurons generally begins and ends later than the estimates obtained for self-stimulation sites in the LH and VTA. The periaqueductal gray and the ventrolateral tegmentum, both situated at the caudal portion of the MFB, have refractory periods ranging from 0.4 to 2.0 msec and 0.8 to 2.0 msec, respectively (Bielajew et al, 1981; MacMillan et al, 1985). The mediodorsal thalamus, found dorsal to the MFB, has the longest recovery from refractoriness reported for self-stimulation neurons, ranging from 1 to 10 msec (Bielajew and Fouriezos, 1985). In rostral reward sites, the anterior basal forebrain recovers from 0.4 to 5 msec (Fouriezos et al, 1987), the caudate-putamen from 0.65 to 6 msec (Trzcinska and Bielajew, 1992), while the medial prefrontal cortex has a refractory period from 0.95 to 6.25 msec (Schenk and Shizgal, 1982; Trzcinska and Bielajew, 1992).

In all cases, except for the medial prefrontal cortex, the refractory period estimates for the periaqueductal gray, the

ventrolateral tegmentum, the mediodorsal thalamus, the anterior basal forebrain, and the caudate-putamen, substantially overlap the values obtained for MFB reward neurons. Studies of the refractory period estimates of the medial prefrontal cortex suggest that this rewarding region is probably part of a system separate or rostral to the MFB reward system (Schenk and Shizgal, 1982). This hypothesis is supported by the results of the 2DG mapping studies which did not find activation in the medial prefrontal cortex (Gallistel et al, 1985; Yadin, Guarini, and Gallistel, 1983). One interpretation for the overlapping estimates of refractoriness in many self-stimulation loci is that a subset of the MFB self-stimulation fibers probably course through these extra-MFB sites.

Collision studies. Direct connectivity between the LH and the VTA for self-stimulation was first reported in 1980 with conduction velocity estimates ranging from 1.0 to 8.3 m/s (Bielajew and Shizgal, 1982; Durivage and Miliaressis, 1987; Shizgal et al, 1980). Combining the collision test with anodal stimulation at one electrode, the direction of conduction of these neurons was shown to be primarily rostrocaudal (Bielajew and Shizgal, 1986). It has also been reported that direct functional connectivity for self-stimulation neurons exists between the LPO and LH with conduction velocities ranging from 0.24 to 11 m/sec (Bielajew et al, 1987).

No evidence of direct connectivity has been observed for

self-stimulation between the medial prefrontal cortex and the LH; this result, coupled with non-overlapping refractory period estimates and low level of double pulse summation at these two sites, has led to the tentative hypothesis that separate fiber systems, with different characteristics, mediate self-stimulation in the medial prefrontal cortex and the LH (Schenk and Shizgal, 1982).

Rationale

The basis for investigating the possibility that the LPO and VTA self-stimulation neurons are anatomically connected is found in a number of studies. Anatomical studies have shown that continuous fibers course between the LPO and the VTA, although it is unclear if any of these play a role in self-stimulation (Nieuwenhuys et al, 1982; Phillipson, 1979; Swanson, 1976). It has also been reported that the LPO contains neurons which can be driven antidromically by stimulation of reward neurons in the MFB (Shizgal et al, 1989). In addition, the estimates of refractoriness for LPO and VTA self-stimulation neurons overlap, suggesting that a subset of these neurons may be common to both sites (Bielajew et al, 1981, 1982; Fouriezos et al, 1987; MacMillan et al, 1985; Schenk and Shizgal, 1982; Yeomans, 1979). This evidence, coupled with the finding that collision is observed between the

LPO and the LH and between the LH and the VTA (Bielajew and Shizgal, 1982; Bielajew et al, 1987; Durivage and Miliaressis, 1987; Shizgal et al, 1980), suggests that there may be an uninterrupted pathway, which is reward relevant, that extends from the LPO to the VTA.

Two major objectives were addressed in this thesis using the parametric techniques that have been described. A mapping study of the LPO was conducted with the intention of delineating those areas within the LPO that support self-stimulation and defining the spatial characteristics of these reward fibers using trade-off functions between current and period. The second objective was to investigate the nature of the anatomical arrangement of reward neurons in the LPO and the VTA using the collision test.

In order to effectively investigate the two objectives of this project, one methodological concern had to be addressed. The problem arose from the frequent appearance of motor seizures occurring following electrical stimulation of the LPO. Efficacious control of the seizures became an objective in order to facilitate the studies to follow. However, because of the concern that the pharmacological agent used to control seizures would affect the membrane properties of the directly stimulated neurons, refractory period tests were conducted to assess any drug induced changes in membrane excitability. Consequently, the first experiment investigated the ability of

the novel benzodiazepine, brotizolam, to control the motor seizures induced by LPO stimulation without altering the refractory period of these neurons.

The second experiment addressed the first major objective of this thesis which was to develop a detailed map of self-stimulation in the LPO using moveable electrodes (Miliaressis, 1981). At each site that supported self-stimulation, the trade-off between current and period was determined, in order to evaluate the spatial configuration of LPO reward neurons.

The third experiment directly addressed the possibility that functional connections exist between the LPO and VTA for self-stimulation. The collision test was used to examine this question; in the event that positive collision results were indicated, the refractory periods of these neurons were determined so that the conduction velocities of the relevant neurons could be estimated.

General Methodology

Unless otherwise indicated, the surgeries, screening and testing procedures for the three experiments were conducted as described below.

Subjects and surgery

The male Long-Evans rats (Charles River Laboratories) were housed separately in plastic cages under a twelve-hour light/dark cycle with lights on at 0700 hours. Food and water were available ad libitum. Subjects weighed between 300 and 400 g at the time of surgery.

Subjects were anaesthetized using a combination of 65 mg/kg intraperitoneal sodium pentobarbital (Somnotol) and 0.05 mL intramuscular xylazine. A subcutaneous injection of 0.20 mL atropine sulfate was administered approximately 15 minutes before surgery in order to minimize respiratory distress.

Surgery was conducted using standard stereotaxic procedures. The flat-skull coordinates used to guide electrode implantation were based on the Paxinos and Watson (1986) atlas.

Two types of monopolar electrodes were used. Dorsoventrally moveable electrodes from Kinetrode Inc., Ottawa (Miliaressis, 1981) were implanted, primarily in anterior brain regions. Fixed electrodes were used mainly in the posterior VTA region; they were constructed from 250 μm diameter, stainless-steel wire and were insulated with Epoxylite to the flattened tips. The indifferent electrode consisted of a gold amphenol pin with

a stainless-steel wire soldered to it. The wire was wrapped around four skull screws and the indifferent electrode was placed contralateral to the implanted electrodes. The entire assembly was anchored to the skull screws using dental acrylic.

Apparatus

The test chambers were 28 cm long X 38 cm wide X 44 cm tall wooden boxes with Plexiglas fronts. In each box, a rodent lever protruded approximately 3 cm above the floor on one side wall. A constant-current amplifier (Mundl, 1980) and an integrated circuit pulse generator, produced in-house, were used to deliver the electrical stimulation. The current was continuously monitored on an oscilloscope by reading the voltage drop across a 1 k precision resistor in series with the rat. In order to prevent polarization at the electrode tip in the absence of a pulse, the output was shunted to ground through 560 resistors.

Each depression of the lever resulted in the delivery of a 500 msec train of rectangular cathodal pulses of 100 usec duration. The pulse period and current were varied as described below.

Screening, training, and stabilization

Animals were permitted to recover from surgery for at least 3 days before screening for self-stimulation began. Conventional operant shaping techniques were used to encourage lever-pressing for moderate electrical stimulation available on

a continuous reinforcement schedule.

Once reliable lever-pressing was exhibited, the animals were introduced to the 60 sec trials, each of which was preceded by five priming stimulations. The priming stimulations, separated by an inter-prime interval of 1 sec, signalled both the start of each trial and the level of the rewarding stimulation available. The current and period were adjusted to produce high response rates.

When lever pressing was consistently initiated within 12 sec of the presentation of the last train of priming stimulation, a descending sequence of periods at a set current was introduced. A response rate/period curve was generated starting with a period at which no responding occurred. Each successive period was a 0.10 common log unit step below the previous one and, therefore, equivalent to an increase in the rewarding value of the stimulation. The periods were decreased until the bar pressing rate exceeded the criterion of 35 responses/minute. A range of currents was tested using this procedure beginning at 80 μA and increasing, in 0.10 common log unit steps, to 1000 μA. The period required to support the criterion response rate of 35 responses/minute was determined at each current by interpolation of the rate/period curve. These values were then plotted to illustrate the trade-off function between current and period.

The procedures to obtain the trade-off function were

repeated until a within session stability criterion was met. A baseline current, usually 200 uA, was administered at the beginning and the end of each session; the criterion for stability was a less than 0.10 common log unit variability between the two baseline threshold determinations.

At the beginning of each session, two or three warm-up determinations of the period threshold were conducted which were not included in the data analysis.

For each experiment, the relevant procedures were replicated until the stability criterion was met. In order to be considered stable, the majority of the standard errors of the mean could not exceed 10% of their associated mean values. Three to six replications were generally required to meet this criterion.

Histology

When all behavioural tests were completed, the subjects were perfused intracardially with a solution of 0.9% saline followed by 10% formalin. The brains were removed and stored in 10% formalin for at least 1 week. The tissue containing the electrode tracks was sectioned at a thickness of 40 um and floated onto gel covered slides. The sections were stained with cresyl violet. The electrode tips were located using the Paxinos and Watson (1986) atlas.

Experiment 1

The examination of self-stimulation sites rostral to the MFB is frequently hampered by the occurrence of stimulation-induced motor seizures. One of these sites is the LPO from which seizures generally develop within the first few stimulation sessions (Fouriezos et al, 1987) and result in significantly longer test sessions and less stable thresholds during the session. The seizures generally worsen over a period of days, sometimes becoming so severe that animals permanently cease responding.

The benzodiazepines are a class of minor tranquilizers that have sedative, anti-anxiety, and, of interest to this study, anti-convulsive properties (Haefely, 1987). The major effects of these compounds appear to arise through their potentiation of gamma-aminobutyric acid's (GABA's) actions at the GABA/benzodiazepine receptor complex; GABA decreases neural excitability by opening chloride channels in the membrane, resulting in neural hyperpolarization (Haefely, 1990) which is the basis of this neurotransmitter's inhibitory action (Weber et al, 1985). The problem with conventional benzodiazepines, for this study, is that their anti-convulsant properties last a relatively short period of time, rendering them impractical for use in our paradigms which generally require individual sessions of three to four hours.

Recently, a novel benzodiazepine, brotizolam, has been developed which appears to have a long-lasting anti-convulsant effect. Like conventional benzodiazepines, this compound has been shown to act at the GABA/benzodiazepine receptor complex to facilitate GABA's ability to decrease membrane excitability, and similar to diazepam, brotizolam appears to be efficacious in controlling seizures. The principal advantage of brotizolam is that it has longer lasting anti-convulsant effects than diazepam (Boke-Kuhn, Danneberg, Kuhn, and Lehr, 1986). Specifically, this drug appears to be effective in controlling motor seizures induced by electrical stimulation for approximately six hours following intraperitoneal injection (Bielajew, Harris, and Parkin, in preparation).

On the surface, brotizolam appears to be an ideal drug for use in studies where the incidence of seizures interferes with data collection. However, since brotizolam interacts with GABA to facilitate reduced membrane excitability, it was essential in our studies to ensure that brotizolam was not altering the membrane properties of the directly stimulated reward neurons. Thus, this experiment examined the ability of the novel benzodiazepine, brotizolam, to control the motor seizures induced by LPO stimulation while not interfering with the poststimulation excitability cycle.

Method

Subjects and surgery

Four male Long-Evans rats (Charles River Laboratories) were used in this study. Electrodes were aimed at the LPO using coordinates 0.6 to 0.92 mm posterior to bregma, 1.3 to 2.0 mm lateral to the mid-sagittal suture, and 8.0 to 8.2 mm ventral to the skull surface reading at bregma. Because three of the four subjects were to be part of experiments 2 and 3, moveable electrodes were implanted in the LPO and fixed electrodes in the VTA, ipsilateral to the LPO; the VTA coordinates were 4.8 mm posterior to bregma, 1.2 mm lateral to the mid-sagittal suture, and 8.0 mm ventral to the skull surface reading at bregma.

Drug

Brotizolam (Boehringer-Ingelheim) was obtained in powder form. The solvent consisted of 55% propylene glycol, 35% saline (concentration 0.9%), and 10% alcohol; it was filtered and placed in a sterile container with the drug and then heated mildly to aid dissolution. The final concentration of the brotizolam solution was 5 mg/mL.

Behavioural testing

The currents were selected to maximize the probability that motor seizures would be elicited and to closely match the currents which would be used during subsequent refractory period and collision tests (800 to 1000 μA).

After a brief warm-up phase, refractory period tests were conducted which consisted of a series of single- and double-pulse (SP and DP, respectively) determinations. Each replication of the refractory period curve began and ended with an SP threshold determination; these thresholds had to meet the previously defined stability criteria (see page 42) for the session to be included in the average refractory period curve. The DP tests which were interposed between the two determinations of the SP threshold, comprised the following eight C-T intervals: 0.2, 0.4, 0.8, 1.2, 2.0, 5.0, 10.0, and 20.0 msec; these intervals were presented in a random order. One or two full refractory period curves, depending on the stability of the SP thresholds, were generated each day. Drug sessions were separated by at least two days.

Once the baseline refractory period curve was established, drug tests commenced during which the estimate of refractoriness was re-evaluated. Pilot tests had been conducted during which different doses of brotizolam were administered; as a result, 7.5 mg/kg i.p. brotizolam was selected as an appropriate dose for the refractory period tests. During each drug session the brotizolam was injected one hour before tests began; the one hour interval was required for the drug-induced sedation to subside. For all sessions, the number and severity of motor seizures was noted. The classification system was based on a five point scale with each

successively severe seizure including the characteristics of the previous classifications: Type 1 consisted of wet dog shakes, Type 2 included mouth and head movements, Type 3, forepaw clonus, Type 4, upright rearing, and Type 5, rearing and falling over (Racine, 1975).

Results

Histology

Three of the four electrode tips (TH22, TH27, and TH29) were located in the LPO region while the remaining tip (TH28) was situated in the LH (see Figure 7). The most anterior placement (TH27) was found to be just lateral to the LPO in the nucleus of the horizontal limb of the diagonal band which is part of compartment 'a' of the MFB (Nieuwenhuys et al, 1982). Similarly, the electrode tip for TH29 was located just lateral and dorsal to the LPO in the substantia innominata. The third electrode (TH22) was positioned within the LPO just dorsal to the nucleus of the horizontal limb of the diagonal band. The final and most posterior electrode (TH28) was located in the dorsal border of the LH just medial to the internal capsule.

Drug Tests

The classification of seizures observed during brotizolam and 'no drug' conditions are summarized in Table 1. For three of the four subjects, the number and severity of seizures were substantially decreased following drug administration. In one case, TH29, the use of brotizolam completely eliminated overt

Figure 7. This figure shows the location of the electrode tips for the four subjects in Experiment 1. The sections are tracings of the Paxinos and Watson (1986) atlas and depict the plates that best represent the electrode tip placements. To the right of each drawing is the anteroposterior coordinate below which the subject is identified.

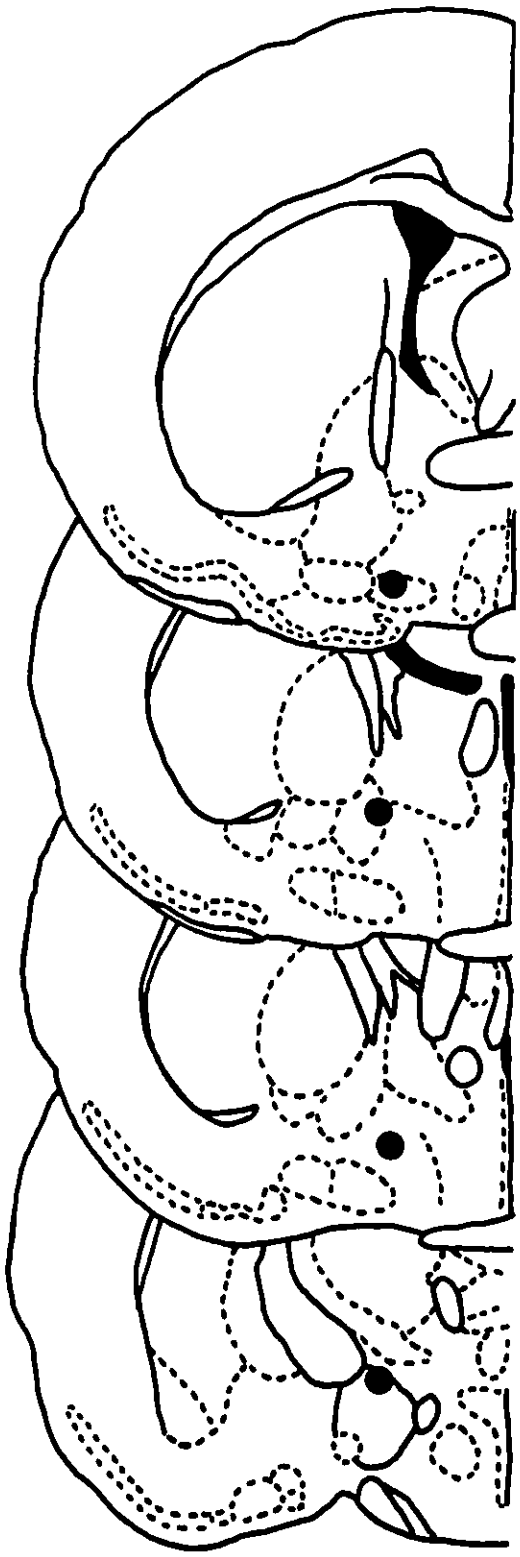
TH27
-0.40
TH29
-0.80
TH22
-0.92
TH28
-1.80

Table 1

Classification of Seizures Observed in Self-stimulation Tests

ID	Condition	Seizure Class					
		1	2	3	4	5	Total
TH27	No Drug	6	1	-	-	5	12
	Brotizolam	-	-	-	-	2	2
TH29	No Drug	7	1	-	-	-	8
	Brotizolam	-	-	-	-	-	0
TH22	No Drug	7	2	1	-	1	11
	Brotizolam	3	-	-	-	1	4
TH28	No Drug	2	-	-	-	-	2
	Brotizolam	-	2	-	-	-	2

seizures during stimulation tests. For the remaining subject, TH28, the incidence and severity of seizures in the 'no drug' condition was minimal; under brotizolam, this subject exhibited the same number of, but slightly more severe, seizures.

The effect of brotizolam (7.5 mg/kg) on the refractory period estimates is shown in Figure 8. Each graph plots the effectiveness of T-pulse stimulation, determined by the equation described earlier (page 14), at different C-T intervals. The subject is identified in the upper left hand corner of each graph above the value of the current at which the refractory period curves were generated. The solid line corresponds to the estimate of refractoriness obtained without drug while the dashed line shows the refractory period result obtained following the administration of 7.5 mg/kg brotizolam.

Inspection of the graphs reveals that the point at which recovery from refractoriness began was between 0.4 and 0.8 msec regardless of the condition under which the curve was generated. In order to examine the later portions of the curve, the C-T intervals corresponding to two proportional cuts of the refractory period curve were determined. For each curve, the intervals at which 50% and 75% of the total effectiveness rise had been completed were found by interpolation; these data are presented in Table 2. For all of the subjects, the interval corresponding to 50% recovery ranged from 1.1 to 1.9 msec and was virtually identical between the

Figure 8. The effect of brotizolam on the refractory period estimates obtained in each subject is illustrated in this figure. The graphs plot the effectiveness of added T-pulse stimulation compared to C-pulse stimulation alone at different C-T intervals. In the upper left hand corner of each graph, the subject number and the current at which the refractory period curves were generated are identified. The solid lines correspond to the 'no drug' refractory period estimates while the dashed lines show the refractory period results following the administration of 7.5 mg/kg brotizolam. The graphs are ordered according to their corresponding electrode placement with the most anterior electrode placement located in the upper left corner and the most posterior placement found in the lower right corner.

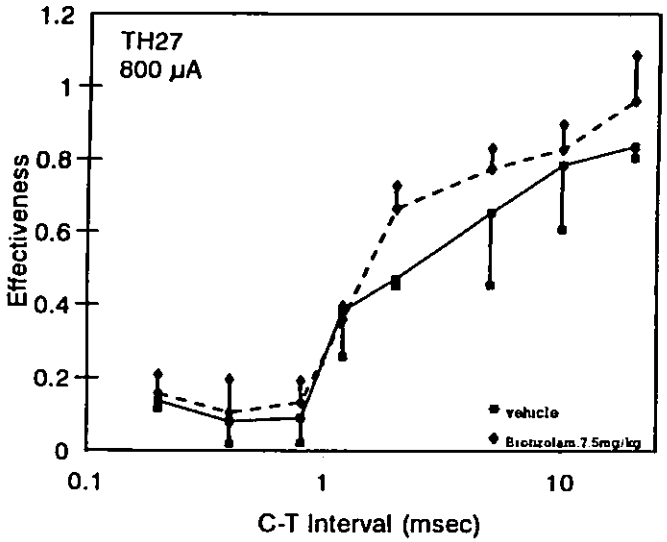
TH27
800 µA
Effectiveness
C-T Interval (msec)
vehicle
Brotizolam:7.5mg/kg

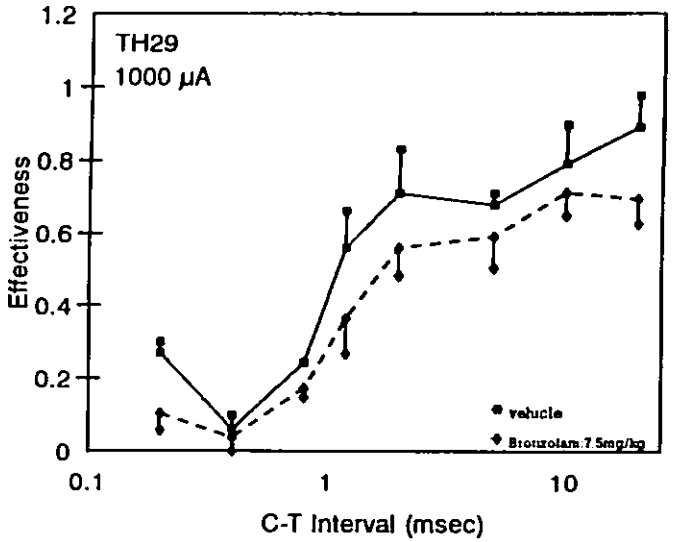
TH29
1000 µA
Effectiveness
C-T Interval (msec)
vehicle
Brotizolam:7.5mg/kg

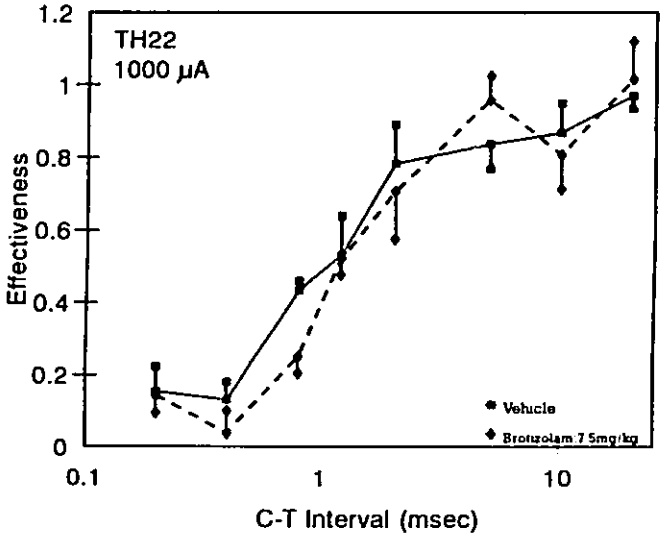
TH22
1000 µA
Effectiveness
C-T Interval (msec)
Vehicle
Brotizolam:7.5mg/kg

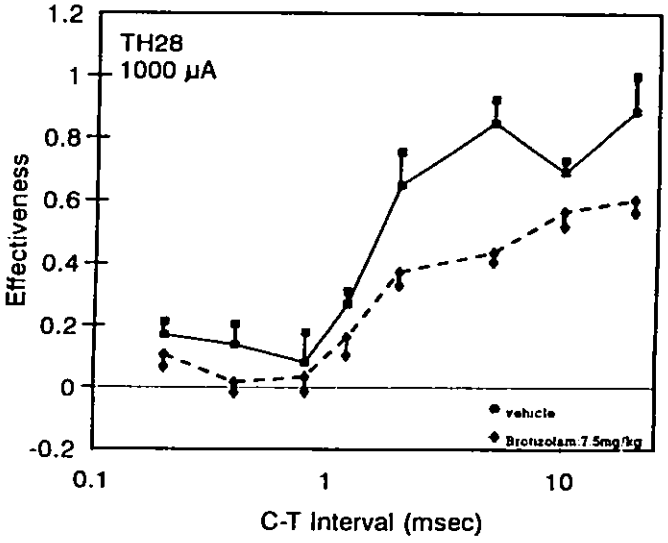
TH28
1000 µA
Effectiveness
C-T Interval (msec)
vehicle
Brotizolam:7.5mg/kg

Table 2

C-T intervals Corresponding to 50% and 75% Recovery from Refractoriness

ID	Condition	C-T Interval (msec)	
		50%	75%
TH27	No Drug	1.9	4.9
	Brotizolam	1.7	4.2
TH29	No Drug	1.1	1.9
	Brotizolam	1.2	1.9
TH22	No Drug	1.3	1.9
	Brotizolam	1.2	2.8
TH28	No Drug	1.7	2.5
	Brotizolam	1.8	5.8

brotizolam and 'no drug' conditions with no difference greater than 0.2 msec. Comparisons of the 75% recovery intervals yielded a range of estimates from 1.9 to 4.9 msec; for three of the four subjects, the difference between the two testing conditions increased but never exceeded 0.9 msec. In the final case, TH28, the difference between the brotizolam and 'no drug' conditions was 3.3 msec, with the 'no drug' curve showing 75% recovery at 2.5 msec and the brotizolam curve exhibiting a slower time course with 75% recovery at 5.8 msec.

The refractory period estimates for the four subjects can be divided into two groups based on the time course of post-stimulation excitability. The three points which have been examined, that is, the beginning of recovery, and the 50% and 75% estimates of recovery from refractoriness, are similar for TH29 and TH22, and for TH27 and TH28. The first pair exhibited shorter C-T interval estimates for the three recovery points than observed in the second pair (see Figure 8 and Table 1).

The statistical analysis consisted of a separate two-way ANOVA for each subject with drug condition and C-T interval as the principal factors (see Table 3). No significant interaction terms were obtained but main effects were observed throughout. As expected, the C-T interval factor was significant ($p<.01$) for all four subjects which is consistent with a refractory period profile. A significant main effect of drug was observed for TH29 and TH28; higher effectiveness values were always obtained in the 'no drug' condition.

TABLE 3

ANOVA Source Tables for Experiment 1

ID	Source of Variation	SS	df	MS	F	p
TH27	C-T interval	6.909	7	0.987	27.331	<.001
	Drug	0.083	1	0.083	2.306	.135
	C-T interval X Drug	0.081	7	0.012	0.319	.942
TH29	C-T interval	3.882	7	0.555	30.886	<.001
	Drug	0.202	1	0.202	11.230	.002
	C-T interval X Drug	0.050	7	0.007	0.401	.896
TH22	C-T interval	6.115	7	0.874	39.986	<.001
	Drug	0.015	1	0.015	0.706	.406
	C-T interval X Drug	0.102	7	0.015	0.669	.697
TH28	C-T interval	4.486	7	0.641	39.103	<.001
	Drug	0.517	1	0.517	31.523	<.001
	C-T interval X Drug	0.234	7	0.033	2.042	.069

Discussion

There are several conclusions that can be drawn from this study. First, brotizolam is clearly effective, for significant periods of time, in controlling the overt seizures that accompany LPO self-stimulation. Second, this drug does not appear to alter the refractory period of the directly stimulated neurons suggesting that the membrane properties of the behaviourally relevant substrate are not compromised by brotizolam.

Control of Seizures

In three of the four subjects, all with electrode placements in or around the LPO, brotizolam proved to be an effective agent in the control of stimulation-induced seizures without altering the time course of the excitability cycle of the directly stimulated neurons. Both the incidence and severity of the seizures exhibited by TH27, TH29, and TH22 were substantially decreased by brotizolam; in the cases of TH27 and TH29, all of the Type 1 (wet dog shakes) and Type 2 (mouth and head movements) seizures were eliminated. The incidence of the most severe class of seizure, type 5 (rearing and falling), was unchanged in TH22, one seizure in each of the drug and 'no drug' conditions, but was controlled in TH27, with a reduction from five to two seizures. From this pattern of results, brotizolam appears to be efficacious, to some extent, in controlling all types of seizures with maximum effectiveness

observed with the less severe classes of seizure (Types 1 to 3) and partial effectiveness with the most severe seizure type.

Refractory Period Estimates

The administration of brotizolam had little or no effect on the refractory period estimates for TH27, TH29, and TH22, as evident by visual inspection of Figure 8 and substantiated by the statistical analysis. The lack of a significant interaction between C-T interval and drug/'no drug' condition was encouraging suggesting that the two curves were parallel and that any effects of brotizolam were not distinguishing the time course of recovery. A significant main effect of C-T interval was expected and is entirely consistent with the profile of refractoriness generally observed, with lower effectiveness values at short C-T intervals and higher ones at longer C-T intervals. The one anomaly to this pattern was the significant main effect of drug for TH29 arising from the consistently lower effectiveness values in the brotizolam condition; a maximum difference of 0.20 was observed between the two conditions. However, as will be discussed, the apparent suppression of effectiveness by brotizolam did not appreciably alter the time course of the post-stimulation excitability cycle for this subject.

The intervals at which recovery was first observed for each subject were identical in the brotizolam and 'no drug' conditions. Similarly, the interpolated intervals at which 50%

of recovery from refractoriness had occurred differed by no more than 0.2 msec. As recovery continued, small differences in the C-T interval estimates for 75% recovery were observed; the largest difference was 0.9 msec. This discrepancy between the brotizolam and 'no drug' refractory period estimates at the 75% recovery point could be accounted for by an artifact of the testing procedure and not to a true effect of the drug; there were substantially larger increments in the tested C-T intervals after 2.0 msec resulting in less precise scaling. Since the 75% recovery intervals occurred around or after the 2.0 msec C-T interval, the larger gap between test points may have resulted in lower resolution of the interpolated values. In addition, the only subject found to have a significant drug effect, TH29, had the best concordance between the brotizolam and 'no drug' intervals at which 50% and 75% of the recovery from refractoriness had occurred (see Table 2). Thus, the results from these three subjects strongly suggest that brotizolam did not substantively alter the time course of recovery from refractoriness in the substrate.

The fourth subject, TH28, was the one case which differed from the above descriptions. The inclusion of this subject was intended to provide a different perspective from which to evaluate brotizolam's effect on neural refractory periods since the electrode was located in the LH rather than the LPO and the incidence of seizures in the 'no drug' condition was minimal. This subject was the only one to show a worsening in the

severity, but not the number, of overt seizures; following brotizolam administration, two type 2 seizures were observed as opposed to two type 1 seizures in the 'no drug' condition.

Portions of the refractory period curve for TH28 appeared to be differentially affected by brotizolam although the ANOVA interaction term was not significant. The earlier parts of the curve, including the intervals at which recovery began and the 50% mark, were unchanged in drug tests. However, much lower effectiveness values, with a maximum difference of 0.41, and substantially delayed recovery, 5.8 msec instead of 2.5 msec, at the point at which 75% recovery from refractoriness had occurred, were observed in the later portions of the curve following brotizolam.

It has been estimated that 70% - 80% of recovery from refractoriness is complete by 1.2 msec for reward neurons in the MFB; beyond this interval, it is unclear what factors, including synaptic events, may account for the remaining contribution to T-pulse effectiveness (Gallistel, Shizgal, and Yeomans, 1981). Thus, the effect of brotizolam at the longer C-T intervals for TH28 may be due, in part, to its action on neural events unrelated to refractoriness. These effects may not have been observed in the other three subjects since the refractory periods of the LPO neurons are known to be longer, between 0.4 msec to 5.0 msec, than those for the LH and VTA (Fouriezos et al, 1987); thus, the post-absolute refractory period events that brotizolam may be influencing would not be

distinguishable from refractory period contributions.

In summary, it appears that brotizolam can control stimulation-induced seizures and that, in animals experiencing seizures, the membrane properties of the directly stimulated neurons, as measured by the post-stimulation excitability cycle, on the whole, are not compromised. Thus, brotizolam may be a useful tool to facilitate the, previously onerous, investigation of seizure-prone self-stimulation sites.

Experiment 2

The LPO, situated rostral to the LH, is linked to the latter by a short transition zone and is considered an important candidate for the cell bodies of origin of the descending pathway that links a subset of the LH and VTA reward neurons (Bielajew et al, 1987; Janas and Stellar, 1987; Murray and Shizgal, 1991; Waraczynski, 1988). In view of the strong arguments to support this hypothesis (Shizgal, 1989), it is surprising that the LPO has not been systematically mapped for self-stimulation.

The purpose of this mapping study was to obtain information about the distribution and spatial organization of reward sites in the region of the LPO. To begin with, the location of self-stimulation sites within and around the LPO was determined. At sites that reliably supported this behaviour, the trade-off relationship between current and period was established in order to characterize the neural density and boundaries of the behaviourally relevant bundle.

Estimates of the relative neural density of elements within the effective stimulation field, at individual sites, can be interpreted from period thresholds if the following assumptions are met (Miliaressis, Rompre, and Durivage, 1982). These are that the system responds only to the total number of pulses delivered irrespective of temporal or spatial characteristics,

that current spread is isotropic, and that different neural populations are uniformly distributed throughout the effective stimulation field (Gallistel et al, 1981).

This model, called the counter model of integration, assumes that the production of a constant behavioural output is a function of the total number of firings that arrive at the downstream synapse; the critical number of firings is the product of the number of activated fibers in the stimulation field (their density) and the number of pulses in the stimulation train (Gallistel, 1978). Maintenance of a constant behavioural output predicts a linear association between neural density and pulse period, assuming that all other stimulation parameters remain unchanged (Miliaressis et al, 1982; Yeomans, Pearce, Wen, and Hawkins, 1984). Thus, when two individual sites are compared, an increase or decrease in period threshold at one site suggests a similar change in neural density.

Additionally, a second property of the substrate, its boundaries, can be estimated from the current/period trade-off relationship. Variations in current level are assumed to proportionally alter the field of excitation; its expansion or contraction should alter the number of fibers within the stimulation field. When this parameter is systematically varied with period, it has been observed that a linear relationship results over a mid-range of currents (Gallistel et al, 1981; Yeomans et al, 1984). The slope of the line

describing the current/period trade-off has been shown to reflect two properties of the directly stimulated neurons - the spatial arrangement and the relative excitability (Schindler, 1983, p. 27; Yeomans, 1990). Under the assumption that neurons having different activation thresholds are randomly distributed throughout the effective stimulation field, the slopes of the trade-off functions are believed to reflect changes in neural density (Miliaressis et al, 1982; Yeomans, 1990).

It is important to reiterate that the absolute number of fibers can not be determined; rather, in comparisons between different stimulation sites, the relative densities at each site can be estimated from the slopes of the trade-off functions. Similarly, when period thresholds at different currents for one site are compared, the spatial limits of the substrate can be inferred since the linear relationship between current and period should fail at currents which exceed the boundaries of the substrate; thus, when the stimulation field is located near the border of the behaviourally relevant fibers, the linearity of the relationship should be compromised at lower currents than at a stimulation site which is located in the center of the fiber bundle (Gallistel et al, 1981; Miliaressis et al, 1982; Yeomans et al, 1984).

Method

Subjects and surgery

Twenty-two rats served as subjects in this experiment.

Moveable electrodes (Kinetrode Inc.) were employed in all but one subject (TH22) which received a fixed electrode. The electrodes were aimed at the LPO; the flat-skull coordinates (Paxinos and Watson, 1986) ranged from 0.2 to 0.92 mm posterior to bregma, 0.6 to 2.0 mm lateral to the mid-sagittal suture, and 7.6 to 8.2 mm ventral to the skull surface reading at bregma. Fixed electrodes were also implanted in the VTA using the coordinates 4.8 mm posterior to bregma, 0.9 to 1.2 mm lateral to the mid-sagittal suture, and 8.0 to 8.4 mm ventral to the skull surface reading at bregma. Those subjects exhibiting reliable and stable bar-pressing for VTA stimulation became part of the subsequent collision experiment.

Screening and training

If a subject did not exhibit self-stimulation after two screening sessions, the electrode was moved a ventral distance of 0.08 to 0.24 mm. For this procedure the rat was anesthetized with a short-acting inhalant, halothane, while the electrode was moved using a calibrated driver. The following day, self-stimulation at the new site was evaluated. This procedure continued until either bar-pressing was established or the full ventral travel of the electrode was used, based on the estimated location of the electrode tip from the Paxinos and Watson (1986) atlas.

The training phase of the study was conducted using a mid-range current value, for example 200 uA. The testing phase,

during which complete trade-off functions were generated, was initiated when stable thresholds were obtained.

Testing

During this phase, the trade-off relationship between the period threshold and current were generated. Each period threshold was determined from a rate/period function. The number of replications of the rate/period curve was determined by the previously described stability criteria (see page 42); as a general rule, fewer replications were required in an experienced subject.

Once the trade-off function was generated at a stimulation site and it was determined that the VTA electrode supported self-stimulation, the procedures described in experiment three were followed. When this phase was completed, the electrode was moved and the site tested anew using the procedure just described.

Results

Histology

The locations of the electrode tips, for both positive and negative self-stimulation sites, are shown in Figure 9a-p. The placements can be categorized into 5 groups: the first was located anterior to the LPO, the second, third, and fourth groups were found within the anteroposterior levels that contain the LPO, and the fifth group was situated posterior to the LPO, in the transition zone between the LPO and the LH.

Figure 9a-p. Results of the mapping study for all subjects in experiment 2. Electrode placements are shown on tracings of plates from the Paxinos and Watson (1986) atlas. Each subject is identified by the alphanumeric designation generally on the left hand side of each sub-figure, below which the anteroposterior coordinate is indicated. The sub-figures are organized with the most anterior placements first. Subjects with the same anteroposterior coordinate are ordered to progress from the most medial to the most lateral stimulation site. The unfilled circles correspond to sites where no self-stimulation was observed; the filled circles represent electrode locations where self-stimulation was found. The vertically oriented symbols, for any subject, represent the electrode. In general, these sites are separated by 0.24 mm except for (p) in which the first three sites were separated by 0.16 mm and the rest by 0.24 mm. On the right of each figure, where applicable, are the trade-off functions generated at each stimulation site; the electrode tip location associated with each function is indicated by a straight line. The data are plotted on a log-log scale with period threshold (msec) against current value (μA). The error bars represent the standard error of the mean. The absence of a trade-off function in positive self-stimulation sites indicates that either the response rate or stability criteria defined in the text were not met.

Ⓐ

+ 0.20

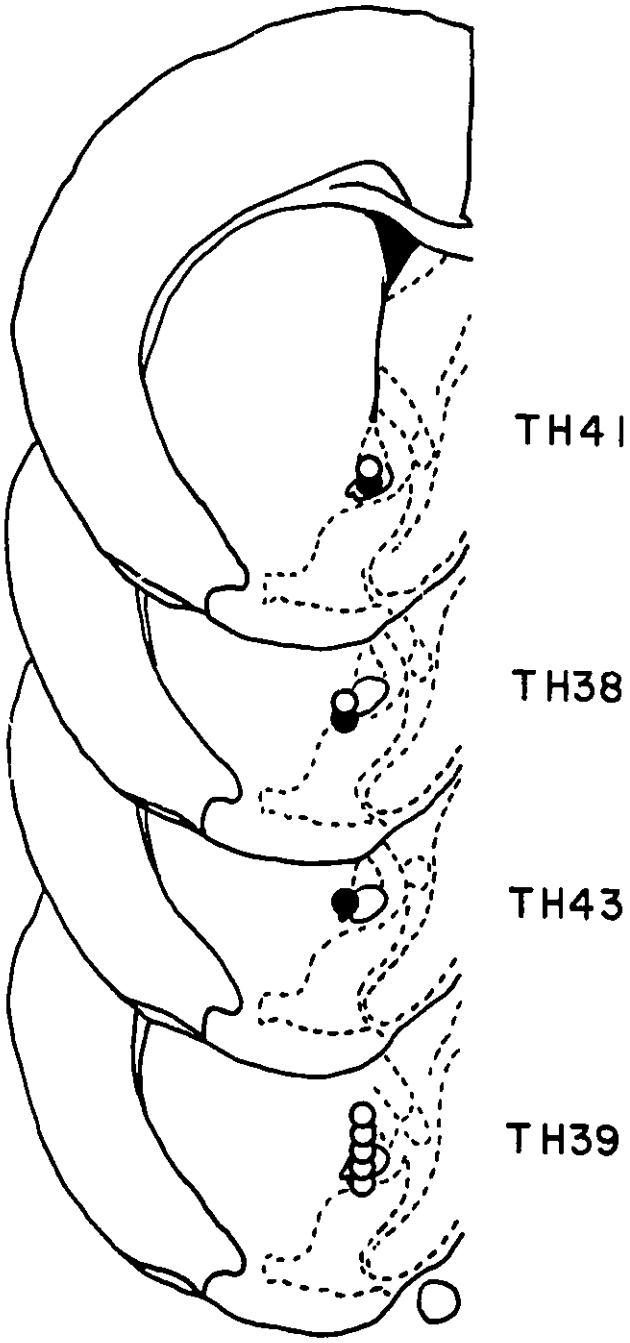

Ⓑ

TH34
-0.40

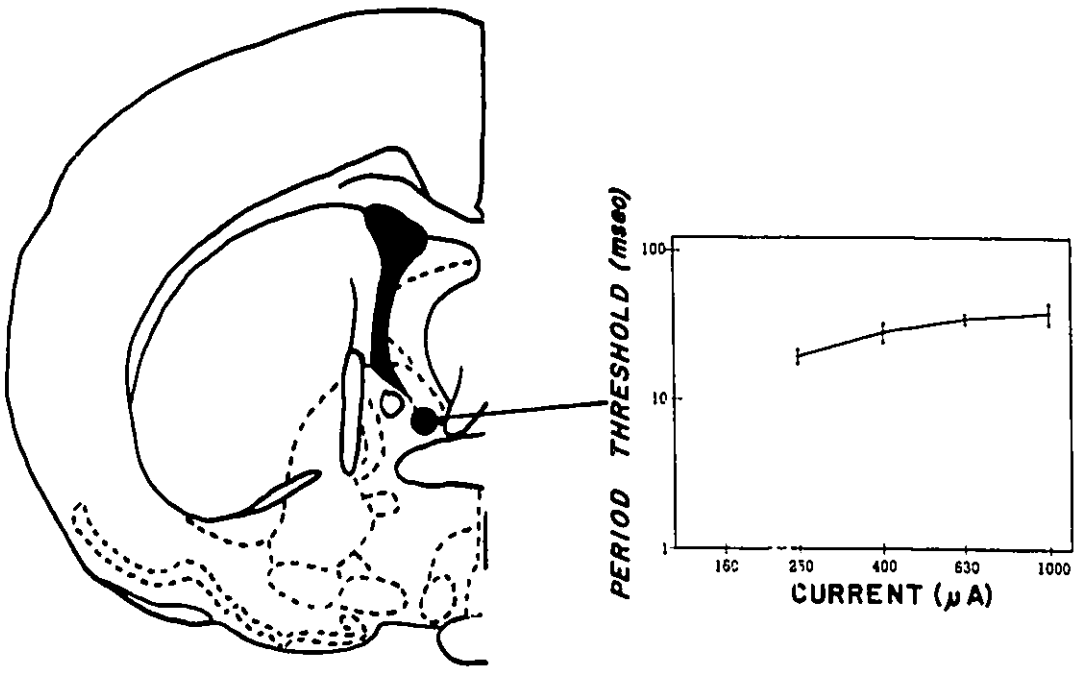
PERIOD THRESHOLD (msec)
100
10
1
160
250
400
630
1000
CURRENT (μA)

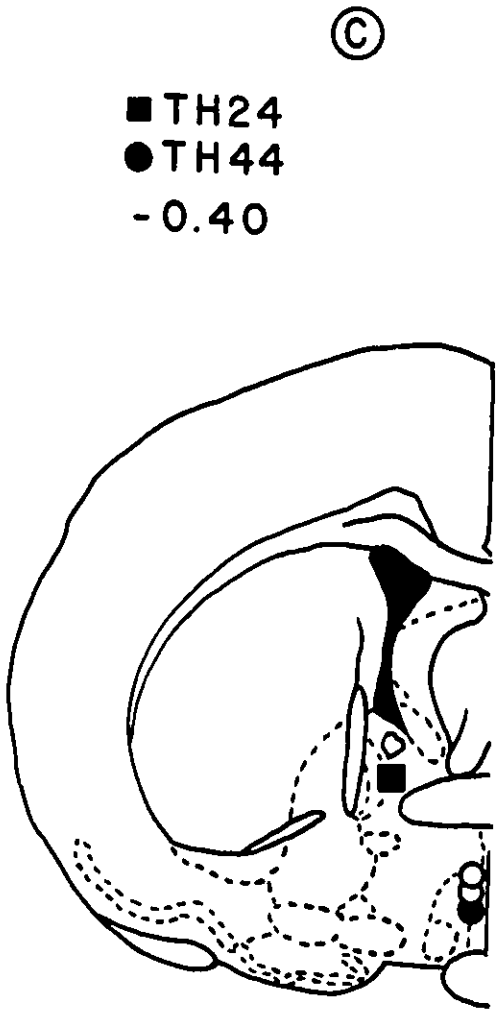
©
■ TH24
● TH44
-0.40

Ⓓ

TH33

-0.40

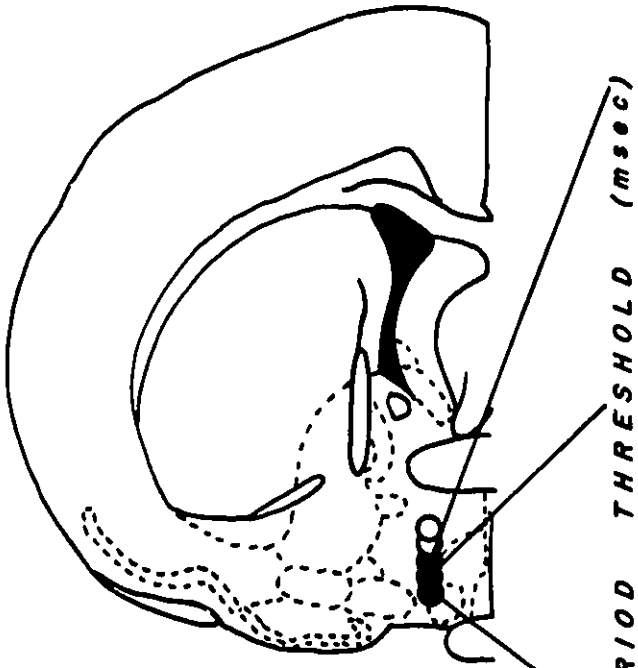

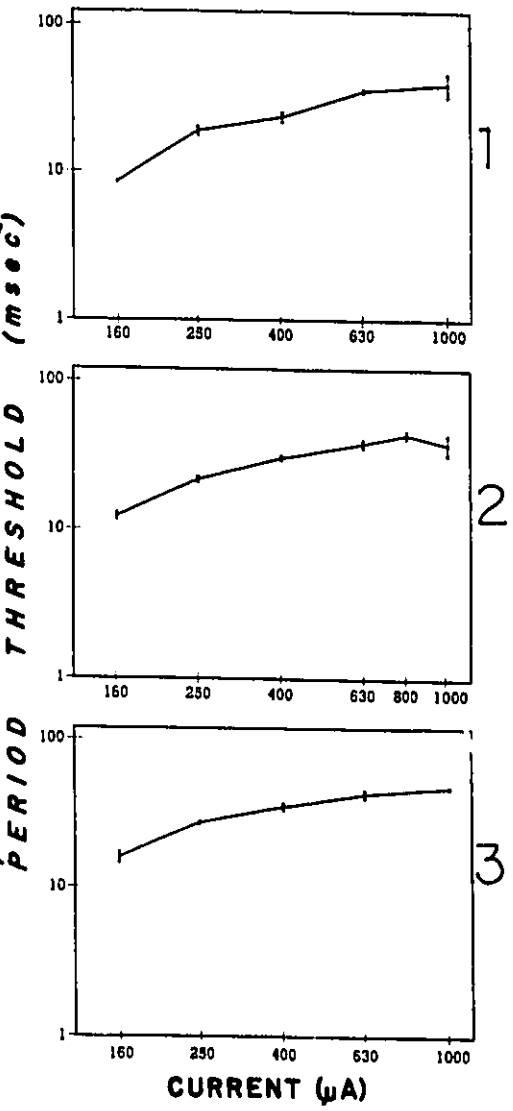
PERIOD THRESHOLD (msec)
100
10
1
160
250
400
630
800
1000
1
2
3
CURRENT (μA)

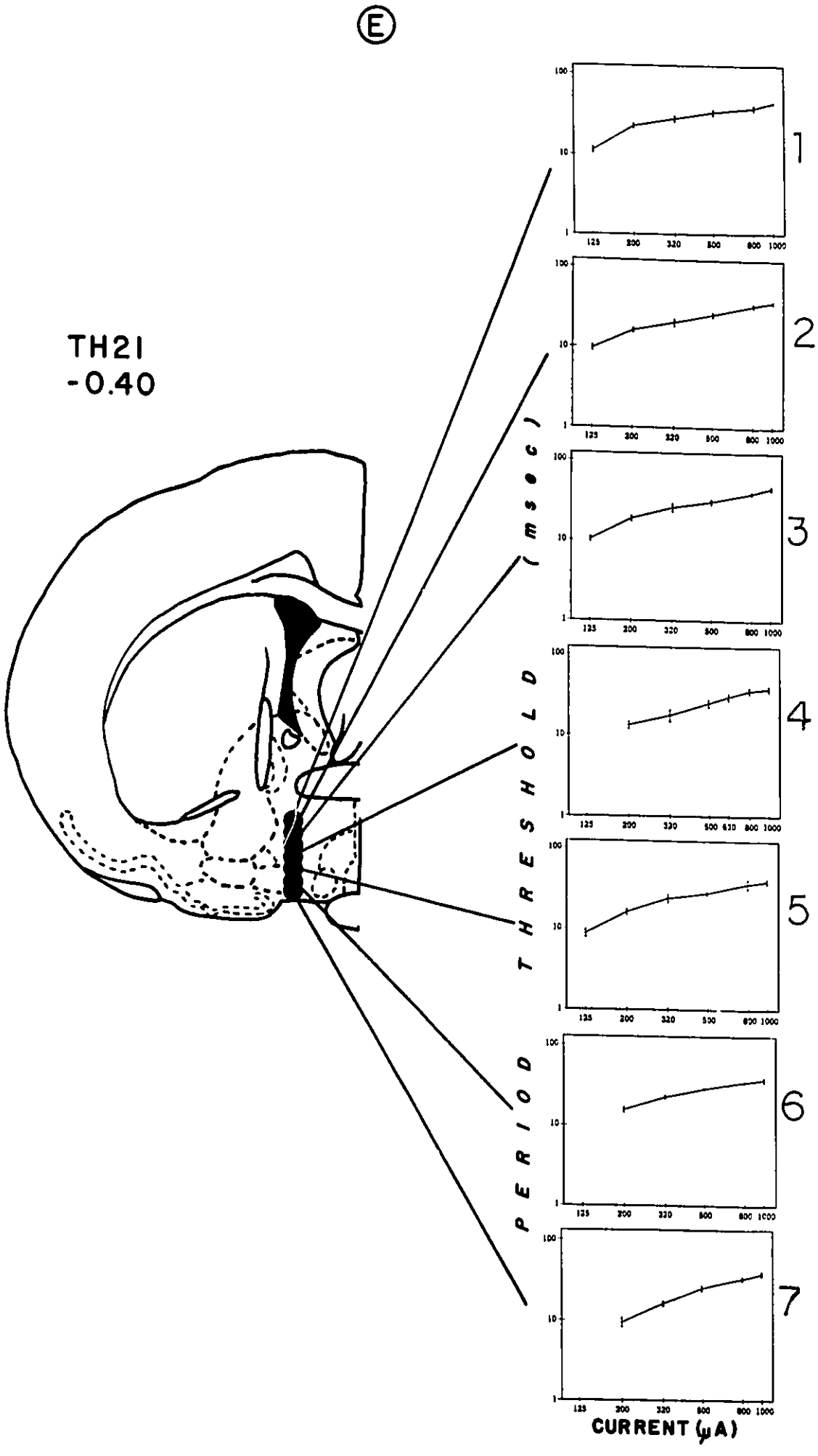
E
TH21
-0.40
PERIOD THRESHOLD (msec)
1
2
3
4
5
6
7
CURRENT (μA)

Ⓕ

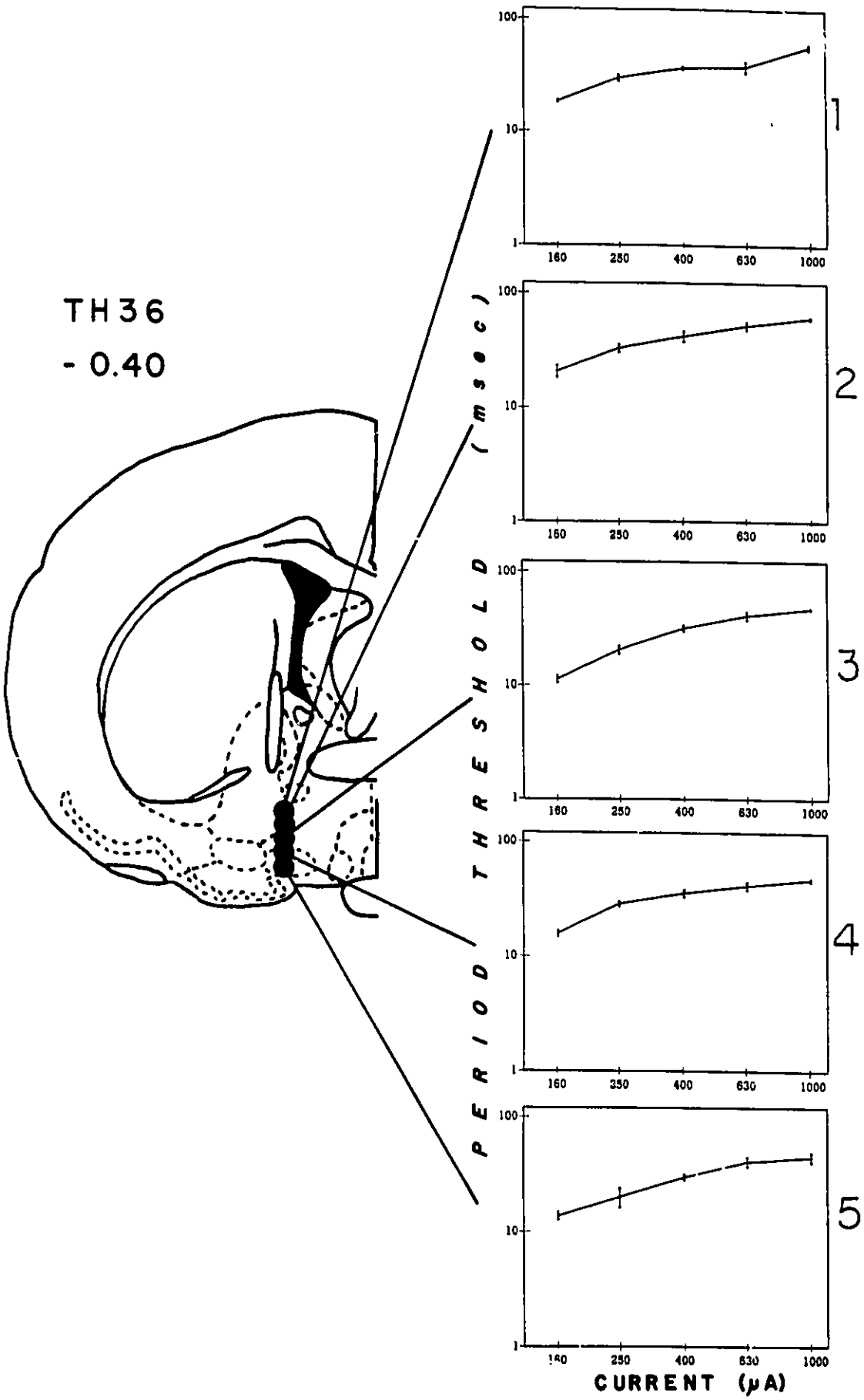
TH36
- 0.40
PERIOD THRESHOLD (msec)
100
10
1
160
250
400
630
1000
1
2
3
4
5
CURRENT (μA)

Ⓖ

TH27
- 0.40

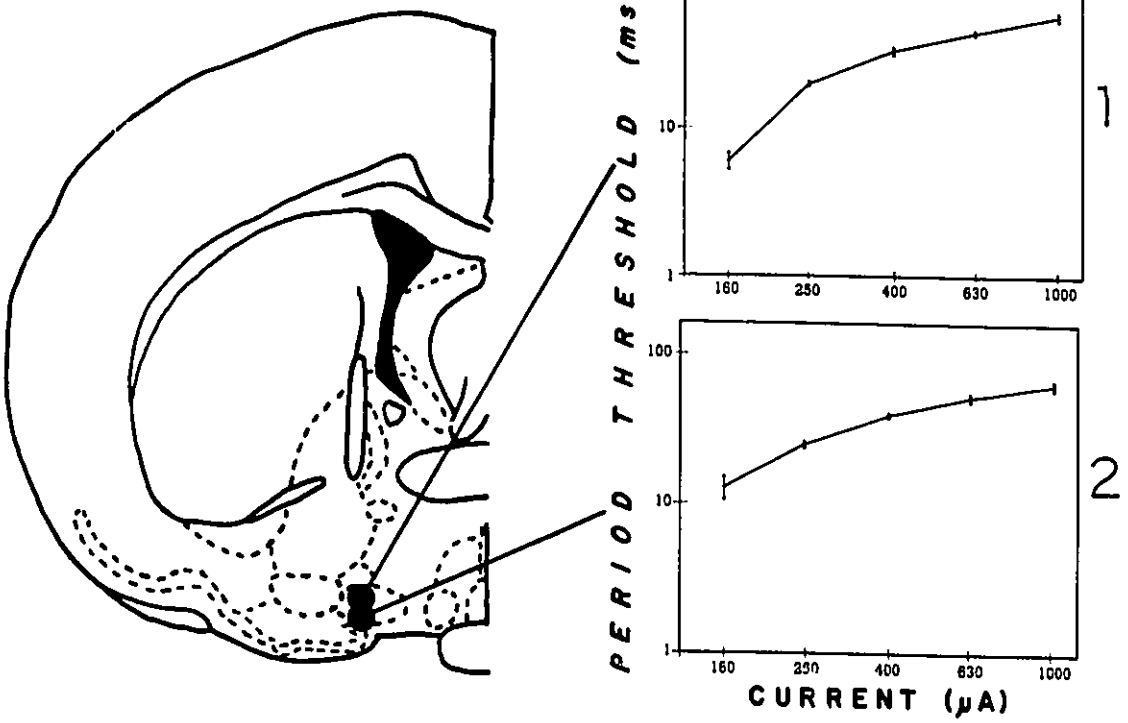
PERIOD THRESHOLD (msec)
100
10
1
160
250
400
630
1000
1
2
CURRENT (μA)

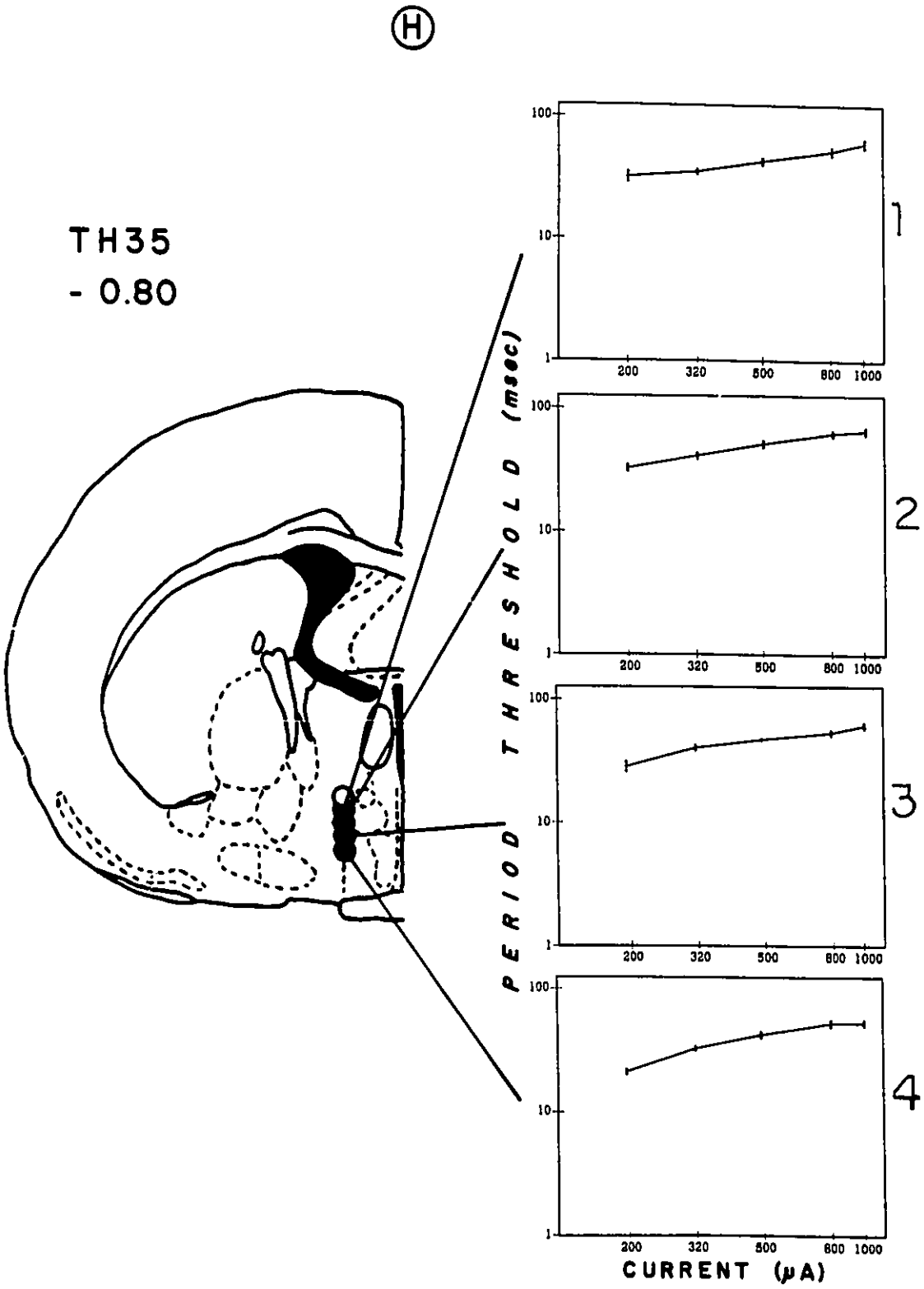
H
TH35
- 0.80
100
10
1
200
320
500
800
1000
PERIOD THRESHOLD (msec)
CURRENT (μA)
1
2
3
4

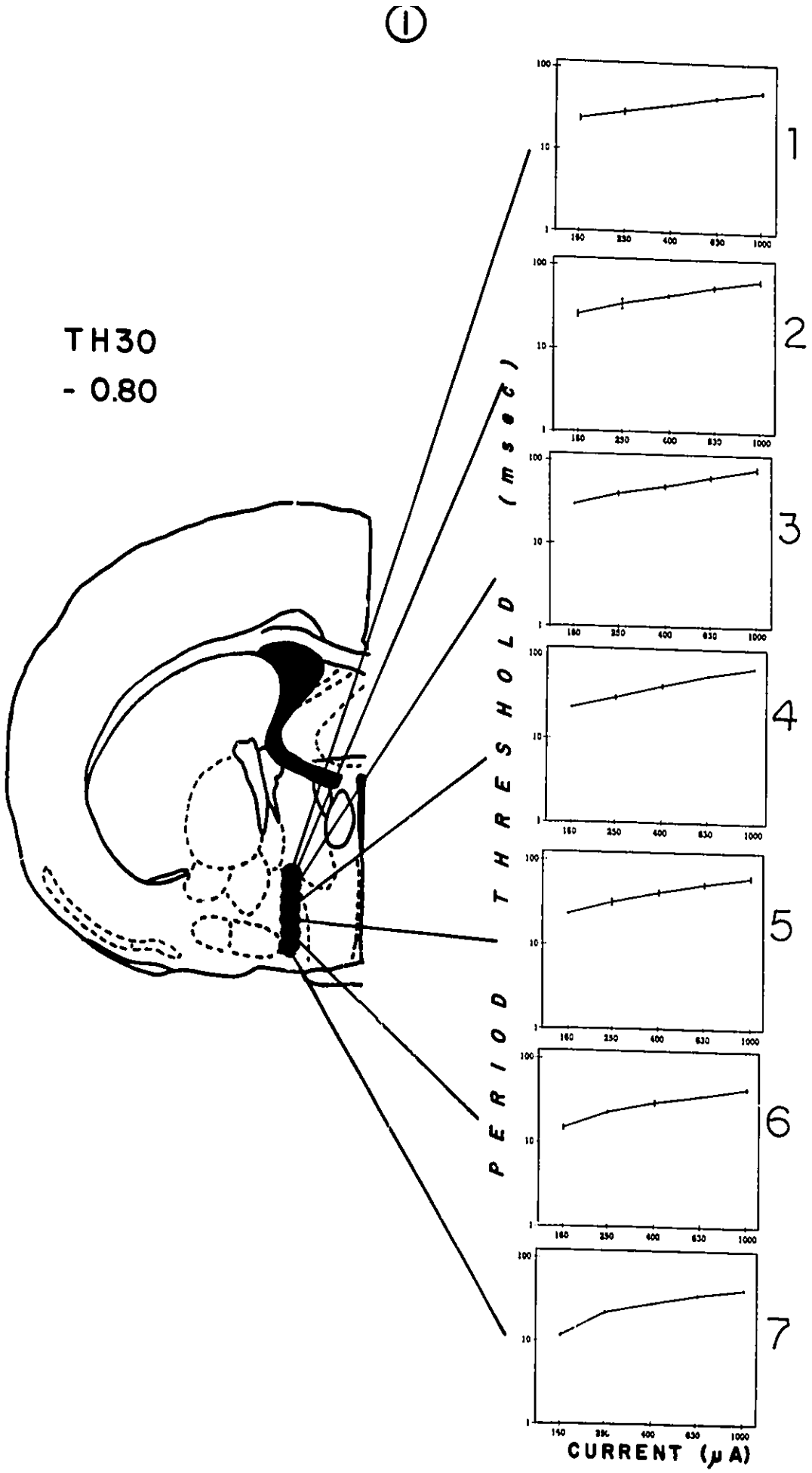
①
TH30
- 0.80
PERIOD THRESHOLD (msec)
100
10
1
150
250
400
630
1000
1
2
3
4
5
6
7
CURRENT (μA)

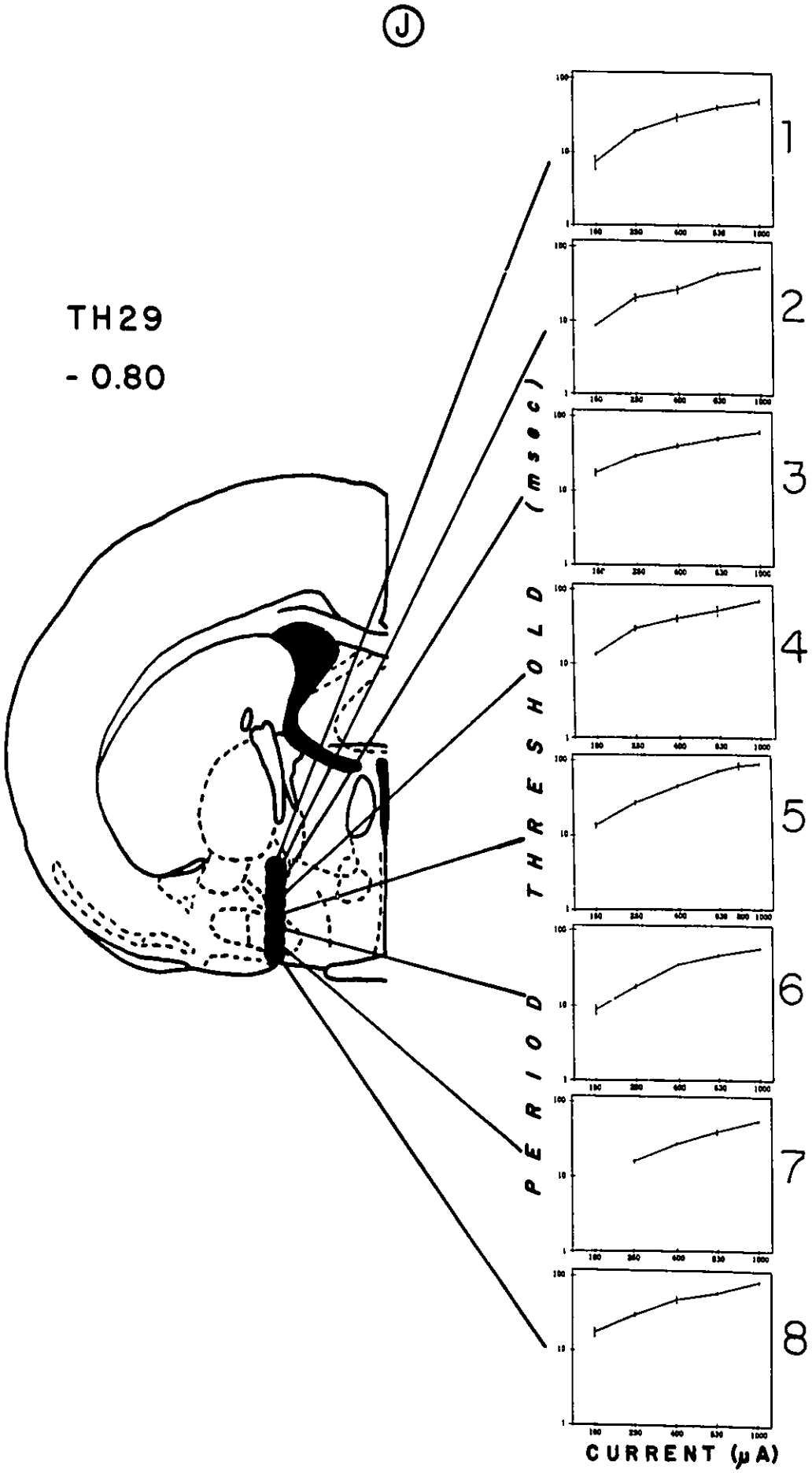
J
TH29
- 0.80
PERIOD THRESHOLD (msec)
1
2
3
4
5
6
7
8
CURRENT (μA)

Ⓚ

⬡ TH42

○ TH37

-0.92

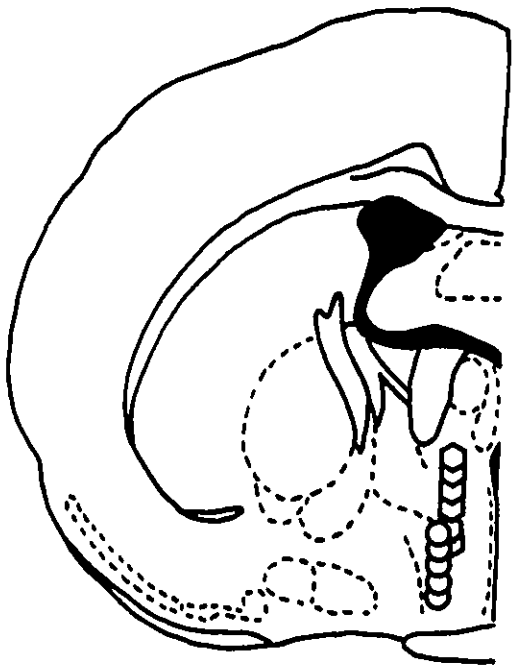

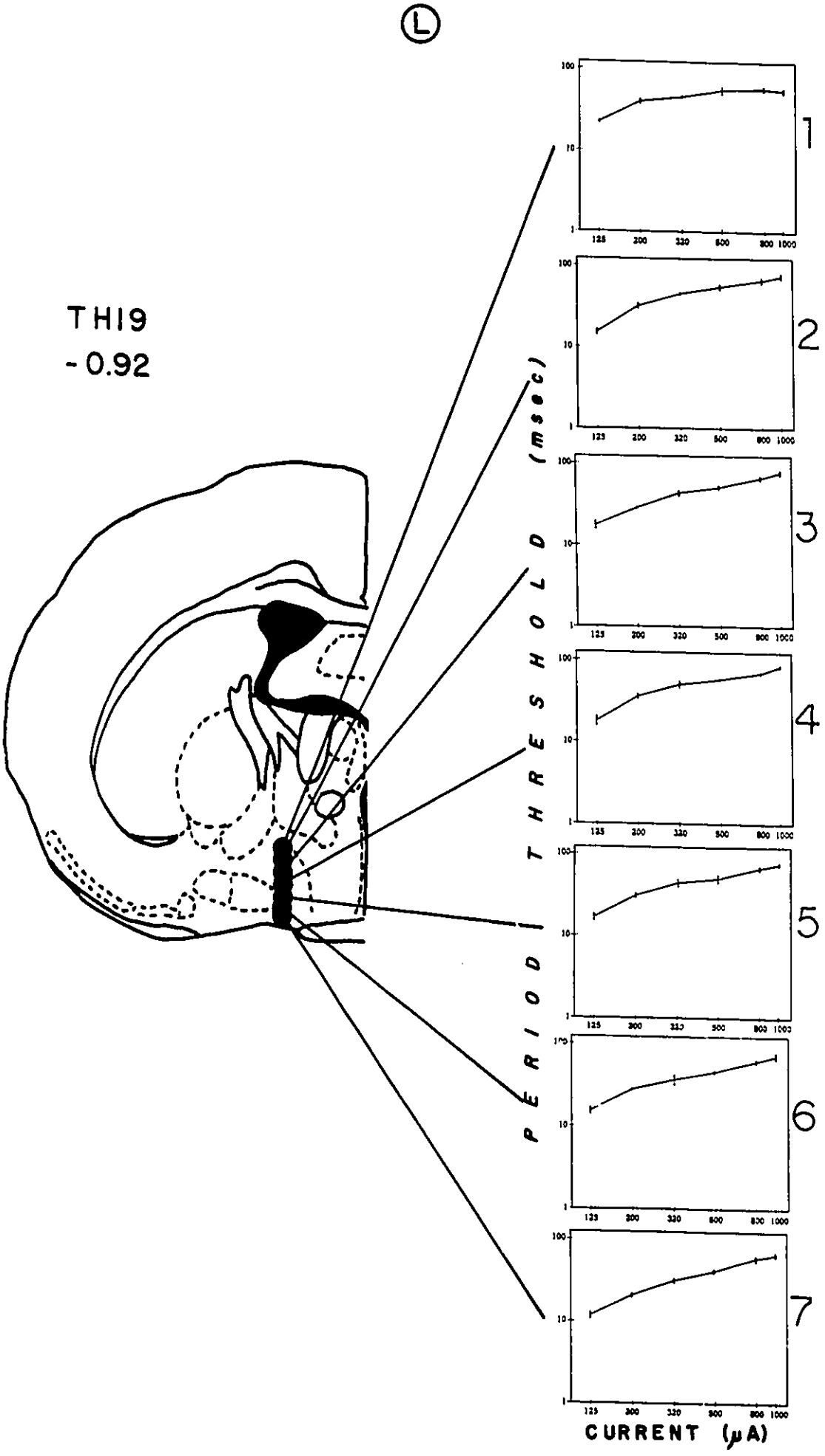
L
TH19
-0.92
PERIOD THRESHOLD (msec)
100
10
1
125
200
320
500
800
1000
1
2
3
4
5
6
7
CURRENT (μA)

Ⓜ

TH22

- 0.92

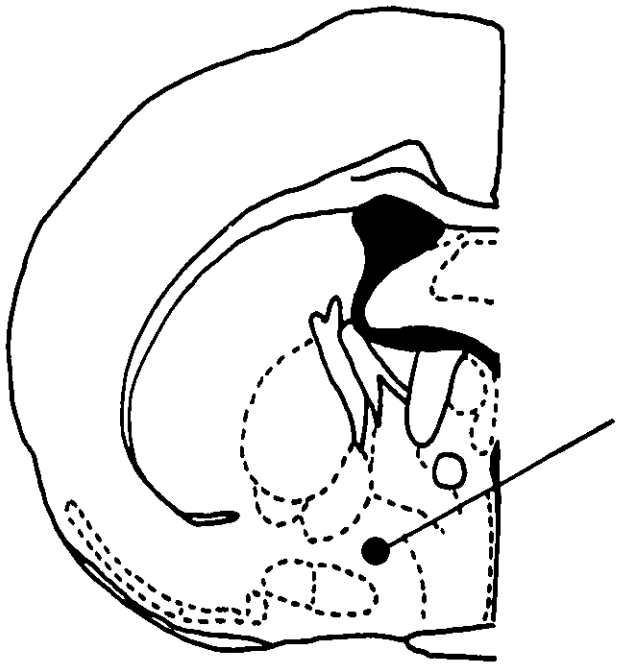

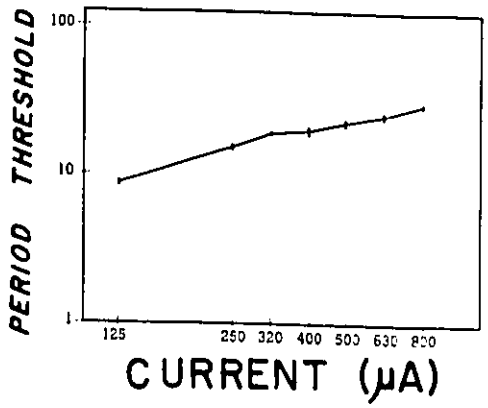
PERIOD THRESHOLD
100
10
1
125
250 320 400 500 630 800
CURRENT (μA)

Ⓝ

○ TH18

○ TH31

-1.30

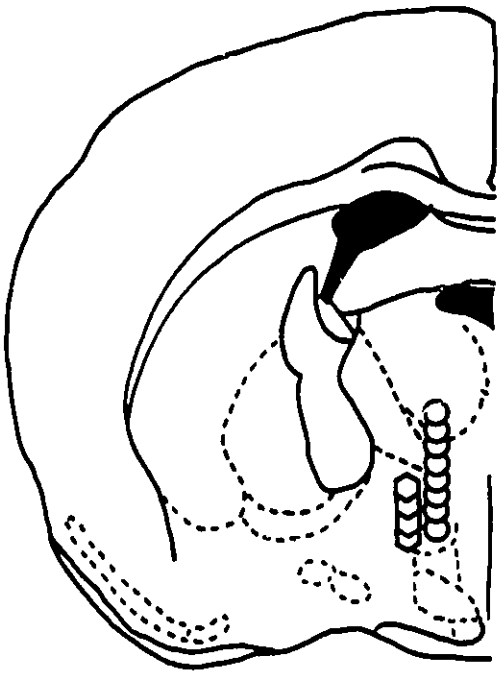

TH25

- 1.40

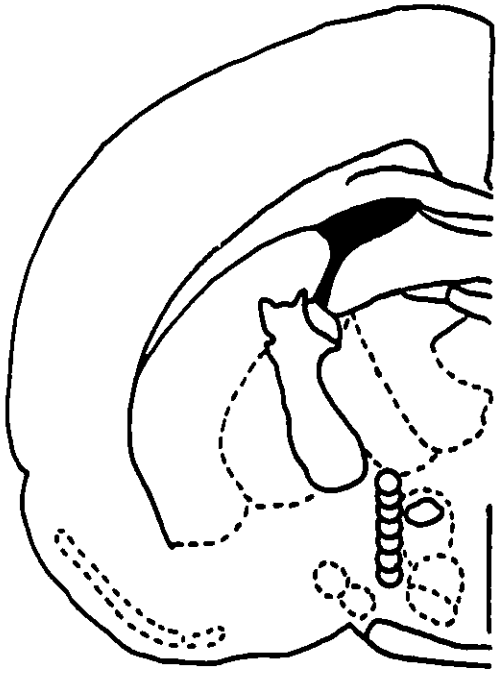

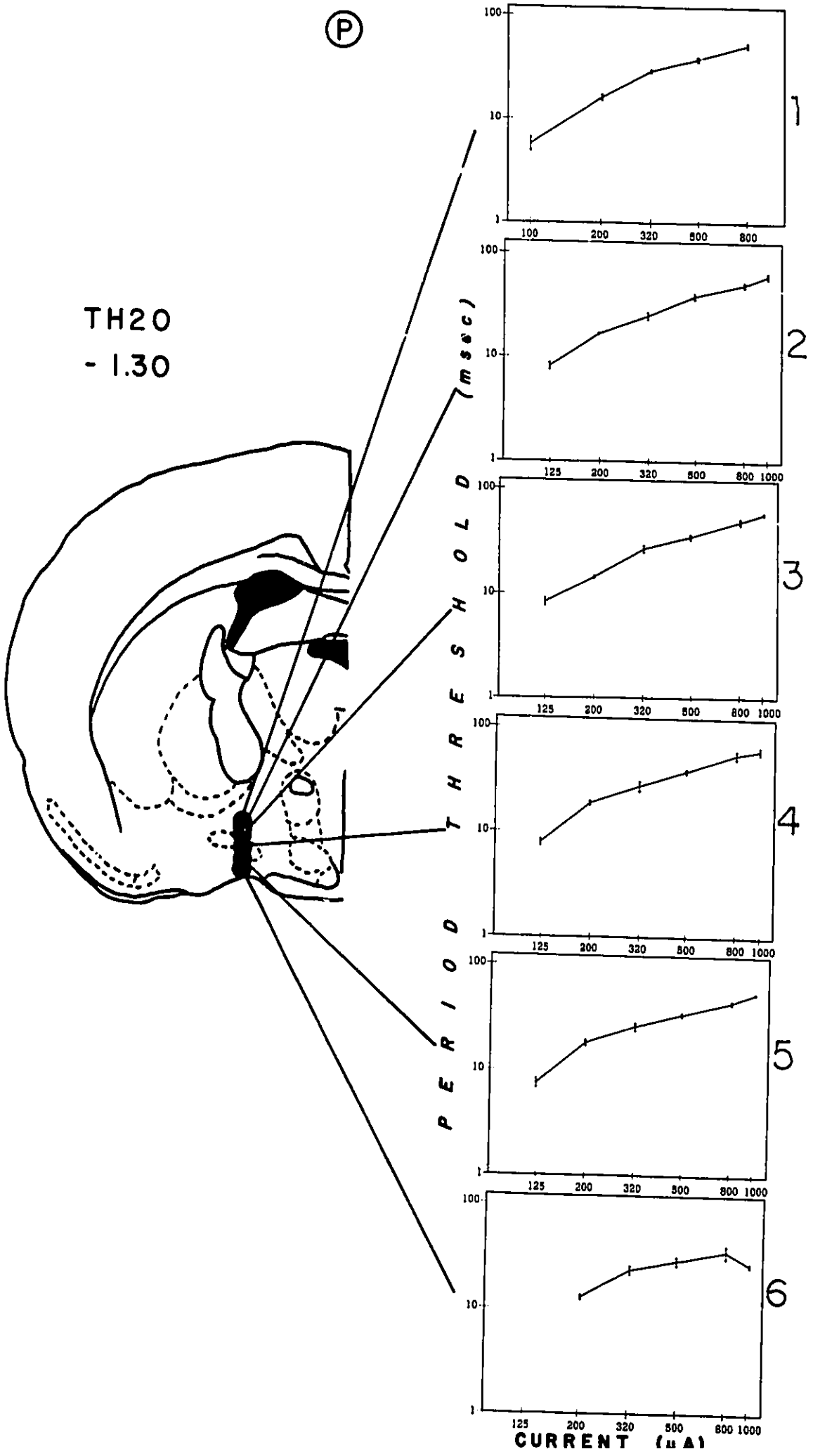
Ⓟ
TH20
- 1.30
PERIOD THRESHOLD (msec)
100
10
1
100 200 320 500 800
125 200 320 500 800 1000
1
2
3
4
5
6
CURRENT (μA)

Anterior group. The first group, which contains four subjects, was found to be just rostral to the midline convergence of the anterior commissure (see Figure 9a). This level is dominated by the caudate putamen and the nuclei of the precommissural septum which includes the horizontal and vertical limbs of the diagonal band, the medial septum, and compartments 'a' and 'b' of the MFB. The four electrodes all passed through the lateral portion of the 'anterior' anterior commissure and were located from the ventral border of the lateral division of the bed nucleus of the stria terminalis to the dorsal border of compartment 'a' of the MFB.

Anterior LPO group. The second group consists of seven subjects with electrodes located around or near the anterior part of the LPO (see Figures 9b-g). At this level, the anterior commissure and the fornix, as yet unbifurcated, are still evident. The LPO is bordered medially by the medial preoptic area, laterally by the ventral pallidum and substantia innominata, dorsally by the bed nuclei of the stria terminalis, and ventrally by the nucleus of the horizontal limb of the diagonal band. The seven electrodes were scattered throughout this level. Two placements, TH24 and TH34 (see Figures 9b-c), were located dorsal to the anterior commissure, lateral to the fornix, and medial to the internal capsule. The electrode for TH44 (see Figure 9c) was situated close to the midline, with the tip passing from the medial preoptic area to the dorsal

border of the anterior medial preoptic nucleus. The next most medial electrode tip, TH33 (see Figure 9d), was found to pass through the border between the LPO and the medial preoptic area from a point level to the dorsal border of the medial preoptic area to the mid-section of the anteroventral preoptic nucleus. The electrode tip for TH21 (see Figure 9e) was located in the lateral portion of the LPO and the medial portion of compartment 'b' of the MFB; the dorsoventral travel of the electrode extended from just ventral to the parastrial nucleus to the ventral border of the MFB. The remaining two electrodes, TH36 and TH27 (see Figures 9f-g), were found in similar locations, with the electrode tip passing through the medial portion of compartment 'a' of the MFB. In the case of TH36 (see Figure 9f), the electrode tip moved from the ventral border of the bed nucleus of the stria terminalis and the medial portion of the ventral pallidum to the ventral border of compartment 'a' of the MFB. The two sites for TH27 (see Figure 9g) were contained entirely within compartment 'a' of the MFB.

Middle LPO group. Three subjects comprise the third grouping of electrode sites (see Figures 9h-j). This level is characterized by a large, well-defined third ventricle, the movement of the medial preoptic area from the midline to a more lateral position, and a more dispersed optic chiasm. The LPO is bordered by the same structures as at the previous rostral level. The most medial electrode placement, TH35 (see Figure

9h), was located at the border of the LPO and medial preoptic area; the dorsoventral movement of the tip began just lateral to the anterior commissural nucleus and ended at the same level as the dorsal border of the MFB. A slightly more lateral placement for subject TH30 was found (see Figure 9i), with the majority of the stimulation sites contained within the LPO; the tip passed from the ventral border of the medial division of the bed nucleus of the stria terminalis to the supraoptic nucleus. The third electrode, TH29 (see Figure 9j), was situated lateral to the LPO, within the substantia innominata and compartment 'b' of the MFB; the electrode tip moved from the ventral border of the globus pallidus and bed nucleus of the stria terminalis to the olfactory tubercle.

Posterior LPO group. The fourth set of subjects had placements at the level where the lateral ventricles collect at the midline (see Figures 9k-m). The LPO is bordered medially by the medial preoptic area, dorsally by the bed nucleus of the stria terminalis, laterally by the horizontal limb of the diagonal band, and ventrally by the supraoptic nucleus at the base of the brain. The two most medial electrode placements, TH37 and TH42 (see Figure 9k), were located in the bed nucleus of the stria terminalis (TH42) and the medial preoptic area (TH37 and TH42). The dorsoventral movement of the electrode tip for TH37 began at the ventral border of the bed nucleus of the stria terminalis and ended dorsal to the suprachiasmatic

nucleus. The initial electrode placement for TH42 was located dorsal to that of TH37, beginning ventral to the thalamic stria medullaris, and terminating within the medial preoptic area, just ventral to the bed nucleus of the stria terminalis. The remaining two electrode tips, identified as TH19 and TH22 (see Figures 9l-m), were located primarily in the LPO with the placement for TH22 contained within the same sites as TH19. The electrode tip for TH19 (see Figure 9l) moved from just ventral to the bed nucleus of the stria terminalis, through the border between the LPO and compartment 'b' of the MFB, to the supraoptic nucleus; the one stimulation site for TH22 (see Figure 9m) was well within the LPO.

LH group. The fifth group was situated posterior to the LPO at the level of the anterior, lateroanterior, and lateral hypothalamic areas (see Figures 9n-p). The most medial electrode placement, TH18 (see Figure 9n), was located at the border between the medial preoptic area and the bed nucleus of the stria terminalis, passing from the ventral part of the anteromedial thalamic nucleus to the ventral section of the bed nucleus of the stria terminalis. Just lateral to this placement, the movement of the electrode tip for TH31 (see Figure 9n) began at the dorsal part of the thalamic stria medullaris and ended ventrolateral to the bed nucleus of the stria terminalis. The electrode site for TH25 (see Figure 9o) was located slightly more posterior and lateral than the ones

for TH18 and TH31; the tip passed from the ventral border of the reticular thalamic nucleus, through the border between the LH and the bed nucleus of the stria terminalis, and ended just lateral to the anterior hypothalamic area. The final electrode placement, TH30 (see Figure 9p), was situated medial to the magnocellular preoptic nucleus and lateral to the supraoptic nucleus; the electrode tip moved from just below the substantia innominata to the lateral border of the supraoptic nucleus.

Mapping of Self-Stimulation Sites

The positive and negative sites for self-stimulation are shown in Figures 9a-p. Of the ninety-seven placements that were evaluated 60 (62%) were positive for self-stimulation. These include five sites from which threshold determinations could not be obtained because the threshold response rate or the stability criteria were not met (see page 42). Positive sites are denoted by filled circles; unfilled circles mark those locations at which self-stimulation could not be elicited.

A composite drawing (see Figure 10) shows both the positive and negative self-stimulation sites; where appropriate, intersecting electrode tracks are combined. Consistent results, negative or positive, were obtained between subjects with closely aligned electrode placements; the one exception was in the most anterior stimulation site (see Figure 9a and 10, plate 1). These four subjects had overlapping electrode

Figure 10. A composite figure indicating the positive and negative self-stimulation sites from all subjects in experiment 2. The sections are tracings taken from the Paxinos and Watson (1986) atlas. Each section is identified by a plate number from 1-6 which is located at the top of each section, and underneath that, by the anteroposterior coordinate (Paxinos and Watson, 1986). The plates are organized from left to right, beginning with the most anterior sites and progressing to the most posterior placements. Positive self-stimulation sites are denoted by filled symbols while negative sites are marked by hatched symbols.

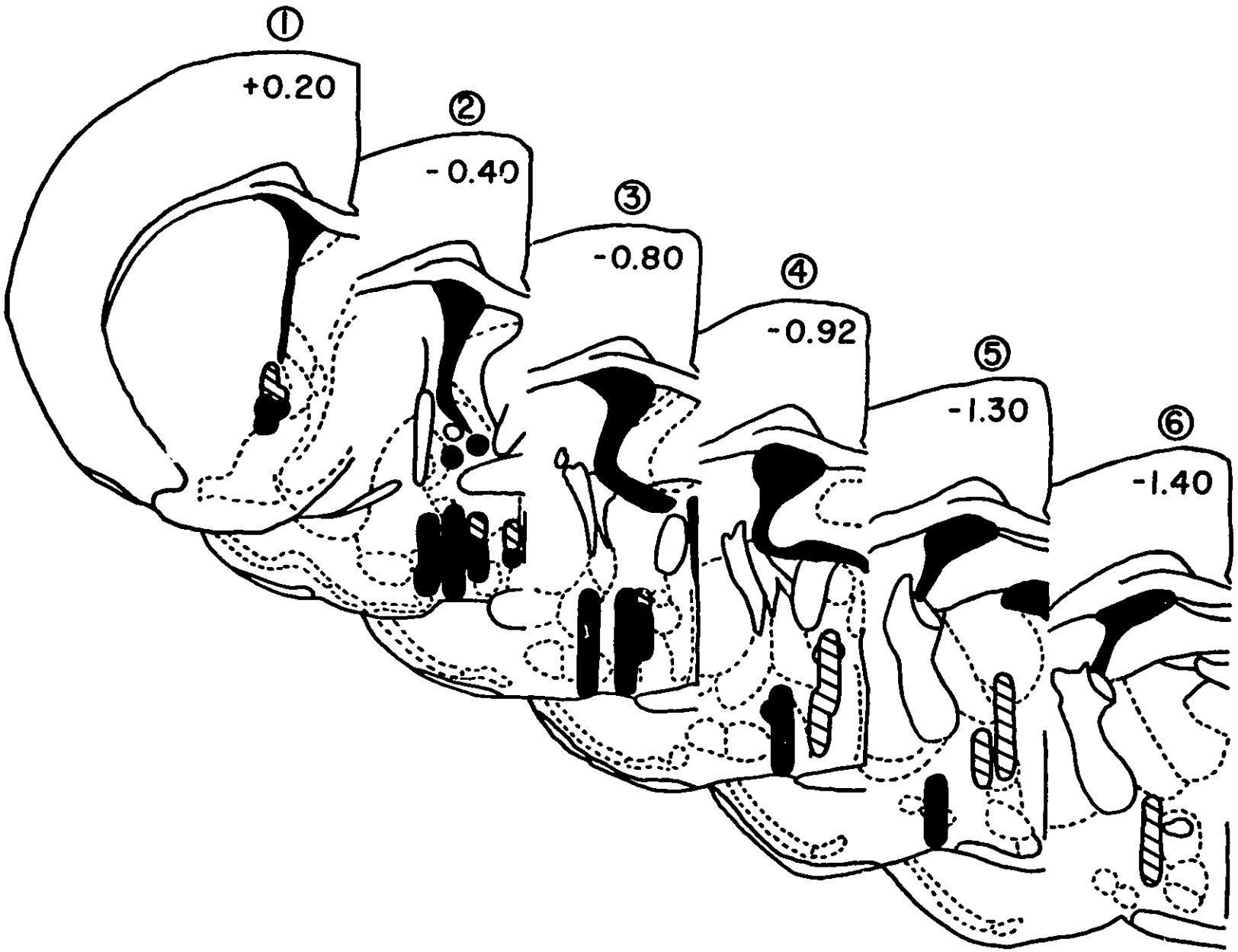
①
+0.20
②
-0.40
③
-0.80
④
-0.92
⑤
-1.30
⑥
-1.40

tracks; in the case of TH41, the location of a positive site was indistinguishable from that of the negative site in TH39 (see Figure 9a), as was also true for TH43 and TH38. However, the positive sites in these pairs did not support stable self-stimulation.

In general, medial sites, including the medial preoptic area and nucleus, did not support self-stimulation, as shown in Figure 10, Plates 2, 4, 5, and 6; if bar-pressing was observed, it was not robust enough to generate trade-off functions (Plate 2). In contrast to the medial preoptic area, the majority of the LPO sites supported vigorous self-stimulation (Plates 2, 3, and 4). The bed nucleus of the stria terminalis, a more dorsal structure, was also positive for self-stimulation (Plate 2) but only in the more rostral sites (Plate 5 and 6). Robust self-stimulation was generally elicited from the compartments of the MFB and the LH (Plates 2, 3, and 5). The lateral sites that consistently yielded high response rates tended to be situated more laterally as the mapping progressed through more caudal regions.

Characteristics of the LPO reward substrate

Trade-off Functions. The trade-off functions generated from the sites with stable self-stimulation thresholds are shown in Figures 9b, 9d-j, 91-m, and 9p. The period threshold is

plotted against current on a log-log scale; the tested current values were usually separated by 0.2 common log unit steps. For each subject, the shape of the trade-off functions across sites were compared in order to determine if there were consistent changes in the relationship as a function of electrode depth.

Anterior LPO Group. The stimulation site for TH34 was situated far more dorsally than any other placement and will not be discussed in the following section (see Figure 9b). For TH33, there was a marked difference between the period thresholds for the lowest current, 160 μA, across sites (see Figure 9d); as the electrode moved ventrally, the stimulation effectiveness at this current increased while there was little change in the period thresholds for the larger currents. In an opposite trend, as more ventral stimulation sites were tested in TH21, more stimulation, as indicated by the decreased period threshold, was required for the lowest current, 125 μA; by the fifth and sixth sites, self-stimulation was consistently absent at this current and more stimulation was required for the next lowest current, 200 μA, at the final placement (see Figure 9e). The period thresholds for the higher currents were relatively invariant across sites for this subject. The trade-off functions for TH36 exhibited few changes as the electrode was moved; after the first site, each curve showed few further increases in period threshold at the highest currents (see

Figure 9f). The two stimulation sites for TH27 were different from each other in one major respect (see Figure 9g); the period threshold for the lowest current, 160 μA, increased substantially when the electrode descended 0.24 mm, while the rest of the curve was relatively unchanged.

Middle LPO Group. The shape of the trade-off functions for TH35 were roughly similar across sites, showing little increases in period threshold with higher currents (see Figure 9h). Likewise, the first five curves for TH30 were almost identical in form and threshold values (see Figure 9i). The final two stimulation sites for this subject showed a marked decrease in period threshold at all currents; this was especially true at the lowest value, 160 μA. In a similar manner, the period thresholds associated with the lowest current, 160 μA, for TH29 showed, initially, a consistent increase over the first three stimulation sites, then a decrease for the next three, culminating in an absence of self-stimulation at the next site; the behaviour at this current was reinstated in the most ventral placement and yielded a period threshold which corresponded to values obtained at more dorsal sites (see Figure 9j).

Posterior LPO Group. In this group, two of the four subjects, TH42 and TH37, did not exhibit bar-pressing and thus are not further discussed in this section (see Figure 9k). Of the remaining two subjects, TH19 and TH22 (see Figure 9l-m),

multiple stimulation sites were only evaluated in TH19. For this subject, the first placement yielded an essentially flat function becoming more steep as the electrode was moved. The second through sixth curves were roughly parallel and exhibited the same range of period thresholds. A steeper function was observed at the last site, due to increased period thresholds at the lower currents, 125 and 200 uA.

LH Group. Only one subject in this group of four exhibited self-stimulation (see Figure 9n-p). For this subject, TH20, the period thresholds for the lowest currents, 100 to 125 uA, were consistently less than 10 msec (see Figure 9p). For sites one through five, there were substantial increases in period threshold over the middle range of currents with few further increases thereafter. At the last stimulation site, several changes were observed; self-stimulation was no longer present at the lowest current, the period threshold for the next current was decreased, and the slope of the function was reduced, with a marked drop-off in period threshold at the highest current.

Regression Analysis

A regression analysis was conducted on the individual 'log-log' transformed trade-off functions and the regression slopes were examined for patterns of change. Only in those cases where the regression R squared value exceeded 0.80, an indicator that the data were reasonably linear, were slope

values included in the comparison. In Table 4 the results of this analysis are presented. Each sub-table represents the values obtained from the previously defined groups; the mediolateral and dorsoventral axes are represented by column and row positions, respectively. The absence of self-stimulation at a site is indicated by a minus sign while the presence of self-stimulation which did not meet threshold or stability criteria is identified by a plus sign.

The R squared value did not exceed 0.80 in five of the fifty-one (roughly 10%) trade-off functions. In three of these cases, TH34, TH35, and TH19, the curves that failed to meet this criterion were observed at dorsal stimulation sites (see Figure 9b, h, and l). A progression was observed over the five stimulation sites in TH35 where the initial placement did not support self-stimulation, a trade-off function that did not meet the R squared criterion was generated in the next site, followed by self-stimulation at three sites which did meet this criterion. The fourth case, TH20, was obtained from the final, ventral test site (see Figure 9p). The fifth case, observed in TH21, was the fourth of seven tested placements (see Figure 9e); there were no apparent distinguishing characteristics relative to the other stimulation sites for this subject and the value of 0.78 was very close to meeting the inclusion value of 0.80. The slope values in Table 4 were examined for

Table 4

Positive and Negative Self-stimulation Sites and Slopes, Derived from Individual Linear Regression Analyses, of the Period/Current Trade-off Functions

A) Anterior LPO Group

Mediolateral Coordinate	0.2	0.9	0.9	1.3	1.4	1.8	1.8
SUBJECT	TH44	TH34	TH33	TH21	TH24	TH36	TH27
Dorsoventral Coordinate							
-6.20		·.48					
-6.50					+		
-7.66				0.56			
-7.84 to -7.92	-		-	0.60		0.55	
-8.08 to -8.16	-		-	0.60		0.56	
-8.32 to -8.40	+		0.79	·.78		0.78	
-8.56 to -8.62			0.69	0.66		0.56	
-8.76 to -8.86			0.65	0.53		0.68	1.15
-9.00 to -9.10				0.86			0.87
Average Value			0.71	0.64		0.63	1.01
Standard error of the mean			0.04	0.05		0.04	0.14

Grand Mean = 0.69; Standard error of the mean = 0.04

B) Middle LPO Group

Mediolateral Coordinate	1.1	1.4	2.0
SUBJECT	TH35	TH30	TH29
Dorsoventral Coordinate			
-7.64 to -7.72	-	0.44	0.94
-7.88 to -7.96	·.72	0.53	0.90
-8.12 to -8.20	0.45	0.54	0.68
-8.36 to -8.44	0.44	0.63	0.83
-8.60 to -8.68	0.56	0.55	1.03
-8.92		0.57	1.04
-9.16		0.67	0.91
-9.40			0.85
Average Value	0.48	0.56	0.90
Standard error of the mean	0.04	0.03	0.04

Grand Mean = 0.70; standard error of the mean = 0.05

Table 4 continued

C) Posterior LPO Group

Mediolateral Coordinate	0.7	0.8	1.6	1.8
SUBJECT	TH42	TH37	TH19	TH22
Dorsoventral Coordinate				
-6.80	-			
-7.04	-			
-7.28	-			
-7.52	-			
-7.76	-			
-7.86 to -8.00	-	-	.75	
-8.10 to -8.20		-	0.69	0.63
-8.34 to -8.42		-	0.68	
-8.58 to -8.66		-	0.66	
-8.82 to -8.90		-	0.66	
-9.06			0.68	
-9.30			0.80	
Average Value			0.70	0.63
Standard error of the mean			0.02	

Grand Mean = 0.69; standard error of the mean = 0.02

Table 4 continued

D) LH Group

Mediolateral Coordinate	0.8	1.2	1.6	2.2
SUBJECT	TH18	TH31	TH25	TH20
Dorsoventral Coordinate				
-6.32	-			
-6.48	-			
-6.64	-			
-6.80	-			
-7.04	-			
-7.26			-	
-7.36 to -7.38	-	-		
-7.50			-	
-7.62 to -7.68	-	-		
-7.74			-	
-7.86		-		
-7.98 to -8.10	-	-	-	
-8.22			-	
-8.36				1.06
-8.46 to -8.52			-	0.93
-8.68 to -8.70			-	0.93
-8.92				0.92
-9.16				0.92
-9.40				*.66
Average Value				0.95
Standard error of the mean				0.03

Grand Mean = 0.95; standard error of the mean = 0.03

\+ positive site but no trade-off obtained
\- negative site
* R squared value less than 0.80

consistent patterns in the anteroposterior, mediolateral, and dorsoventral axes. A within-subject comparison revealed that there were no uniform patterns of change in the slope values obtained in the dorsoventral direction. Within each of the previously defined groups, anterior LPO, middle LPO, posterior LPO, and LH, the average slope for each subject was calculated; no clear progression in a mediolateral direction was observed. However, when a grand mean for each anteroposterior plate, collapsed across mediolateral and dorsoventral placements, was calculated, the three LPO groups, anterior, middle, and posterior, had similar slope values which were substantially lower than the slope for the one subject in the LH group (see Table 4). The single subject in the LH group was found to have a comparable slope value to those reported in other LH placements (Harris and Bielajew, 1988).

In order to summarize the information contained in the trade-off functions and ease its interpretation, the changes in period threshold at a low and high current were examined at each site (see Figure 11a-d). Each sub-figure reports the results of subjects that had electrodes located at the same anteroposterior coordinate; for individual subjects, the period thresholds corresponding to a high and a low current, generally 1000 μA and 200 or 250 μA respectively, are plotted for each stimulation site.

The results for the anterior LPO group are shown in Figure

Figure 11a-d. The period thresholds corresponding to a low current, 200 or 250 μA, and a high current, generally 1000 μA, for each LPO stimulation site in individual subjects are shown. The sub-figures are grouped according to the anteroposterior coordinate that best represents the location of the electrode tips (Paxinos and Watson, 1986); this coordinate is located in the upper left hand side of each sub-figure. The left column contains the histological results with each subject identified near the top of each drawing. The right column contains the graphs relating the low and high current period thresholds obtained at each stimulation site. The period threshold (msec) is plotted on a log scale ranging from 10 to 100 msec except for subject TH21 in sub-figure A where the period threshold values range from 1 to 100 msec. The period thresholds associated with the low current are represented by a continuous line, and the equivalent for the high current by a dashed line.

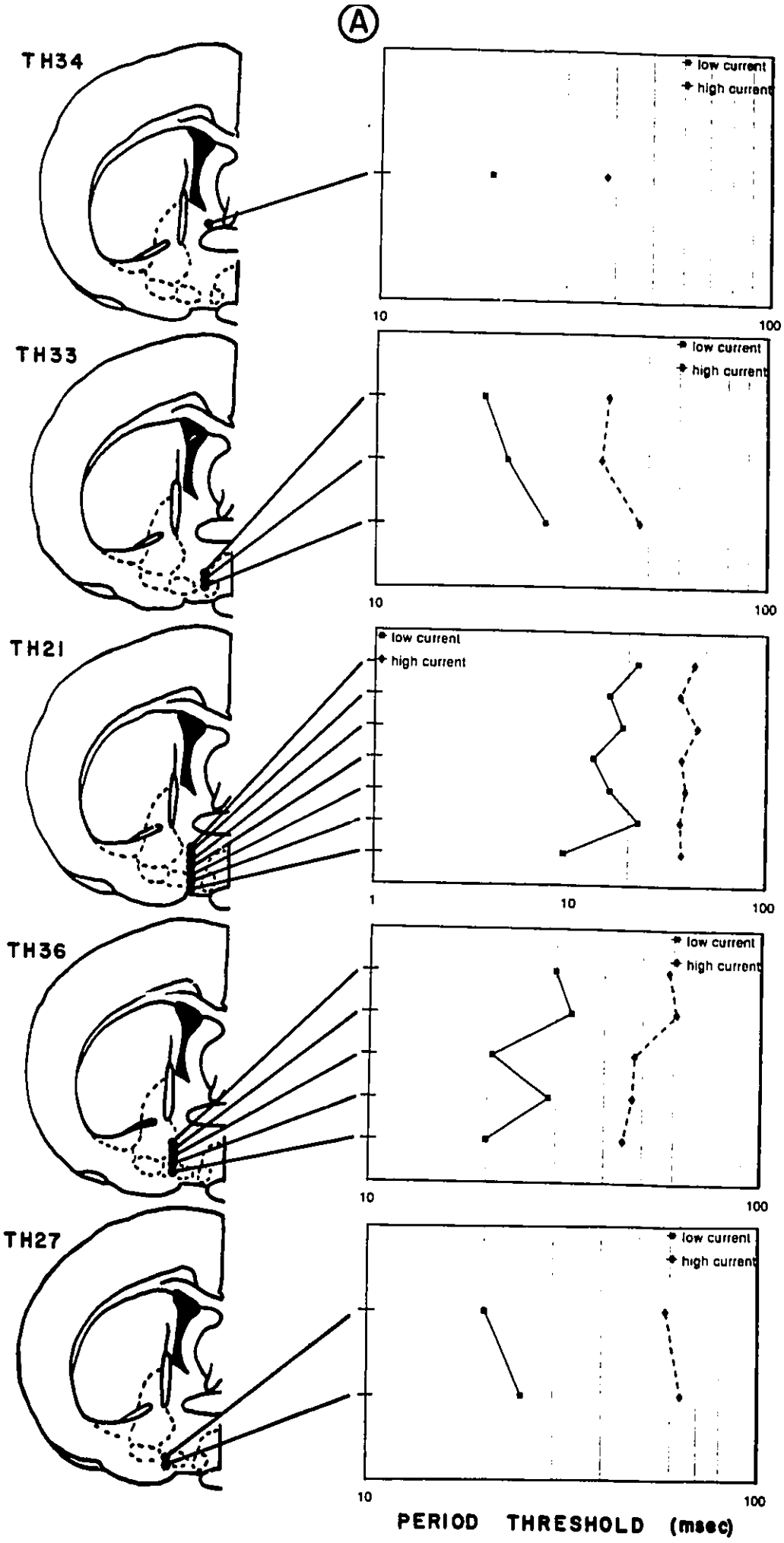
A
TH34
low current
high current
10
100
TH33
low current
high current
10
100
TH21
low current
high current
1
10
100
TH36
low current
high current
10
100
TH27
low current
high current
10
100
PERIOD THRESHOLD (msec)

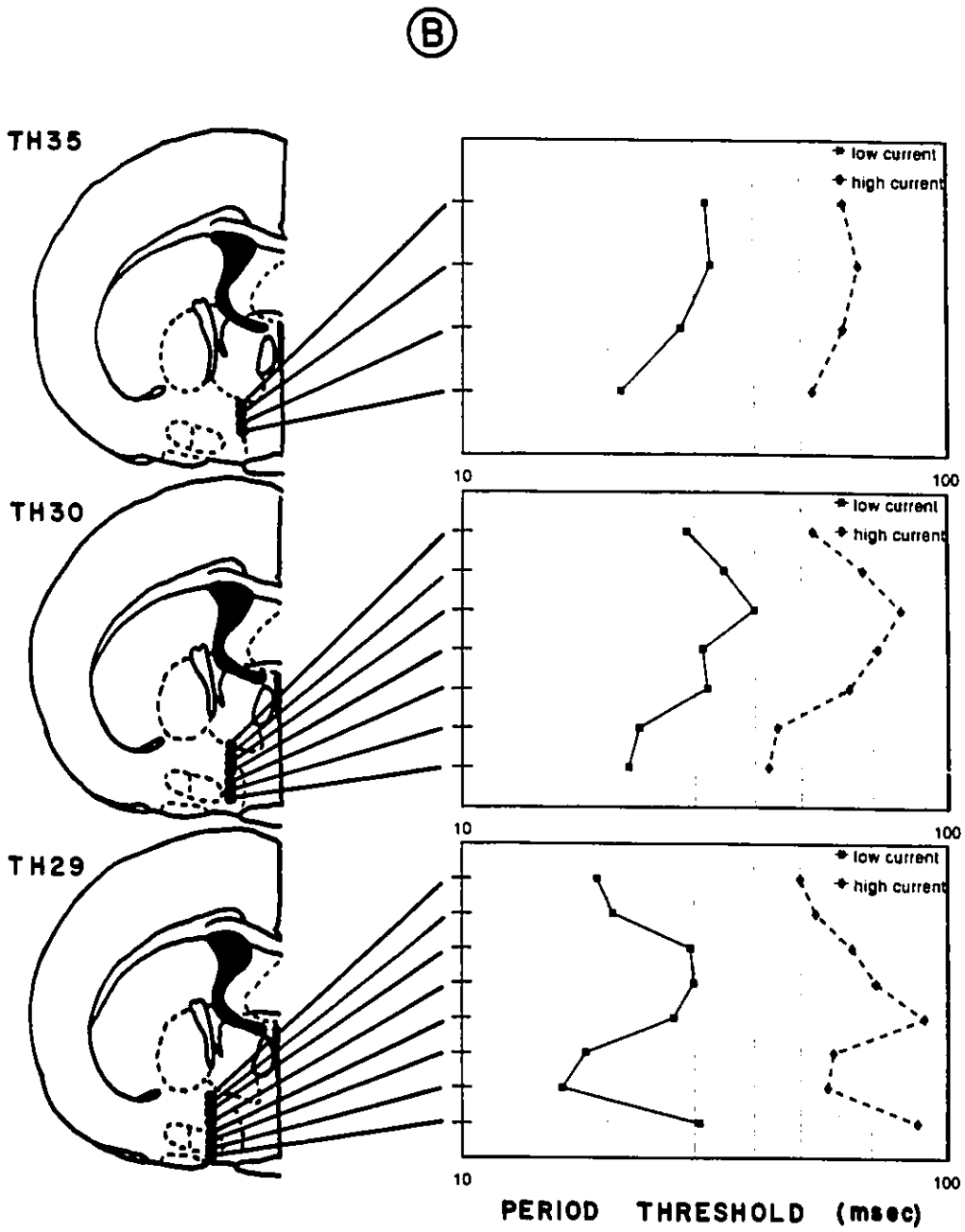
B
TH35
TH30
TH29
low current
high current
10
100
PERIOD THRESHOLD (msec)

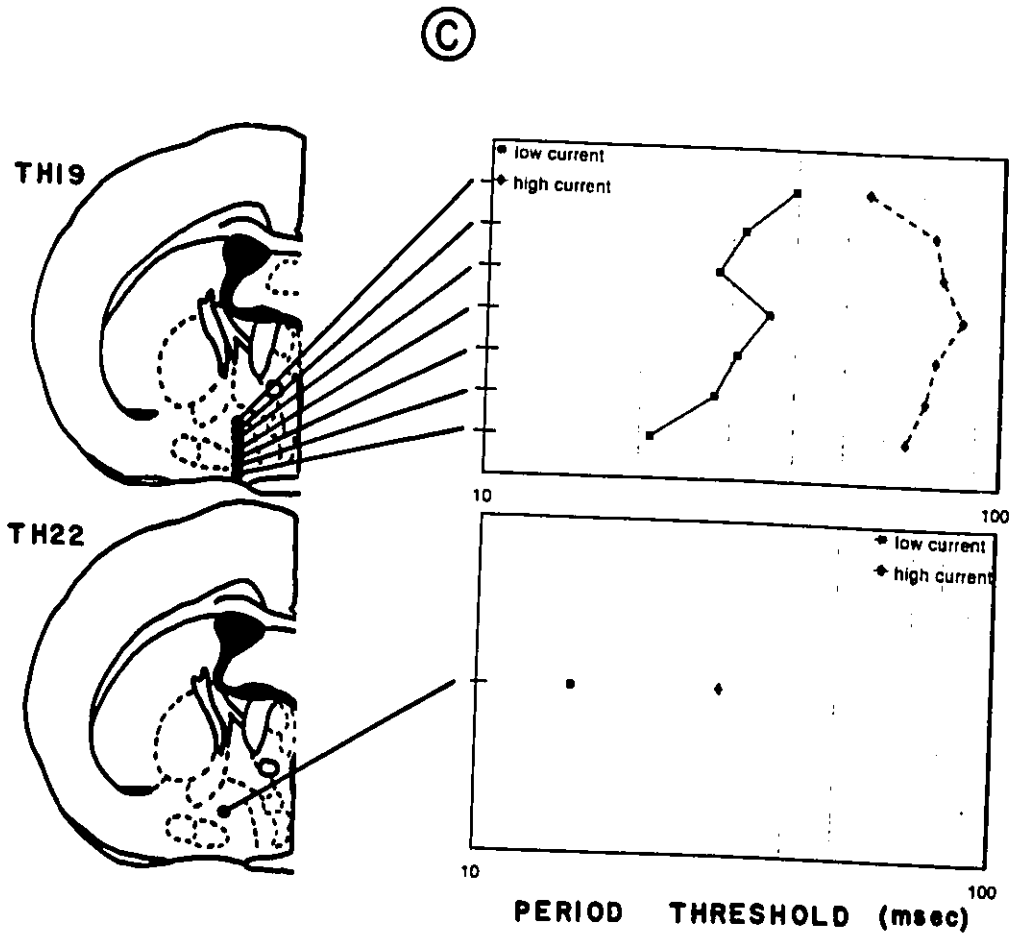
©
TH19
low current
high current
10
100
TH22
low current
high current
10
100
PERIOD THRESHOLD (msec)

Ⓓ

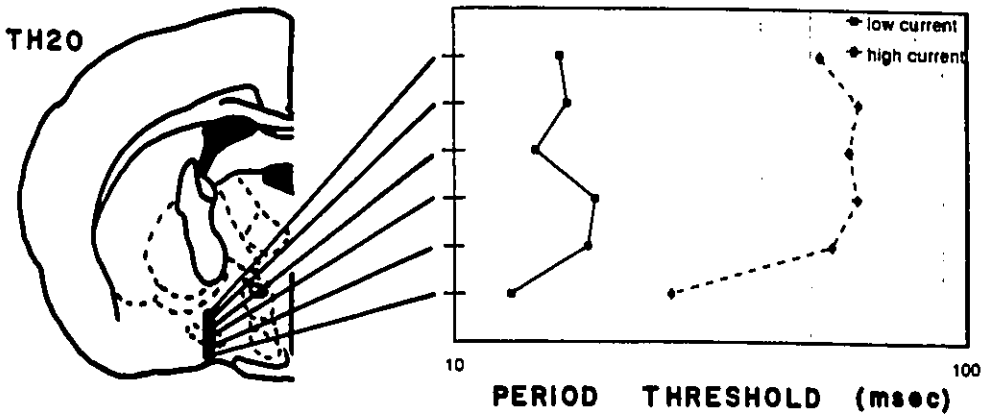
TH20
low current
high current
10
100
PERIOD THRESHOLD (msec)

11a. Approximately the same range of period thresholds, from 20 to 30 msec for the low current, was observed; the one exception was TH21 where the thresholds ranged from 12 to 18 msec, about a 0.1 log unit decrease. The two most lateral stimulation sites, TH36 (first two sites) and TH27, exhibited period thresholds for the high current that were 0.2 common log units larger than those for the three medial placements at the same current values. For the middle and posterior LPO groups, the period thresholds appeared higher, on average, than those of the anterior LPO group. Larger threshold values were observed at more dorsal sites in two of the five subjects (see Figure 11b-c) while two of the remaining three subjects, TH29 and TH19, exhibited similar profiles with the highest thresholds being observed following stimulation of middle sites. For these four subjects, smaller threshold changes, no more than 0.2 log unit shift, between sites, were generally observed at the low current while the period threshold shifts at the high current ranged from 0.1 to almost 0.4 log units. The results for the single subject, TH20, in the LH group are shown in Figure 11d. The period thresholds associated with the low current had values less than those observed for all subjects except TH22 while the period thresholds at the high current were fairly representative.

Discussion

The LPO is a structure that has been examined in a variety of experimental paradigms intended to discover the origin of the cell bodies for the descending pathway linking the LH and VTA reward neurons. While the results of LPO lesions on subsequent MFB self-stimulation, of cell responses in the LPO following rewarding stimulation in the MFB, and of the metabolic consequences of LPO neurons attributable, in part, to MFB self-stimulation have suggested that the LPO may be an important structure in the MFB reward pathway (Gallistel et al, 1985; Janas and Stellar, 1987; Murray and Shizgal, 1991; Shizgal et al, 1989; Waraczynski, 1988), a systematic investigation of self-stimulation in this area has not been reported. The results of this study suggest that self-stimulation can be elicited throughout the LPO and that the directly stimulated fibers appear to be organized in a more diffuse bundle than in the LH and the VTA.

Mapping of the self-stimulation substrate

Self-stimulation could be elicited from activation of sites located throughout the LPO and compartments 'a' and 'b' of the MFB. For all groups, except the most anterior one, the dorsal sites were less likely to support the behaviour; this was especially true if a dorsal site was medially situated. The presence or absence of self-stimulation at a particular

location was generally consistent between animals with the exception of the most anterior group; the behaviour obtained from these particular placements never exceeded either the criterion response rate or the stability requirement. These erratic results may reflect a paucity of reward-relevant neurons in this area or the recruitment of inhibitory or competing systems which interfere with the elicitation of self-stimulation.

The location of positive and negative self-stimulation sites, extending from the area anterior to the midline convergence of the anterior commissure caudally to the transition area between the LPO and LH, suggests a projection that moves more laterally as it progresses in the caudal direction. For example, it was possible to elicit self-stimulation from a medial site, 0.9 mm lateral to the midline, in the anterior LPO group, while in the LH group, negative sites were observed up to 1.6 mm lateral to the midline. Indeed, except for the most anterior group, lateral placements always supported self-stimulation while medial sites were far less likely to do so.

The general pattern of results is in accordance with studies examining the metabolic activation of structures following caudal MFB self-stimulation (Gallistel et al, 1985) and parallels the lateral progression of the rostrocaudal trajectory of the MFB described by anatomists (Paxinos and

Watson, 1986). The MFB pathway can be portrayed as a horizontal 'C' with the medial top of the C representing the LPO, the lateral middle of the C, the LH, and the medial bottom of the C corresponding to the location of the VTA. It can be seen that, for the portion of the trajectory relevant to this study, namely the LPO to the LH, both the MFB and the positive reward sites move from medial to more lateral positions.

Characteristics of the LPO reward substrate

The period/current trade-off function, allowing for the assumptions underlying the counter model (Gallistel, 1978), can provide estimates of both the neural density and the spatial boundaries of the critical substrate. Exploiting the advantage of stimulating consecutive sites using moveable electrodes, the trade-off functions of individual subjects can be examined for departures from linearity and asymptotic current; these observations can then be used to infer the spatial limits of the reward substrate in question. Regrettably in this study, no consistent pattern was found in either the correlation between electrode placement and the observation of a curvilinear function or the current intensity at which the curve began to asymptote for the subjects.

The relative density of the behaviourally relevant neurons at separate stimulation sites can be compared from the slopes of the regression lines relating period threshold to current intensity. These values were essentially identical for all LPO

stimulation sites, especially when the average slopes within each group (anterior, middle, and posterior LPO) were considered. In contrast, the mean slope value across sites for the single subject in the LH group, TH20, which was comparable to slope estimates obtained at other LH placements, was substantially greater, suggesting that the reward neurons in the LPO could be less densely packed than in the LH.

Within the LPO, certain trends were observed that suggested an increase in neural density as more caudal sites were stimulated. While the group average of the slopes for the trade-off functions was virtually identical for the three LPO groups, there was an observable trend, as the group anteroposterior orientation progressed caudally, for increasing period thresholds at the low and high currents (see Figure 11a-d). This trend is consistent with the previously discussed slope data suggesting an increase in packing density of reward fibers from the LPO to the LH.

The anatomical literature supports this interpretation. Studies suggest that the MFB becomes smaller, and possibly more dense, as it moves from the LPO, through the LH, and caudally towards the VTA (Nieuwenhuys et al, 1982). Since self-stimulation can be obtained in all of these areas, it may be that the reward substrate shares this characteristic; indeed, the slopes of period/current trade-off functions derived from stimulating self-stimulation sites in the LH and VTA have been

reported to increase substantially between these two loci (Harris and Bielajew, 1988). Based on the similarity of the slopes obtained in the LPO trade-off functions, one could argue that the distribution of reward neurons in the LPO appears to be uniformly dense; the trend towards increasing period thresholds and steeper slopes can be attributed to the contribution of more densely packed reward neurons at caudal sites.

Of particular relevance to the interpretation of this study is the assumption that neurons with varying thresholds for activation are homogeneously distributed within the effective stimulation field. If this assumption is violated, the slope of the period threshold/current trade-off function could also reflect differences in excitability thresholds of the reward relevant neurons (Schindler, 1983, p. 27; Yeomans, 1990). It has been shown that the LPO comprises mainly diffuse, thin, and poorly myelinated fibers; this is in contrast to the LH which contains a wide variety of fiber types ranging from small unmyelinated to small and large, coarsely myelinated neurons, many of which extend to the VTA (Veening, Swanson, Cowan, Nieuwenhuys, and Geeraedts, 1982). A potential difference in composition between the LPO and LH reward substrate is supported by the behaviourally derived measures of refractoriness and estimates of conduction time between these two structures (Bielajew et al, 1987; Fouriezos et al, 1987).

Thus, both differing neural density and thresholds of activation could be contributing to the observed slope patterns.

In order to address this concern, one needs to establish whether the neurons that give rise to LPO self-stimulation are the same reward neurons that have been characterized elsewhere in the MFB. One direct manner to determine whether the same neurons underlie self-stimulation in the LPO and more caudal MFB sites is to employ the behavioural adaptation of the collision test (see experiment 3). Without this information, no adamant conclusions can be drawn; however, based on the evidence in this, and prior, studies, the LPO appears to contain a relatively homogenous population of reward neurons.

Experiment 3

There is persuasive evidence to suggest that the LPO is a rostral continuation of the MFB reward system, and may contain the cell bodies of origin of these fibers. Medial forebrain bundle self-stimulation has been shown to antidromically activate neurons in the LPO (Shizgal et al, 1989) and lesions of the area surrounding, and including, the LPO can lead to at least transient decreases in the rewarding value of MFB self-stimulation (Janas and Stellar, 1987; Murray and Shizgal, 1991; Waraczynski, 1988). The LPO has also been shown to be metabolically activated following rewarding brain stimulation of the caudal MFB (Gallistel et al, 1985). A subset of the neurons of the LPO have the same electrophysiological characteristics as MFB reward neurons (Bielajew et al, 1981, 1982; Fouriezos et al, 1987; MacMillan et al, 1985; Schenk and Shizgal, 1982; Yeomans, 1979) and finally, the results from behavioural studies using the collision test (Shizgal et al, 1980) have suggested that the same axon bundle mediates self-stimulation elicited by LPO and anterior LH electrodes (Bielajew et al, 1987).

The nature of the anatomical connection between the LPO and more posterior regions of the MFB remains unclear. There are fiber bundles within the MFB that course reciprocally between the VTA and the LPO (Nieuwenhuys et al, 1982; Phillipson, 1979;

Swanson, 1976). Self-stimulation of the VTA can be, at least transiently, reduced by LPO lesions (Janas and Stellar, 1987; Murray and Shizgal, 1991) while LPO neurons have been found to be antidromically activated by rewarding stimulation of the VTA (Shizgal et al, 1989). As stated above, at least a subset of LPO reward neurons appear to share an axon bundle with the anterior LH (Bielajew et al, 1987) and, in separate collision tests, it has been demonstrated that anterior LH and VTA self-stimulation sites arise from activation of the same fiber bundle (Bielajew and Shizgal, 1982; Durivage and Miliaressis, 1987; Shizgal et al, 1980). Thus, in the above tradition, the purpose of this study was to examine the nature of the reward-relevant connection between the LPO and the VTA, using the behavioural adaptation of the collision test.

Method

Subjects and surgery

Nine Long-Evans rats were used in this experiment. The coordinates for the moveable LPO electrodes ranged from 0.3 to 0.92 mm posterior to bregma, 1.3 to 2.0 mm lateral to the mid-sagittal suture, and 7.6 to 8.2 mm ventral to the skull surface reading at bregma. The fixed VTA electrodes were implanted using the cocrdinates 4.8 mm posterior to bregma, 0.9 to 1.2 mm lateral to the mid-sagittal suture, and 8.0 to 8.4 mm ventral to the skull surface reading at bregma.

Screening, training, and stabilization

These phases were conducted as in experiment 2.

Behavioural Testing

The general protocol for the collision test began with the selection of currents for the LPO and VTA that equated the single-pulse (SP) period thresholds obtained from these two sites. After two or three warm-up trials, a typical collision session consisted of, first, determining the SP thresholds for the LPO (anterior or A site) and the VTA (posterior or P site). Double-pulse (DP) tests followed with the random presentation of 8 C-T intervals: 0.2, 0.6, 0.8, 1.2, 2.0, 5.0, 10.0, and 20.0 msec. The session ended with a second determination of the SP thresholds for the LPO and the VTA. If the stability criteria were not met (see page 42), the session was discarded.

In general, each session resulted in the completion of two full collision curves, one of which resulted from the delivery of the C pulse to the LPO and the T pulse to the VTA (A-P condition) and a second where the conditions were reversed (P-A condition). The across session stability criteria was defined as the majority of the standard errors of the mean not exceeding a value of 0.10 which was 10% of the theoretical maximum effectiveness value.

If a sudden rise in effectiveness (E) at longer C-T intervals was reliably observed, then the double-pulse technique for assessing the neural refractory period was

conducted at each site in order to be capable of computing the conduction velocity (see page 24) should a reliable collision effect be obtained.

When all tests were completed, the LPO electrode was moved a ventral distance of 0.24 mm and the trade-off procedures described in experiment 2 were applied to the new site, followed by collision tests between the new LPO site and the VTA. To ensure stability of the fixed VTA electrode, periodic checks of the period/current trade-off function were conducted.

Statistical Analysis

Individual two-way ANOVAs were conducted on the collision curves generated at each stimulation site; the main factors were C-T interval and AP/PA condition. In cases where the only significant factor was the AP/PA condition, further analyses were not done. However, when the C-T interval factor was significant, indicating a change in E value over the tested intervals, the data were examined using a modified version of the asymptote test, originally developed to estimate the first C-T interval at which the E value associated with a refractory period curve had reached a plateau (Bielajew et al, 1981).

To employ this test, the means and associated standard errors of the two longest C-T intervals are compared; if these ranges overlap, they are combined and a new mean and standard error are calculated. These new values are compared with the corresponding mean and standard error of the next shortest C-T

interval; if they overlap, the data are again combined. This horizontal stepwise procedure is continued until the pooled mean and standard error no longer overlap the mean and standard error of the next shortest C-T interval. The point at which the E value approaches an asymptote is defined as the shortest C-T interval to contribute to the pooled mean and standard error.

As mentioned above, the original version of this test, a 'top-down' approach, was applied to the collision curves in this study when the C-T interval factor was significant in order to estimate the interval at which the change in E approached an asymptote. In addition, the same procedure was applied to the early portion of the curves in order to determine the longest C-T interval at which the E value had not yet begun to increase. Both asymptote tests were executed on the individual AP and PA curves if the ANOVA yielded significant main effects of the C-T interval and AP/PA factors; in the case where only the C-T interval factor was significant, the two curves associated with the AP and PA conditions were collapsed and the asymptote test was conducted on the one composite collision curve.

Results

The results will be presented on a per subject basis; due to the dependence of the observations on the particular electrode orientations, between subject comparisons are not appropriate. The subjects were ordered so that the data for the animal with the most anterior electrode placements are presented first. For each subject, the histological findings, a descriptive overview of the collision curves, and then the results of the statistical analyses are presented. As a general rule, when an increase in E was observed, only those cases where the E difference was at least 0.20 were the results considered notable; this value was selected as it exceeded the permissible standard errors of the mean in this study. Individual source tables are provided in Appendix 1.

TH27. The anterior electrode was located lateral to the LPO with the first site contained within compartment 'b' of the MFB and the second site at the ventral border of this structure; the posterior electrode was situated in the LH, which at this level is considered part of the MFB, just medial and slightly ventral to the cerebral peduncle (see Figure 12a). The currents used for the collision tests were unusual in that the posterior site required a substantially higher current than the anterior location, a requirement which was not observed in

Figure 12a-i. The histological and collision test results for each of the nine subjects in experiment 3 are shown. The sections are tracings from the Paxinos and Watson (1986) atlas that best represent the locations of the electrode tips; the anteroposterior coordinates for the anterior (A) and posterior (P) electrode placements are located in the upper left hand corner of the figure. The alphanumeric combination that identifies each subject is located in the upper left hand corner of each sub-figure. The collision graphs, located on the right side of the figure, show the effectiveness of double-pulse stimulation, relative to the single pulse condition, plotted against C-T interval. The solid lines correspond to the AP condition in which the C pulses were delivered to the anterior (LPO) electrode and the T pulses to the posterior (VTA) electrode; the PA condition, C pulses to posterior (P) electrode and T pulses to anterior (LPO) electrode, is represented by the dashed lines. The error bars symbolize the standard error of the mean. The LPO and VTA currents at which the tests were conducted are shown in the upper left hand corner of each collision graph; the presence of a 'B' just below indicates that some of the replications were conducted following the administration of brotizolam. The solid lines connect each anterior stimulation site with its corresponding collision curve.

Ⓐ

TH27

A: -0.40
P: -3.80

●—● AP
●-● PA

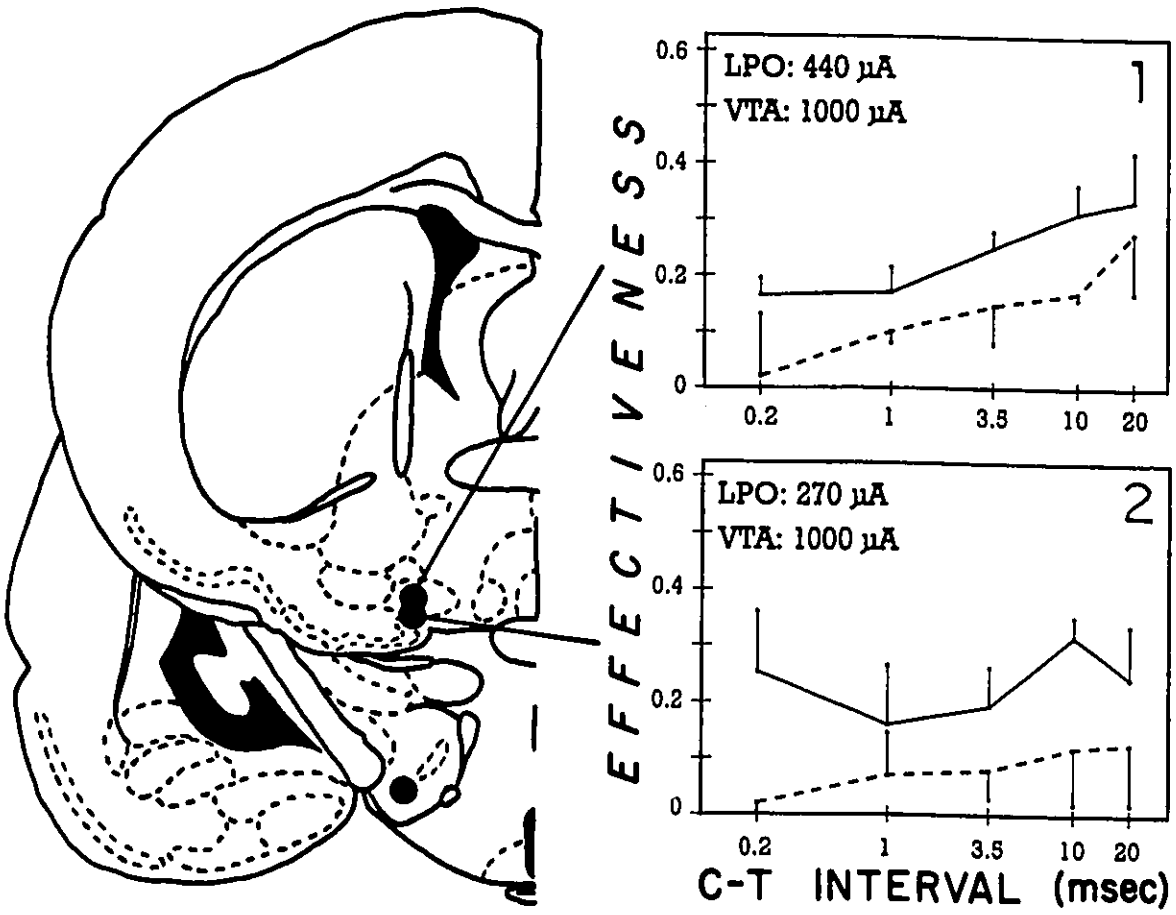

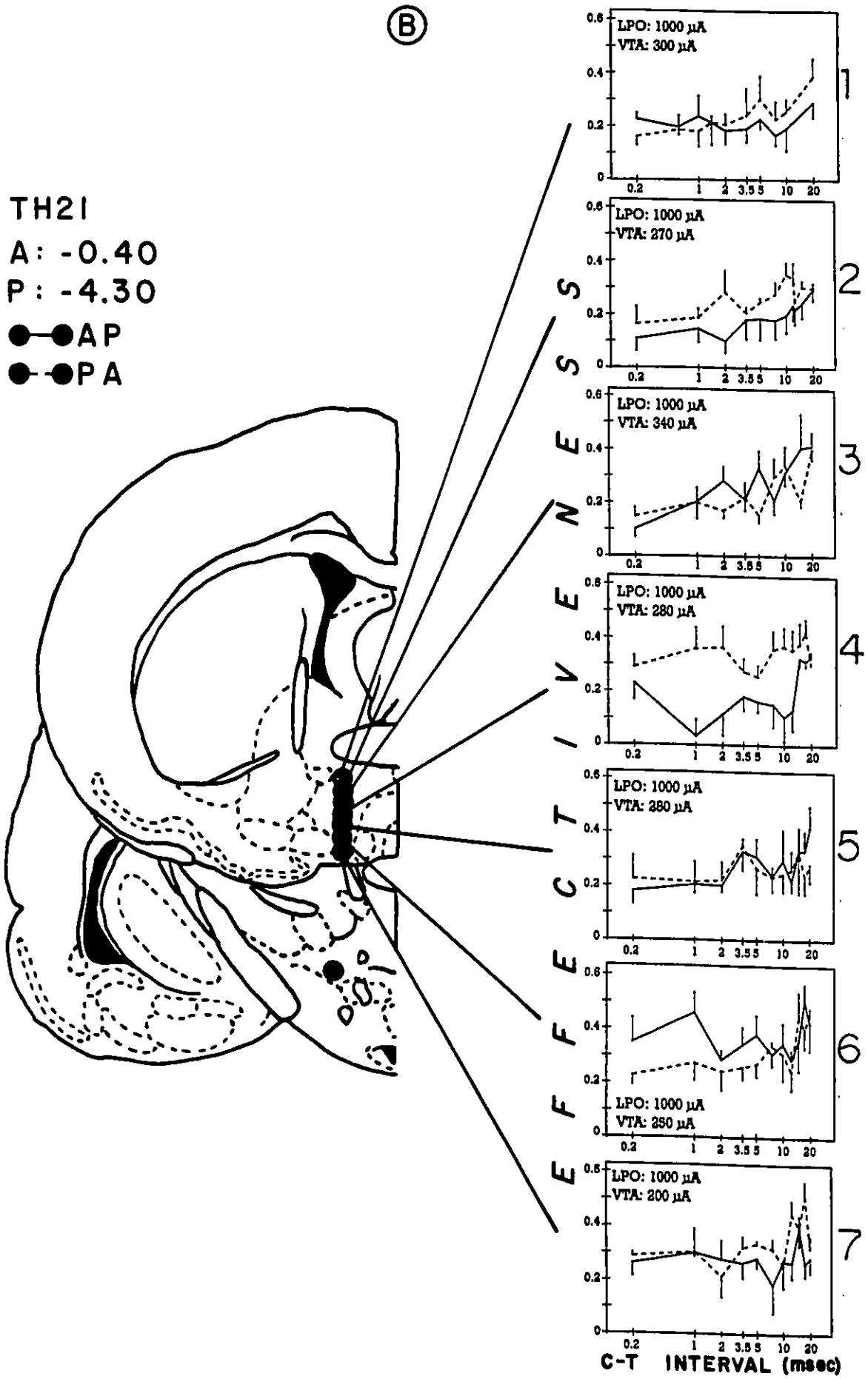
B
TH21
A: -0.40
P: -4.30
AP
PA
LPO: 1000 μA
VTA: 300 μA
LPO: 1000 μA
VTA: 270 μA
LPO: 1000 μA
VTA: 340 μA
LPO: 1000 μA
VTA: 280 μA
LPO: 1000 μA
VTA: 280 μA
LPO: 1000 μA
VTA: 250 μA
LPO: 1000 μA
VTA: 200 μA
1
2
3
4
5
6
7
0.6
0.4
0.2
0
0.2
1
2
3.5
5
10
20
EFFECTIVENESS
C-T INTERVAL (msec)

TH34

A: -0.40
P: -4.52

●—●AP
●-●PA

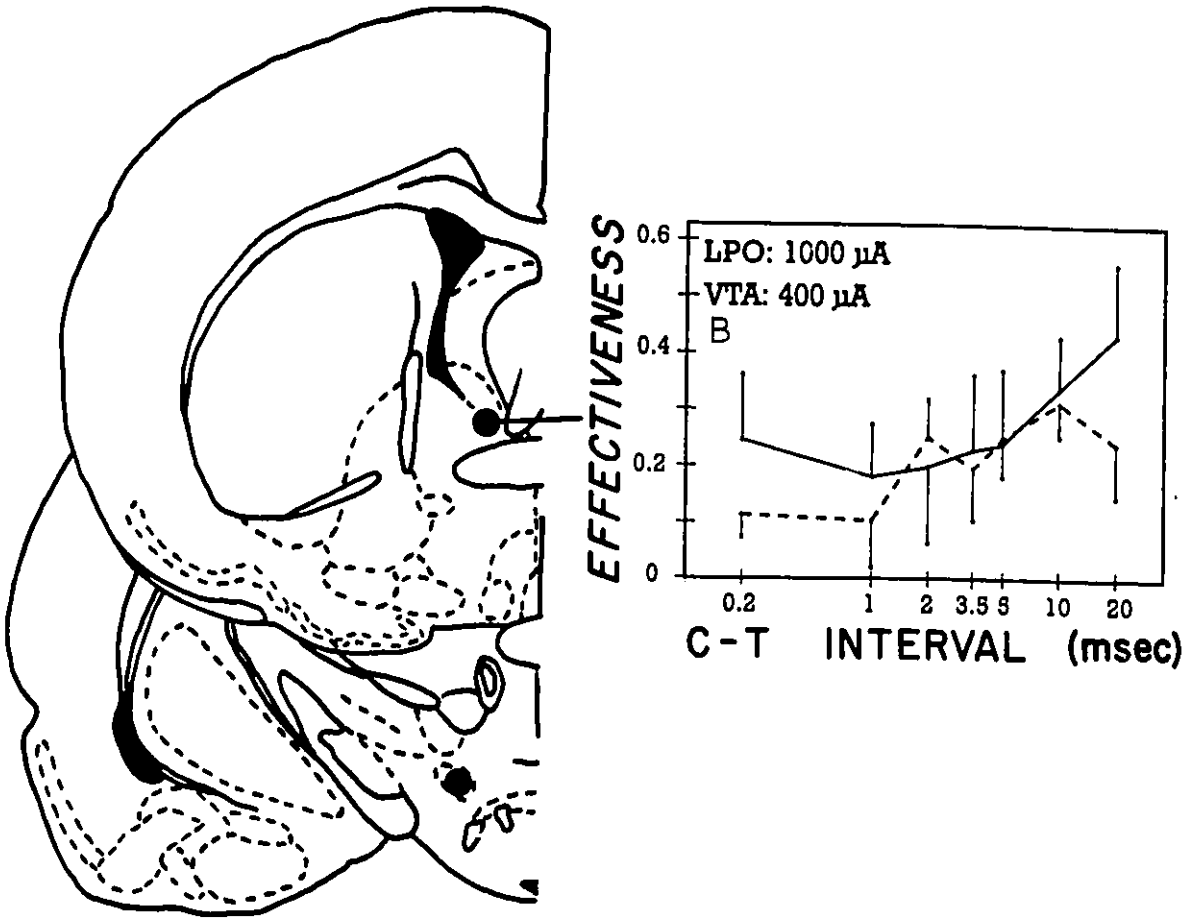

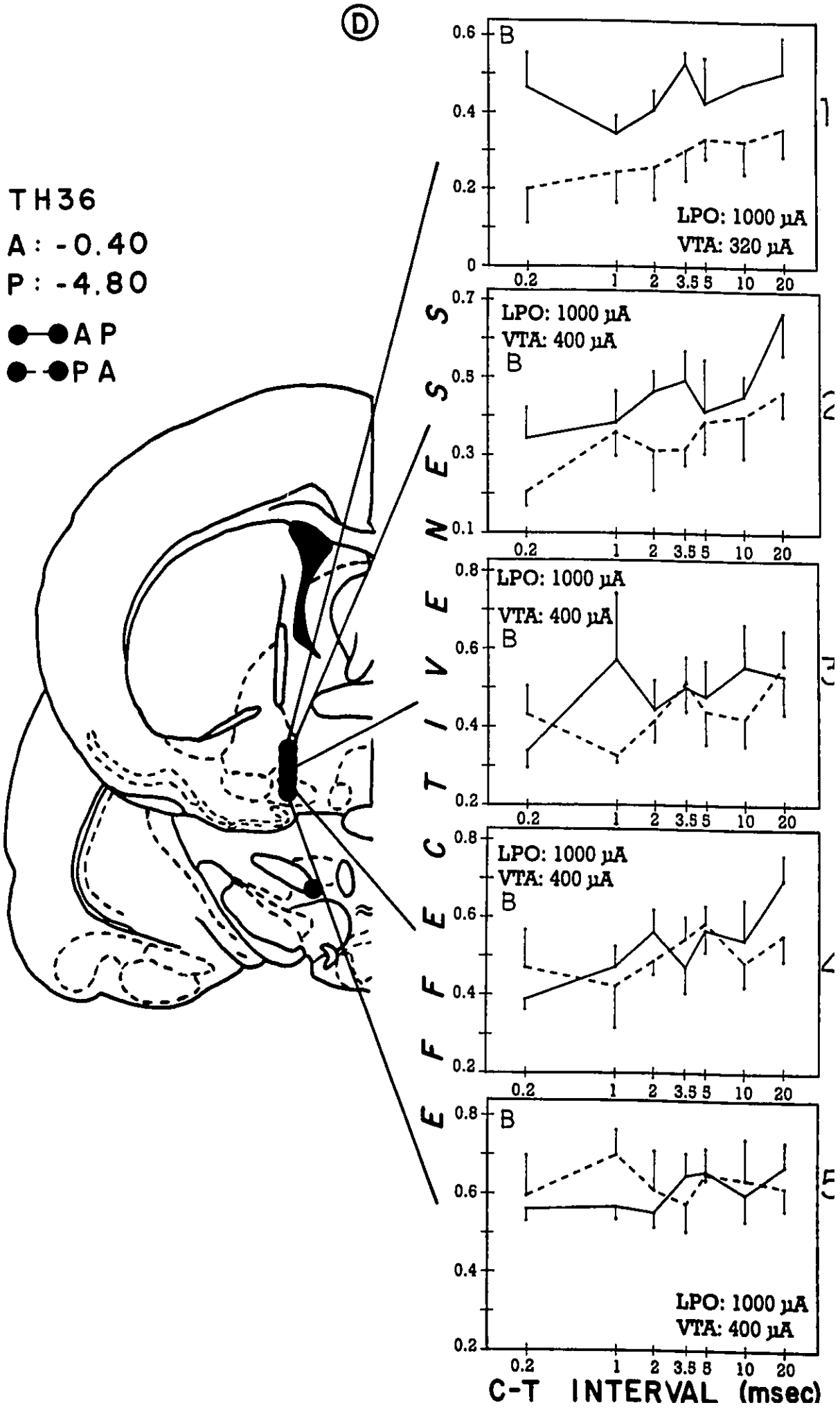
Ⓓ
TH36
A: -0.40
P: -4.80
AP
PA
B
LPO: 1000 µA
VTA: 320 µA
LPO: 1000 µA
VTA: 400 µA
B
LPO: 1000 µA
VTA: 400 µA
B
LPO: 1000 µA
VTA: 400 µA
B
B
LPO: 1000 µA
VTA: 400 µA
EFFECTIVENESS
0.2 1 2 3.5 5 10 20
C-T INTERVAL (msec)

Ⓔ

TH33

A: -0.40

P: -4.80

●—●A P

●—●P A

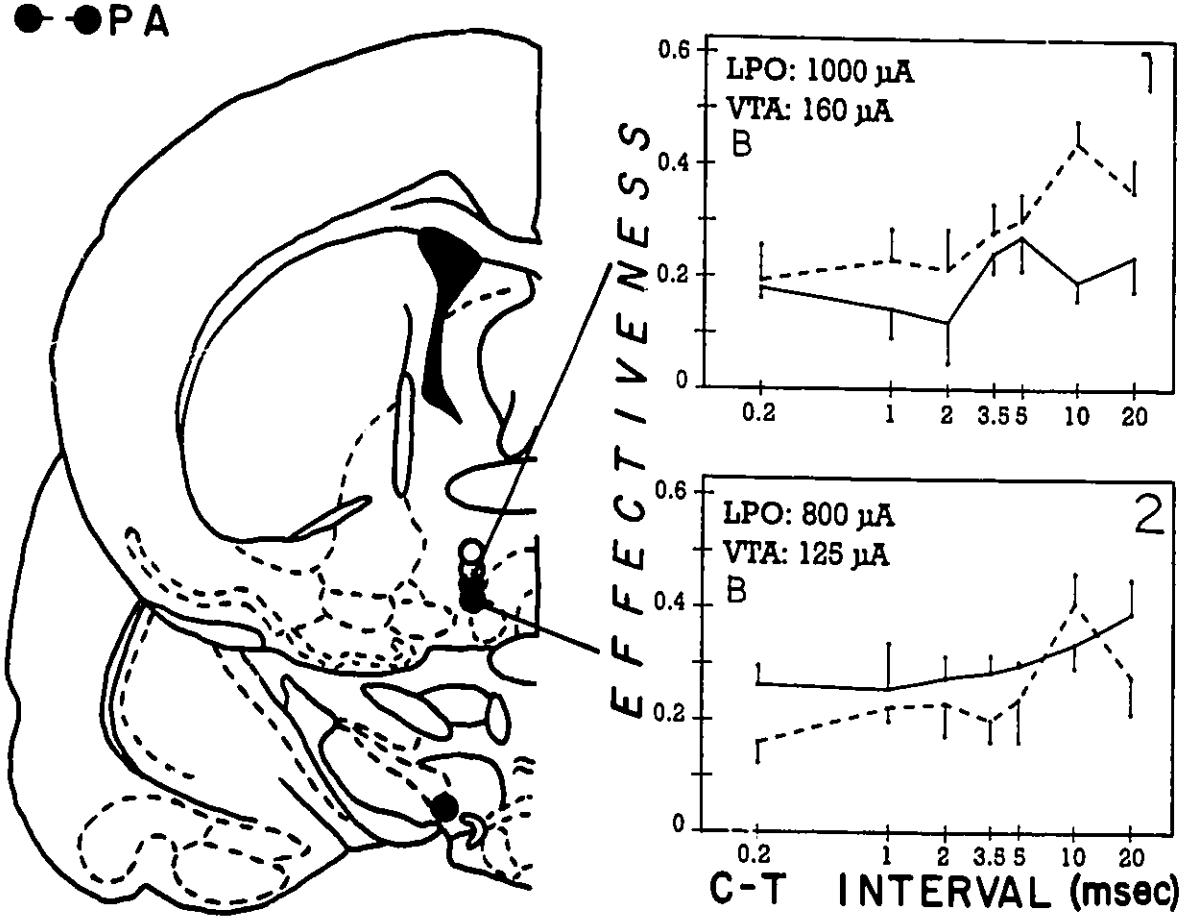

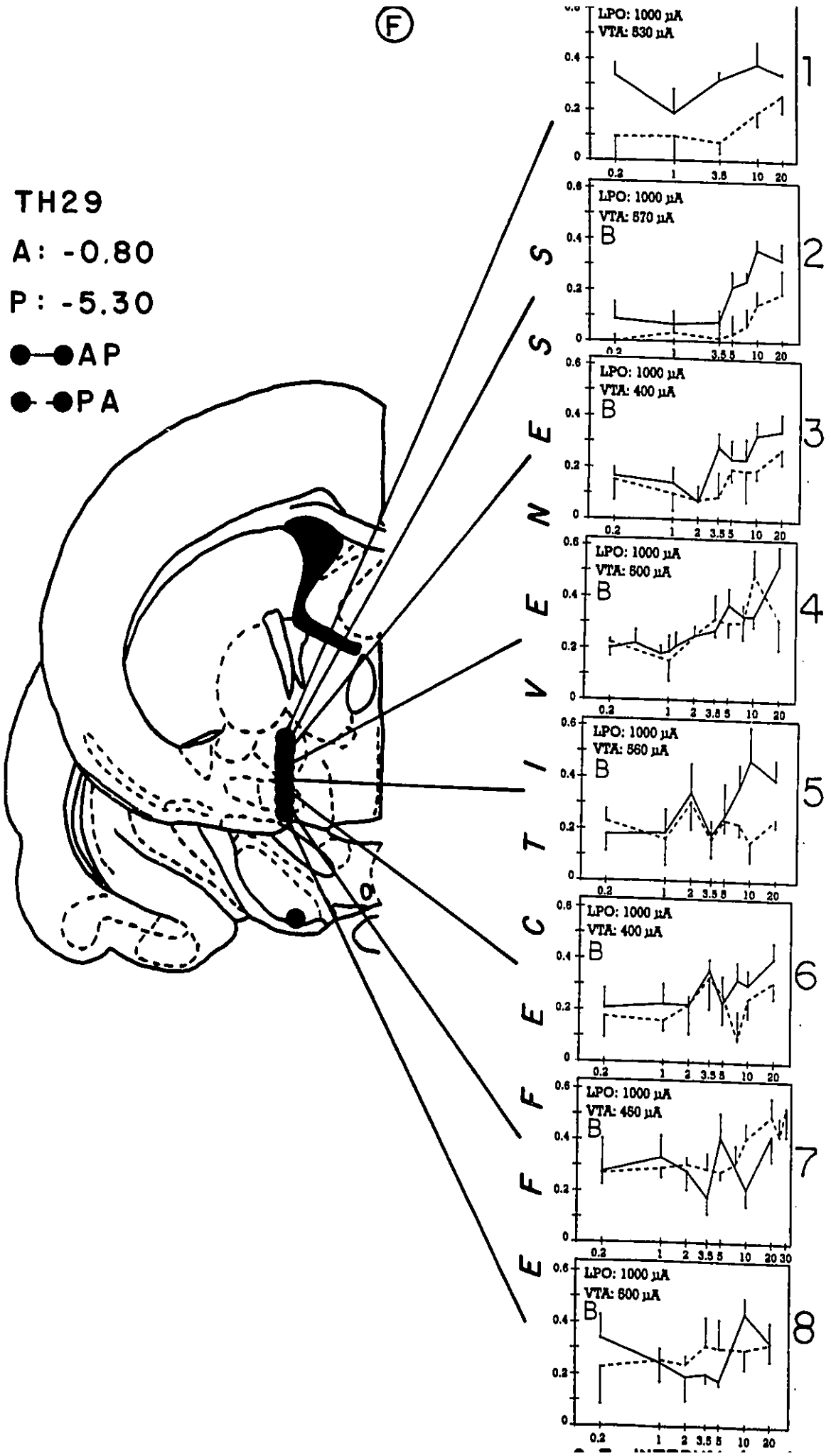
F
TH29
A: -0.80
P: -5.30
AP
PA
EFFECTIVENESS
LPO: 1000 µA
VTA: 830 µA
1
LPO: 1000 µA
VTA: 570 µA
B
2
LPO: 1000 µA
VTA: 400 µA
B
3
LPO: 1000 µA
VTA: 600 µA
B
4
LPO: 1000 µA
VTA: 560 µA
B
5
LPO: 1000 µA
VTA: 400 µA
B
6
LPO: 1000 µA
VTA: 460 µA
B
7
LPO: 1000 µA
VTA: 600 µA
B
8

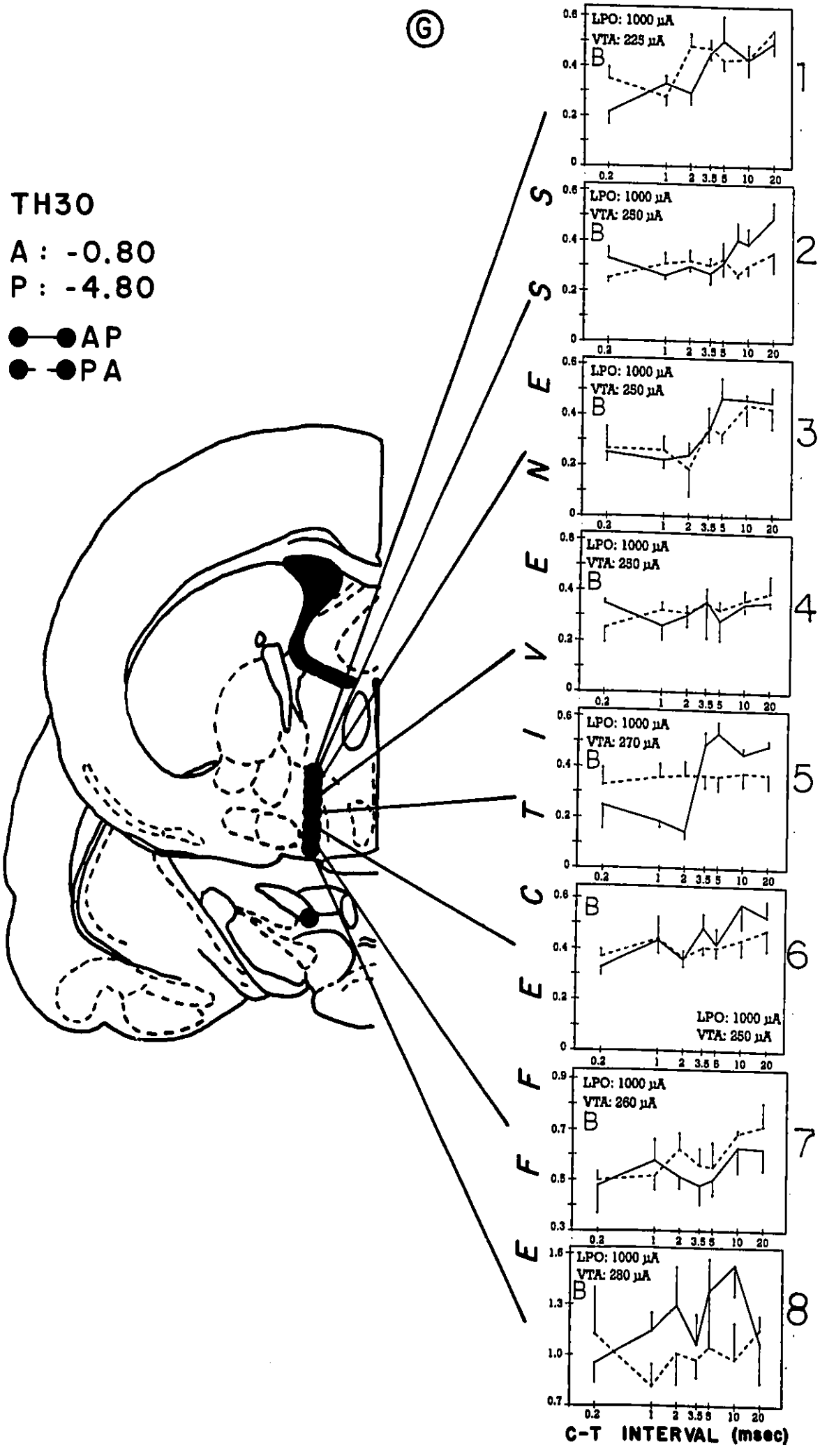
TH30
A : -0.80
P : -4.80
AP
PA
G
EFFECTIVENESS
LPO: 1000 µA
VTA: 225 µA
B
1
LPO: 1000 µA
VTA: 250 µA
B
2
LPO: 1000 µA
VTA: 250 µA
B
3
LPO: 1000 µA
VTA: 250 µA
B
4
LPO: 1000 µA
VTA: 270 µA
B
5
B
LPO: 1000 µA
VTA: 250 µA
6
LPO: 1000 µA
VTA: 260 µA
B
7
LPO: 1000 µA
VTA: 280 µA
B
8
0.2 1 2 3.5 5 10 20
C-T INTERVAL (msec)

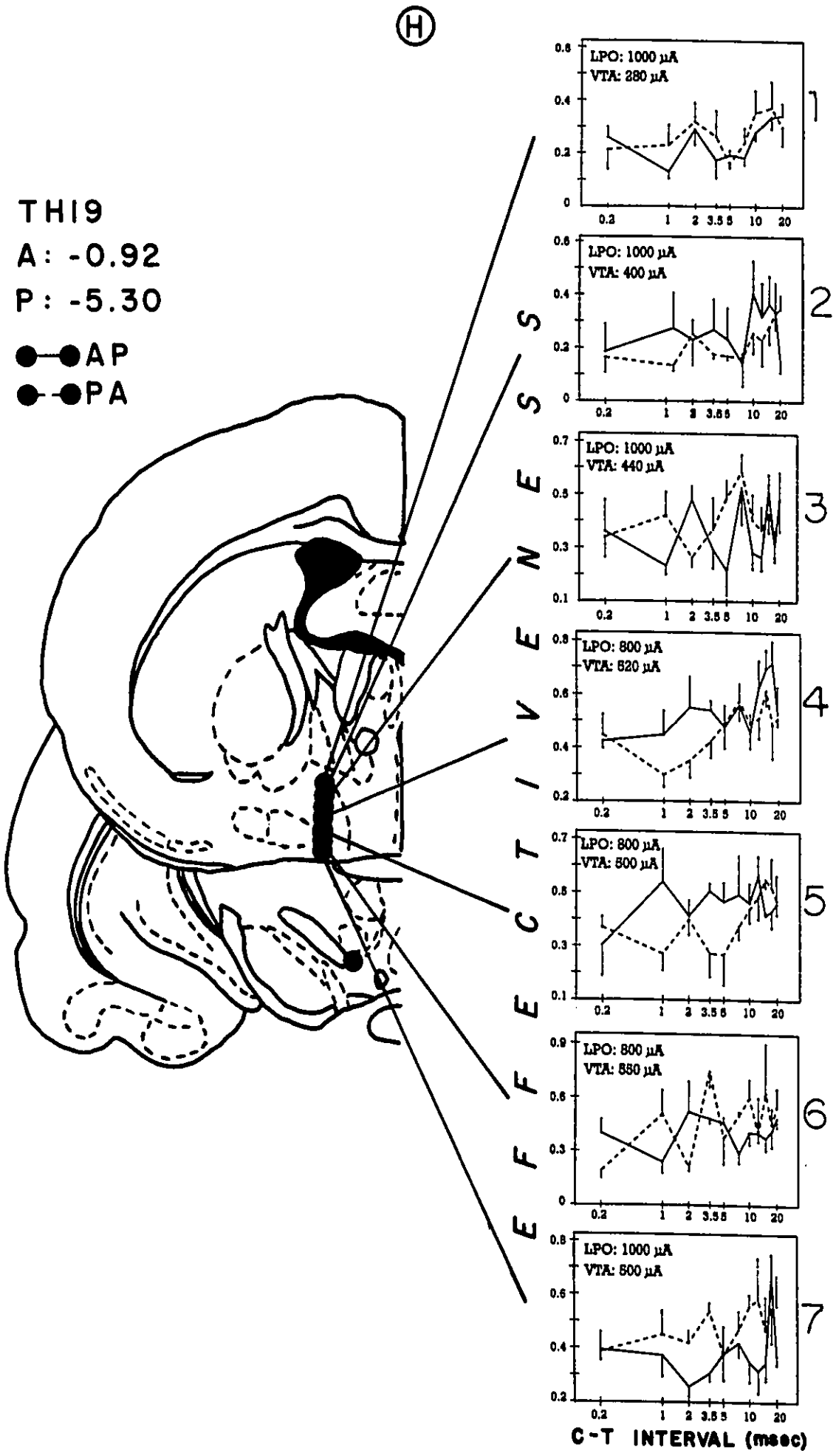
H
TH19
A: -0.92
P: -5.30
AP
PA
EFFECTIVENESS
LPO: 1000 µA
VTA: 280 µA
1
LPO: 1000 µA
VTA: 400 µA
2
LPO: 1000 µA
VTA: 440 µA
3
LPO: 800 µA
VTA: 520 µA
4
LPO: 800 µA
VTA: 600 µA
5
LPO: 800 µA
VTA: 880 µA
6
LPO: 1000 µA
VTA: 600 µA
7
0.2 1 2 3.5 5 10 20
C-T INTERVAL (msec)

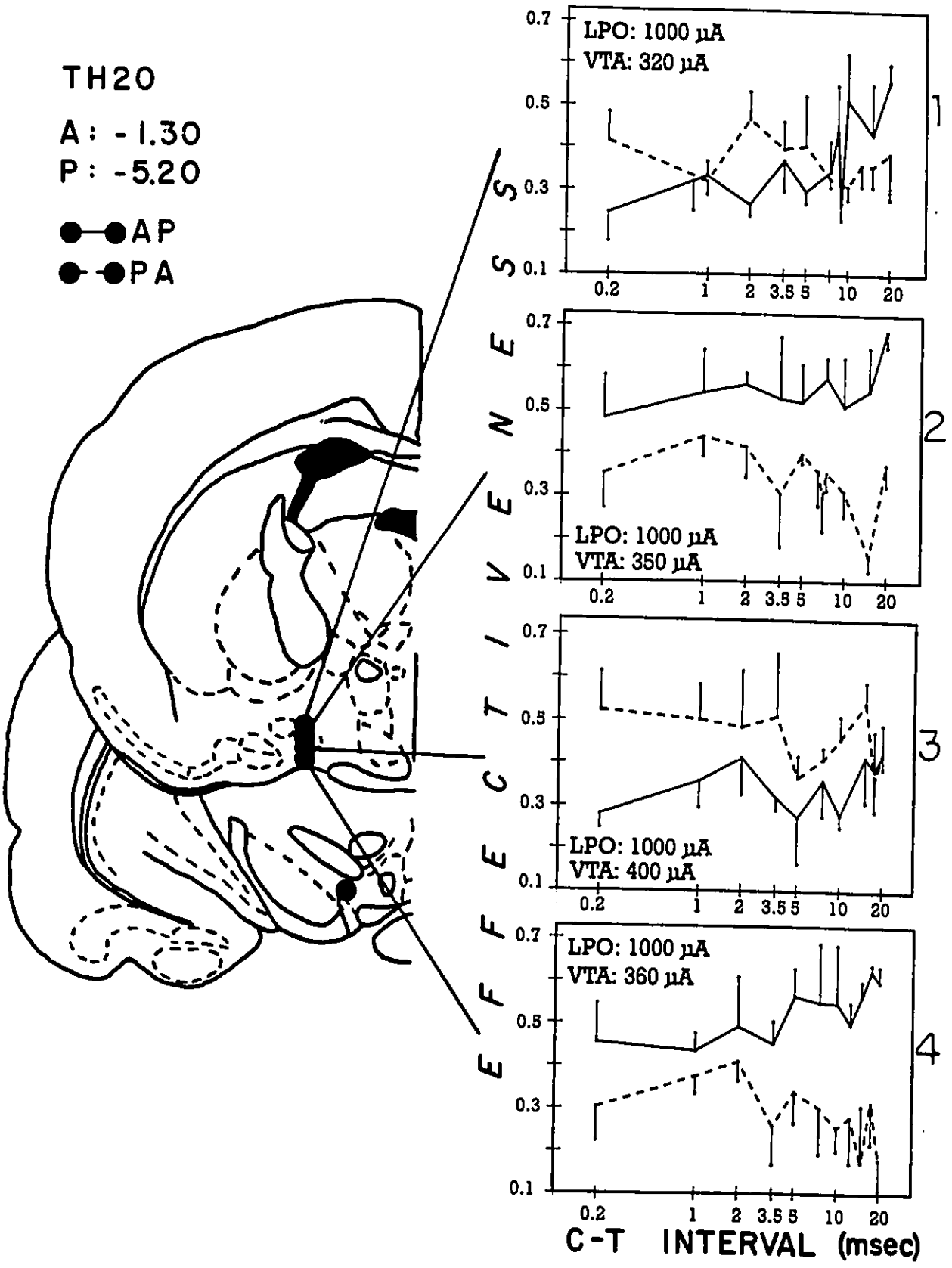
TH20
A : - 1.30
P : - 5.20
AP
PA
LPO: 1000 µA
VTA: 320 µA
LPO: 1000 µA
VTA: 350 µA
LPO: 1000 µA
VTA: 400 µA
LPO: 1000 µA
VTA: 360 µA
EFFECTIVENESS
0.7
0.5
0.3
0.1
0.2
1
2
3.5
5
10
20
1
2
3
4
C-T INTERVAL (msec)

any of the other subjects. The AP condition exhibited consistently higher E values than the PA curves for the two sets of collision curves, a range of 0.23 to 0.25 (AP) compared to 0.08 to 0.14 (PA). At the first site, both the AP and PA curves exhibited a gradual rise in E; this profile was absent in the second site.

The statistical analysis revealed a significant main effect of both factors, C-T interval and AP/PA condition, for the first stimulation site. The asymptote test indicated that, in the AP condition, the increase in E occurred between 1.0 and 3.5 msec while, in the PA condition, the same interval, 3.5 msec, was found to define both the upper and lower limits suggesting a continual rise (see Table 1). The AP/PA condition was the only significant factor that was obtained for the second stimulation site. The means collapsed across C-T interval were 0.23 in the AP condition and 0.08 in the PA.

TH21. The anterior electrode was found to pass through the LPO beginning just medial to the lateral division of the bed nucleus of the stria terminalis and ending just at the base of the brain; a total of seven sites were examined. The posterior electrode was located just dorsal to the LH and lateral to the submammillothalamic nucleus (see Figure 12b).

The collision profiles from the first four stimulation sites exhibited a fairly consistent pattern with the E levels for the PA curve usually higher than the AP one. Both curves showed a

Table 5

The Results of the Asymptote Test - Estimates of the Lower and Upper C-T Intervals Forming the Range Over Which E Values Increased.

Subject	Site	Curve	Lower C-T Interval	Upper C-T Interval	E Difference
TH27	1	AP	1.0	3.5	0.13
	1	PA	3.5	3.5	inconsistent
TH29	2	AP	3.5	10.0	0.26
	2	PA	7.5	5.0	inconsistent
	3	collapsed	3.5	3.5	inconsistent
	4	collapsed	1.0	10.0	0.23
	7	collapsed	10.0	20.0	0.17
TH30	1	collapsed	1.0	20.0	0.23
	2	collapsed	10.0	20.0	0.13
	3	collapsed	2.0	5.0	0.19
	6	collapsed	0.2	10.0	0.16
TH33	3	AP	2.0	3.5	0.09
	3	PA	5.0	10.0	0.16
	4	collapsed	5.0	10.0	0.11
TH36	2	AP	10.0	20.0	0.24
	2	PA	0.2	5.0	0.21
TH19	1	collapsed	1.0	10.0	0.12
	4	AP	10.0	12.5	0.15
	4	PA	3.5	5.0	0.14
TH21	3	collapsed	0.2	10.0	0.23

tendency to rise in the first three sites which appeared to start earlier as more ventral sites were tested. By the fourth site, the AP and PA curves appeared to be best described as flat lines with the PA curve exhibiting a higher average E value, 0.34, than the AP curve, 0.19. The results of the collision test for the remaining three sites yielded relatively flat profiles with a tendency for E values to increase at the longest C-T intervals.

Significant statistical results were obtained for four of the seven electrode placements, namely sites 2, 3, 4, and 7. The AP/PA factor was significant for site 2; the corresponding means were 0.19 (AP) and 0.26 (PA). The third stimulation site revealed a main effect of C-T interval due to the higher E values obtained as C-T interval was increased. When the AP and PA curves were collapsed, the asymptote test indicated that E increased between 0.2 and 10 msec (see Table 1). A significant AP/PA factor was obtained for site 4 with the PA curve exhibiting higher E values over almost the entire range of C-T intervals; the means were 0.19 (AP) and 0.34 (PA). This factor was also significant at site 7; the mean E values were 0.28 (AP) and 0.34 (PA).

TH34. The single anterior electrode site for this subject was located just ventromedial to the lateral ventricle at the border of the medial division of the bed nucleus of the stria terminalis and the septohypothalamic nucleus, a placement which

was the most dorsal of all the collision subjects. The posterior electrode was located within the lateral portion of the rostral VTA which, at this level, is not yet considered to be part of the MFB (see Figure 12c).

The AP and PA collision curves exhibited rises in E beginning at approximately the same C-T interval (1 msec); however, due to the large error associated with the E estimates, the results of the statistical analyses were not significant.

TH36. The anterior electrode was situated at the lateral border of the LPO and the ventral pallidum; the dorsoventral travel of the electrode, which gave rise to five stimulation sites, began at the most medial portion of the ventral pallidum and ended just dorsal to the ventral border of compartment 'b' of the MFB. The posterior electrode was located at the medial tip of the medial lemniscus just dorsal to the VTA which is classified as part of the MFB at this level (see Figure 12d).

The most prominent features of the five sets of collision curves were the increases in average E across sites and the disparity in E between the AP and PA curves. The AP curves rose from roughly 0.45 to 0.61 across sites and 0.29 to 0.63 in the PA case. Thus, the difference in E values between the two conditions was no longer evident in the more ventral sites and both curves exhibited concomitant increases in average E values at the last three stimulation sites.

Statistically significant results were obtained only in the first two sites. For site 1, the AP/PA factor was significant with respective means of 0.45 and 0.29. In the second stimulation site, both factors, AP/PA and C-T interval, reached significance; hence the asymptote test was conducted on the AP and PA curves separately; the estimated interval over which the E value increased was 10 to 20 msec for the AP curve and 0.2 to 5.0 msec for the PA curve (see Table 1).

TH33. The two anterior stimulation sites were located at the border between the LPO and the medial preoptic area just dorsal to the anteroventral preoptic nucleus. The posterior electrode was situated at the lateral border of the VTA and the substantia nigra pars compacta; the VTA is contained within the MFB at this level (see Figure 12e).

The two sets of collision curves for this subject showed a clear 'step', that is, an increase in E values, in the PA condition; the step occurred earlier at the first site, 2 versus 3.5 msec, but ended at the same interval, 10 msec, in both sites. A similar pattern was observed in the AP condition of site 1 but not site 2.

Statistically significant effects were obtained for both stimulation sites in this subject. The collision curves for the first placement yielded significant C-T interval and AP/PA factors. The intervals over which E increased were 2.0 to 3.5 msec for the AP curve and 5.0 to 10.0 msec for the PA curve

(see Table 1). At the second stimulation site, only the main effect of C-T interval reached significance; when the AP and PA curves were collapsed, the interval associated with increased E values was 5.0 to 10.0 msec.

TH29. The anterior electrode was situated just lateral to the LPO with the stimulation sites beginning in the dorsal portion of the substantia innominata and ending at the ventral border of compartment 'b' of the MFB; a total of eight sites was tested. The posterior electrode was located in the medial portion of the substantia nigra pars reticulata at the border between this structure and the cerebral peduncle (see Figure 12f).

The development of a step-like pattern appeared in the collision curves for the first four stimulation sites, with the rise in E values occurring earlier in the AP condition than in the PA one. The corresponding PA curves exhibited a similar, though reduced step pattern. This pattern, which was largely absent in sites 5 and 6, reappeared in site 7, but only in the PA condition and occurred between 5 to 20 msec.

The results from five of the eight electrode placements, sites 1 to 4, and site 7, were statistically significant, and are consistent with the observed patterns. There was a significant main effect of AP/PA condition in site 1 with mean E values of 0.31 (AP) and 0.14 (PA). Both factors, C-T interval and AP/PA condition, achieved significance in site 2;

the intervals over which the E values rose were 3.5 to 10 msec in the AP curve and 7.5 to 5.0 msec in the PA curve (see Table 1). Only the main effect of C-T interval was significant in sites 3 and 4; thus, the AP and PA curves were combined in each case. For site 3, both the upper and lower C-T interval was 3.5 msec, suggesting a gradual rise in this case, and 1.0 to 10 msec for site 4. Finally, the factor, C-T interval, was significant in site 7; in this case, the E value increased over intervals of 10.0 to 20.0 msec.

TH30. The anterior electrode for this subject passed through the center of the LPO beginning at the ventral border of the bed nucleus of the stria terminalis and ending at the supraoptic nucleus; this placement was slightly more medial than that for TH29. The posterior electrode was located dorsal to the VTA at the medial tip of the medial lemniscus (see Figure 12g).

Several of the stimulation sites for this subject gave rise to substantial step-like patterns in the AP condition, a less frequent observation when PA stimulation was delivered. At the first site, the rises in E values occurred at different C-T intervals, appearing earlier in the PA condition, 1 to 2 msec, than in the AP condition, 2 to 3.5 msec. A rise, observed later, was apparent only in the AP condition in the second stimulation site. At the third site, the steps reappeared, beginning at the same interval, 2 msec, but approaching an

asymptote earlier in the AP condition, 5 msec, versus 10 msec in the PA case. Again, the collision curves generated from the fifth stimulation site repeat the pattern seen at a more dorsal site (#2), although the step contributed by AP stimulation was the largest observed in the study. This profile was not evident at the next site; the sixth and seventh sites are characterized by higher E values in both conditions and relatively parallel functions. Exceptionally high E values and standard errors were observed at the most ventral site.

The main effect of C-T interval was significant in the first three stimulation sites. The collapsed AP and PA curves yielded the following estimates of the interval over which E increased - 1.0 to 20.0 msec, 10.0 to 20.0 msec, and 2.0 to 5.0 msec, respectively (see Table 1). Not surprisingly, at the fifth stimulation site, the distinctive shapes of the AP and PA conditions yielded a significant interaction term, between C-T interval and condition. Note that this was the only significant interaction recorded in the 44 analyses of this study. The data from the sixth stimulation site resulted in a significant C-T interval factor; the application of the asymptote test to the collapsed AP and PA curves revealed a rise in E between 0.20 and 10.0 msec (see Table 1).

TH19. The anterior electrode for this subject passed through the LPO, which at this level forms part of the MFB, beginning just ventral to the bed nucleus of the stria

terminalis and ending in the supraoptic nucleus; seven sites were tested. The posterior electrode was situated in the dorsal portion of the VTA at the medial tip of the medial lemniscus (see Figure 12h).

The collision curves for the first three stimulation sites exhibited highly variable E values from which no consistent pattern could be discerned. However, in the next two sites, the curves generated in the PA condition were more step-like in appearance, especially in site 4, while the AP curves were, on average, flat. The suggested step in site 4 extended over C-T intervals of 2 and 7.5 msec; the asymptotic E values in the PA curve and the average E value in the AP case were similar, 0.53 (PA) and 0.55 (AP). The final two stimulation sites showed highly irregular results in both the AP and PA conditions.

The findings from three of the seven stimulation sites, numbers 1, 4, and 7, yielded significant statistical effects. In the first site, the main effect of C-T interval was significant; the increase in E occurred between 1.0 and 10.0 msec (see Table 1). Both factors, C-T interval and AP/PA condition, reached significance in the fourth site; the E value increased between 10.0 and 12.5 msec in the AP condition and 1.0 and 10.0 msec in the PA condition (see Table 1). The most ventral stimulation site, number 7, gave rise to a significant difference between the average E values for AP and PA stimulation, 0.38 in the AP and 0.49 in the PA condition.

TH20. This subject had the only anterior placement located at the level of the LH; the electrode tip was found to originate at the dorsal border of the horizontal limb of the diagonal band and end at the supraoptic nucleus. The posterior electrode was situated in the lateral portion of the VTA just ventral to the medial lemniscus (see Figure 12i).

The shape of the four sets of collision curves for this subject appeared to be generally flat with large differences observed between the AP and PA conditions in sites 2 to 4; however, there was no consistent pattern observed in the position of the AP and PA curves. Indeed, for sites 2 and 4, the E values associated with the AP condition were faithfully higher than the E values obtained from PA stimulation while this pattern was reversed in site 3.

There was a significant difference between average E values associated with the AP and PA curves in all but the first stimulation site. At site 2, the means were 0.55 (AP) and 0.35 (PA), at site 3, 0.35 (AP) and 0.46 (PA), and 0.53 (AP) and 0.29 (PA) for site 4.

Refractory period results

A comparison of the effectiveness values obtained in the LPO and the VTA using the refractory period paradigm is illustrated in Figure 13. The data averaged across four subjects, TH29, TH30, TH27, TH22, are shown; for the LPO, 7 sites from both TH29 and TH30 and one site from TH27 and TH22 contribute to the

Figure 13. The composite refractory period curves obtained from the LPO and VTA are shown. The effectiveness of T pulse stimulation, relative to the C pulses alone, is plotted against C-T interval. The solid line represents the results from the LPO while the dashed line corresponds to the VTA data. The error bars indicate the standard error of the mean. The LPO estimate is based on 16 average refractory period curves, 7 sites in TH29 and TH30 and one site from TH27 and TH22. The use of fixed electrodes in the VTA permitted one refractory period estimate in each subject; thus, the VTA excitability cycle is based on 4 average refractory period curves.

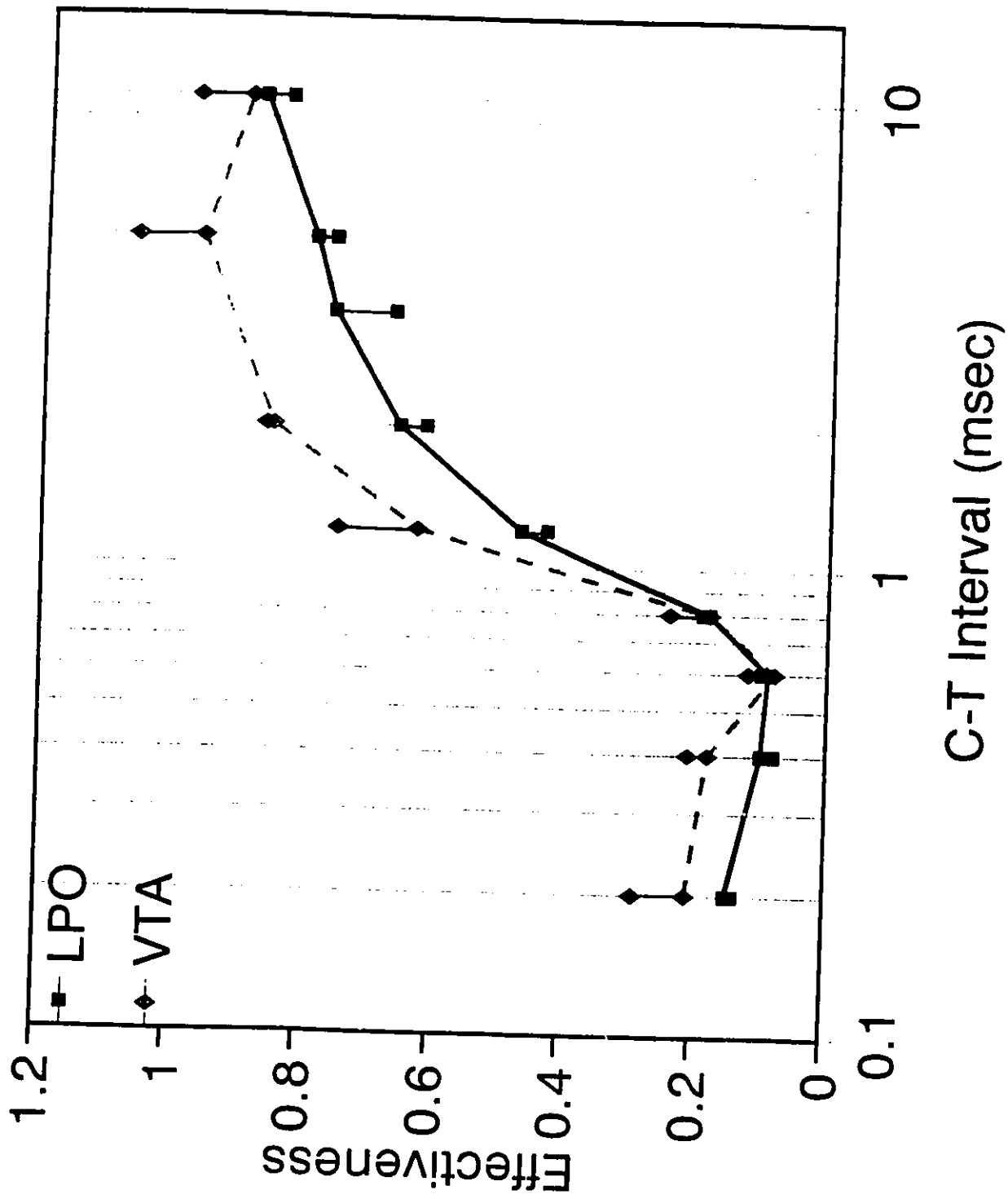
LPO
VTA
Effectiveness
1.2
1
0.8
0.6
0.4
0.2
0
0.1
1
10
C-T Interval (msec)

refractory period curve while for the VTA curve, which was evaluated with fixed electrodes, the data are based on the average results from each subject. Thus, the LPO curve comprises 16 average refractory period curves while the VTA result is based on 4 estimates. It appears that both sites began to recover from refractoriness at the same C-T interval, 0.6 msec; however, the asymptotic point, based on visual inspection, for the VTA occurred earlier, 2 msec, than in the LPO, 5 msec. The low standard error of the mean observed in both refractory period curves suggests that these collapsed curves are representative of the refractory period profile in individual sites and are consistent with those reported in other studies (Bielajew et al, 1981, 1982; Fouriezos et al, 1987; MacMillan et al, 1985; Schenk and Shizgal, 1982; Yeomans, 1979).

Discussion

The primary focus of this study was to determine if direct axonal connections exist between LPO and VTA reward neurons. In order to investigate this question, the behavioural adaptation of the collision paradigm (Shizgal et al, 1980) was employed which tests for collisions between orthodromic and antidromic action potentials produced by stimulating the same axon bundle at two different locations. Collision is inferred when there is an increase in double-pulse effectiveness over a

short range of C-T intervals and when the same profile occurs regardless of which site is stimulated first. None of the collision profiles in this study were consistent with the characteristics of axonal collision; instead, a model that has been developed to explain transynaptic collision (Shizgal, personal communication; Yeomans, 1990; Yeomans and Buckenham, 1992) is applied to the observed collision curves.

Axonal Collision

The simplest model of collision is one in which a direct axonal connection exists between two sites (Shizgal et al, 1980); the 'axonal' collision model, which has been the theoretical basis for such studies to date (Bielajew and Shizgal, 1982, 1986; Bielajew et al, 1987; Durivage and Miliaressis, 1987; Schenk and Shizgal, 1982; Shizgal et al, 1980), predicts that when the effectiveness of double-pulse stimulation is plotted against the C-T interval, a characteristic profile will result. At C-T intervals less than the interelectrode conduction time and refractory period, typically short intervals, during which collisions occur, double-pulse effectiveness will be low. Second, at intervals longer than the sum of the conduction time between the electrodes and the refractory period, effectiveness values will be high. Third, the delivery of the first pulse of each pair (C pulse) to either the anterior or posterior electrode should not affect the shape of the profile; that is, the two curves,

whether the C pulses are delivered to the anterior or posterior electrode first, should be symmetrical. When functions generated by the behavioural collision test meet the above criteria, the simplest interpretation is that at least a subset of the neurons underlying the behaviour at the two sites share the same axons.

In order for the axonal collision model to be a viable explanation in this study, the collision profiles had to yield the following statistical effects. First, only a significant main effect of C-T interval was expected; a significant AP/PA factor would have suggested an asymmetry in the two curves. Second, the results of the asymptote test had to yield reasonable estimates of the collision interval; for example, the estimated upper interval could not be shorter than the corresponding lower interval. Third, the increase in E over the collision interval had to be at least 0.20 units, a cut-off value that exceeded the permissible standard errors of the mean. Of the 44 sets of collision curves obtained, only three, TH21 site 3, TH30 site 1, and TH29 site 4, appeared to suggest, on visual inspection and the results of the statistical analyses, that axonal collision had occurred.

In each of the three candidate cases, there is reason to suspect the applicability of the axonal collision model. In the first case, site 3 for TH21 (see Figure 12b), the estimated collision interval ranged from 0.2 to 10.0 msec. This interval

must exceed the sum of the conduction time between electrodes and the refractory period; since the start of recovery from refractoriness for both LPO and VTA reward neurons began at 0.4 msec, the above collision interval is far too short to propose that collision-like effects were being observed. The first stimulation site for TH30 (see Figure 12g) yielded a collision interval of 1.0 to 10.0 msec over which E increased 0.23 units; however, on inspection of the graph, it is apparent that the two collision curves rise over different intervals, 1.0 to 2.0 msec for the PA condition and 2.0 to 3.5 msec for the AP condition. This pattern does not fit the symmetric profile predicted by the axonal collision model. The final stimulation site was site 4 for TH29 (see Figure 12f) in which the collision interval was estimated to range from 1.0 to 10.0 msec. As in the previous case, an inspection of the collision curves indicates an asymmetry in the duration of the collision intervals, 1.0 to 5.0 msec (AP) versus 1.0 to 10.0 msec (PA); however, it is possible that the early symmetrical step reflects some contribution of axonal collisions. In general, though, the axonal collision model does not appear to characterize the profiles.

Transynaptic Model

An alternative to the axonal collision model is one in which a synapse is interposed between the two electrodes, termed the 'transynaptic' collision model (Shizgal, personal

communication; Yeomans, 1990; Yeomans and Buckenham, 1992). The principal effect of a synapse, due to the unidirectional nature of synaptic transmission, is that collisions between antidromic and orthodromic action potentials can occur only on the post-synaptic membrane between the soma and the stimulating electrode. As a result, the delivery of C pulses to either the anterior or posterior electrode influences the shape of the collision profiles, yielding asymmetric AP and PA functions. In order to simplify the derivation of collision profiles predicted by the transynaptic collision model several assumptions must be made. First, as in the axonal collision model, the component of the excitability cycle that is assumed to contribute, in part, to the collision interval is the absolute refractory period. Second, the synaptic transmission time is presumed to vary randomly. Third, the antidromic action potentials generated at the post-synaptic stimulation site have no effect on the conduction characteristics of the soma of the post-synaptic neuron.

Given these assumptions, there are three important time intervals to be considered (see Figure 14). These are the time for the orthodromic action potential generated at electrode A to conduct to the initial segment of the post-synaptic neuron (referred to as the pre-synaptic conduction time or t_1), the time for the antidromic action potential generated at electrode B to travel to the soma (called the post-synaptic conduction

Figure 14. The three collision profiles predicted by the transynaptic collision model are illustrated (Shizgal, personal communication). At the top of the figure is shown a simplified model of the collision test when a synapse is located between the two stimulating electrodes, A and B. The pre-synaptic conduction time, denoted by t_1, represents the time for an orthodromic action potential to travel from electrode A to the initial segment of the second neuron. The post-synaptic conduction time, t_2, denotes the time for an antidromic action potential to travel from electrode B to the soma of the second neuron. The three collision graphs illustrate the different profiles that are predicted as a result of altering the relationship between t_1 and t_2. The solid line shows the condition where the C pulse is delivered to electrode A and the T pulse to electrode B; the dashed line represents the opposite condition where the C pulse is delivered to electrode B and the T pulse to electrode A.

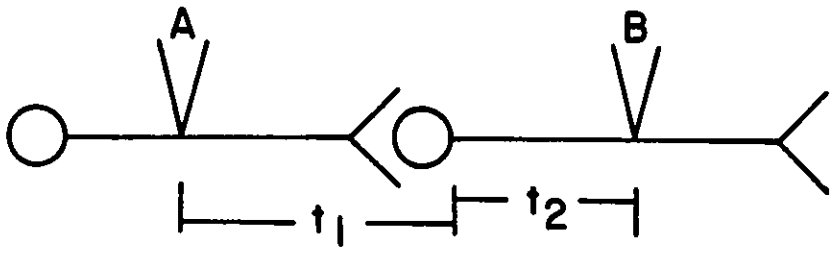

A) $t_1 > t_2$

——A - B

- - - -B - A

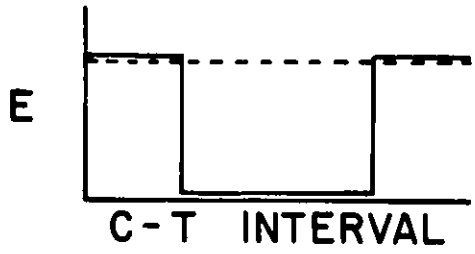

B) $t_1 < t_2$

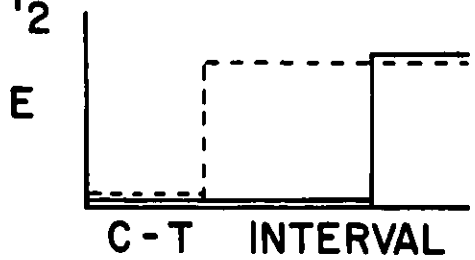

C) $t_1 = t_2$

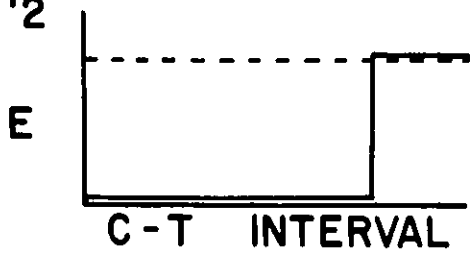

time or t_2), and the refractory period of the membrane that is directly stimulated by electrode B (r_B). When all possible relationships between t_1 and t_2 are taken into account, $t_1 > t_2$, $t_1 < t_2$, and $t_1 = t_2$, three 'ideal' collision profiles can be modelled.

The collision curves that result when $t_1 > t_2$ are illustrated in Figure 14a. When the C pulse is delivered to electrode A, collision will be observed when the C-T interval is greater than the difference between the pre-synaptic and post-synaptic conduction times ($t_1 - t_2$) and less than the total time for the C pulse to conduct past electrode B plus the time for the membrane under electrode B to recover from refractoriness ($t_1 + t_2 + r_B$). Before and after this collision interval, double-pulse effectiveness will be maximal. When the C pulse is delivered to electrode B, collision will never be observed since the T pulse (to electrode A) can not be delivered at a sufficiently short C-T interval to reach the post-synaptic membrane before the effects of the antidromic action potential generated at B have dissipated; thus, double-pulse effectiveness will always be at a maximum.

When $t_1 < t_2$, a collision profile similar to that shown in Figure 14b is theorized. When the C pulse is delivered to electrode A, collision will occur at all C-T intervals that are less than the total time for the orthodromic action potential from site A to conduct past electrode B plus the time for the

membrane to recover from refractoriness ($t_1 + t_2 + r_B$); this would result in a longer collision interval than in the first scenario. The delivery of the C pulse to electrode B would result in collision being observed only when the C-T interval was less than the difference between the post-synaptic and pre-synaptic conduction times ($t_2 - t_1$); the collision interval in this instance would be shorter than the one observed when the C pulse was delivered to electrode A.

The final variation to the transynaptic collision model arises from the case in which $t_1 = t_2$ (see Figure 14c). When the C pulse is delivered to electrode A, collision will be observed at every C-T interval that is less than the conduction time of the orthodromic action potential generated by electrode A to pass electrode B and the membrane under B to recover from refractoriness ($t_1 + t_2 + r_B$). In the other condition, when the C pulse is delivered to electrode B, collision will never occur since, at any C-T interval, the T pulse, delivered to electrode A, will not have time to reach the post-synaptic element before the effects of the antidromic action potential generated at electrode B have dissipated.

Before the transynaptic model can be applied to data obtained in behavioural studies, several alterations to the above 'ideal' collision curves must be made. It was assumed that each pre-synaptic action potential would generate a post-synaptic action potential 100% of the time; in reality, this

would likely not occur. The probability of initiating a post-synaptic action potential should set the upper limit for the size of the observed collision effect, suggesting that the increases in double-pulse effectiveness should be smaller for transynaptic collision than for axonal collision. A further limit on the size of the collision effect is the case in which the electrodes are misaligned; as in the axonal collision model, the collision effect would be decreased since only a subset of the behaviourally relevant fibers would be stimulated by both electrodes. An additional caveat to the 'ideal' transynaptic model is that the experimentally obtained collision intervals should span a wider range than those observed in axonal collision since the pre- and post-synaptic conduction times in the stimulated population will undoubtedly vary more (Yeomans, 1990).

With this model in mind, the collision curves obtained in this study were re-examined. In four of the nine subjects, curves resembling two of the three variations of the transynaptic model were observed. The second type of collision curve (see Figure 14b), where both the AP and PA curves rise but at offset intervals, was seen in TH29 sites 2 and 3 (see Figure 12f) and TH30 sites 1 and 3 (see Figure 12g). The third transynaptic collision profile (see Figure 14c), where one curve exhibits a rise in E while the other has consistently high values, was observed in TH33 site 2 (see Figure 12e), TH19

site 4 (see Figure 12h), and TH30 site 5 (see Figure 12g). In general, the electrodes in these subjects, both the anterior and posterior ones, were correctly located in the LPO and VTA and were situated more caudally than those for the other subjects.

The collision intervals generally had a wider range of values, compatible with the expectation that the conduction velocities of the population of pre- and post-synaptic neurons would not be the same. The longer collision intervals were suggestive that the directly stimulated population had slower conduction times than in other collision studies (Bielajew and Shizgal, 1980; Durivage and Miliaressis, 1987; Shizgal et al, 1980); this was reflected by the LPO refractory period estimates (see Figure 13) which showed continued recovery until 5.0 msec.

One disadvantage of the transynaptic model is that, unlike the axonal one, the two stimulated populations are not required to have, and likely do not have, matching conduction velocities; as a result, it is difficult to use these data to estimate conduction velocities. However, an advantage of the transynaptic model is that the direction of conduction can be inferred from the obtained collision profiles without additional tests (Bielajew and Shizgal, 1986; Yeomans, 1990); each of the three predicted collision curves can be obtained by only one particular orientation of the substrate. In this

study, the earlier rise in the AP curve observed in sites 2 and 3 for TH29 and site 3 for TH30 correspond to the second transynaptic profile (see figure 14b) while site 5 for TH30 and site 2 for TH33 fit the third model (see figure 14c); in all of these cases, caudorostral conduction, from the VTA to the LPO, was implicated. A rostrocaudal orientation, LPO to VTA, was suggested for the remaining case, site 1 in subject TH30, since the PA curve exhibited an earlier rise in effectiveness. Thus, a caudorostral direction of conduction accounts for six of seven cases.

Miscellaneous patterns

Of the remaining collision curves in this study none fit the three profiles described by the transynaptic collision model. An overall characteristic of the curves was the low levels of E that were observed, ranging generally, between 0 and 0.30. In addition, there were several patterns of results that were consistently obtained. For the most part, these curves were flat lines; gradual increases in E, with no discernable 'step', as the C-T interval increased to a maximum of 20.0 msec, were frequently observed. This pattern is inconsistent with the predictions of either the axonal or transynaptic collision model; both of these models require a step-like pattern in at least one of the curves. However, they do parallel the shapes of effectiveness curves obtained from double-pulse stimulation of the LH and PAG (Bielajew et al, 1981).

Substantial differences in summation levels between the AP and PA curves were often noted; the AP curve exhibited higher average E values than the PA condition in 10 instances, while the reverse, PA greater than AP, was seen in 4 cases. A third pattern that was observed was an increase in E values in the same animal as more ventral sites were tested; this was especially evident in the case of subject TH36. Finally, the last profile was the observation of a step-like pattern in one of the collision curves associated with low E levels and a flat line in the other curve; although reminiscent of one of the profiles predicted by the transynaptic model, the summation values associated with the flat lines were too low.

Conclusion

The purpose of this study was to evaluate whether direct axonal connections exist between self-stimulation neurons in the LPO and the VTA. While axonal collision was not observed, its absence should not be interpreted to suggest that such an organization does not exist. A number of reasons could account for the negative result including the possibility that the electrodes were misaligned, a prospect that becomes more of a factor as the distance between the electrodes is increased. In order to account for some of the recurring patterns that were observed in the 44 pairs of sites, the transynaptic collision model was examined; the profiles exhibited by the majority of the collision curves could not be accounted for by this model.

However, four of the nine subjects exhibited, at a few sites, profiles indicative of a caudorostral direction of conduction. This result is different from that reported by Bielajew and Shizgal (1986) where a combination of the collision test and an anodal block technique indicated a rostrocaudal direction of conduction between reward neurons in the LH and VTA.

The behavioural adaptation of the collision test is, at present, the only means by which the functional connectivity between two sites can be directly addressed. While the introduction of moveable electrodes has immeasurably enhanced the probability of observing axonal collision, a further refinement would be the addition of electrophysiological techniques. Already, single unit collision tests have been conducted on cells that were antidromically activated by LH and VTA stimulating electrodes (Rompre and Shizgal, 1986); this procedure, if introduced as a pre-screening strategy, has significant merit. Collision would likely not be observed between two sites that fail to exhibit antidromic activation following electrical stimulation at the opposing location, while the observation of antidromic activation suggests some form of connectivity, which potentially may be related to reward fibers. Thus, the use of an electrophysiological pre-screening procedure coupled with moveable electrodes has the prospective to significantly improve the current hit rate of the collision test.

General Conclusion

These studies comprise a detailed examination of BSR in the LPO. The specific issues that were addressed were 1) the stability of the refractory periods of these neurons to benzodiazepine challenge, 2) the spatial organization and density of LPO reward fibers, and 3) their functional connectivity to a caudally located site, the VTA.

It is well known that stimulation-elicited behaviours in anterior brain sites, such as the LPO, are often accompanied by the development and full production of motor seizures. The first experiment in this dissertation showed that brotizolam, a novel benzodiazepine with anticonvulsant properties, may be a useful tool in BSR studies. Not only was this drug capable of controlling the incidence of motor seizures during repeated test sessions, but it did so for up to six hours with no apparent decrease in efficacy; this property is important given the lengthy test sessions that characterize parametric paradigms in BSR. In addition, estimates of the refractory period were unchanged following brotizolam administration, indicating that, at least this electrophysiological property of the directly stimulated neurons was not altered by the drug.

The investigation of LPO self-stimulation included the determination of the relative density of the substrate. In experiment 2, it was found that sites that supported BSR were

located throughout the extent of the LPO and compartments 'a' and 'b' of the MFB while negative sites were situated medially, for example in the medial preoptic area, and at more anterior locations. The positive placements followed a trajectory that moved progressively more laterally towards caudal sites, a pattern that is consistent with anatomical descriptions of the MFB (Paxinos and Watson, 1986). The LPO has been described as a diffusely organized region (Veening et al, 1982); similarly, the results of this study suggest that the reward substrate in the LPO is homogeneously organized with a distribution less dense than that found in the LH.

There is a myriad of evidence, derived from anatomical, metabolic, electrophysiological, and parametric studies, to suggest that direct functional connectivity exists between LPO and VTA self-stimulation neurons (Bielajew et al, 1981, 1982, 1987; Fouriezos et al, 1987; Gallistel et al, 1985; Janas and Stellar, 1987; MacMillan et al, 1985; Murray and Shizgal, 1991; Nieuwenhuys et al, 1982; Phillipson, 1979; Schenk and Shizgal, 1982; Shizgal, 1989; Shizgal et al, 1980, 1989; Swanson, 1976; Waraczynski, 1988; Yeomans, 1979). The third experiment, which directly examined this hypothesis using the behavioural adaptation of the collision test (Shizgal et al, 1980), did not yield typical examples of collision-like effects; indeed, in only one of forty-four cases, was the presence of axonal collision between the LPO and VTA intimated. Far more

prevalent were double-pulse effectiveness profiles that were suggestive of transynaptic collision effects (Yeomans, 1990); the most prominent feature of these collision curves was the marked asymmetry between the AP and PA conditions.

While estimating conduction velocity is difficult in the case of transynaptic collision, due to factors such as the unknown positions of the electrodes relative to the synapse, the duration of synaptic delay, and the possibility of different pre- and post-synaptic neurons, the model does allow the direction of conduction to be inferred from the shapes of the curves (Shizgal, personal communication). That is, under the assumptions of the model, each observed profile can be obtained from only one of three possible configurations. While a rostrocaudal direction of conduction has been suggested between the LH and the VTA using the anodal block technique (Bielajew and Shizgal, 1986), a caudorostral direction of conduction was implicated in six of seven sites in this study.

The MFB is known to contain significant numbers of both ascending and descending fiber components (Nieuwenhuys et al, 1982); one of the more important ascending systems, originating in the VTA, that has played a pivotal role in BSR history is the mesolimbic dopaminergic system (Ungerstedt, 1971). However, in this study, the results are not consistent with a role of the ascending dopaminergic system in mediating the collision-like effects; the suggestion of at least one synapse

located between the VTA and LPO eliminates the continuous mesolimbic dopamine system as a candidate fiber system.

The observation of collision-like effects consistent with the axonal model strongly suggests that the two sites in question are functionally connected by the same fiber bundle. However, the interpretation is less clear when such effects are not observed. In this study, the absence of axonal collision profiles may not reflect the lack of direct functional connectivity between the LPO and VTA reward neurons; a plausible explanation is that the effective stimulation fields were misaligned. However, an alternative arrangement, as inferred from the transynaptic model, can be proposed in which at least one synapse interrupts neural conduction flowing between the VTA and the LPO. One implication of this hypothesis is that the LPO sites investigated in the third study are not the location of the cell bodies of origin for the descending reward pathway that has been shown to course between the LH and VTA self-stimulation (Bielajew and Shizgal, 1986); the transynaptic model and the direction of conduction imply that these LPO reward neurons are both separate and lie downstream from the VTA reward substrate.

"The state of mind which enables a man to do work of this kind is akin to that of the religious worshipper or lover. The daily effort comes...straight from the heart."

Albert Einstein

References

Bielajew, C. H. (1983). Psychophysical inference of the direction of normal conduction in the substrate for medial forebrain bundle self-stimulation. Unpublished doctoral dissertation, Concordia University, Montreal.

Bielajew, C. H. (1991). Distribution of cytochrome oxidase in response to rewarding brain stimulation: effect of different pulse durations. *Brain Research Bulletin*, **26**, 379-384.

Bielajew, C. and Fouriezos, G. (1985). Post-stimulation excitability of mediodorsal thalamic self-stimulation. *Behavioural Brain Research*, **17**, 97-102.

Bielajew, C., Harris, T., and Parkin, E. (in preparation). Brotizolam attenuates stimulation-induced motor seizures without altering refractory periods of reward neurons in the LPO.

Bielajew, C., Jordan, C., Ferme-Enright, J., and Shizgal, P. (1981). Refractory periods and anatomical linkage of the substrates for lateral hypothalamic and periaqueductal gray self-stimulation. *Physiology and Behavior*, **27**, 95-104.

Bielajew, C., Lapointe, M., Kiss, I., and Shizgal, P. (1982). Absolute and relative refractory periods of the substrates for lateral hypothalamic and ventral midbrain self-stimulation. *Physiology and Behavior*, **28**, 125-132.

Bielajew, C. and Shizgal, P. (1980). Dissociation of the substrates for medial forebrain bundle self-stimulation and stimulation-escape using a two-electrode stimulation technique. *Physiology and Behavior*, **25**, 707-711.

Bielajew, C. and Shizgal, P. (1982). Behaviorally derived measures of conduction velocity in the substrate for rewarding medial forebrain bundle stimulation. *Brain Research*, **237**, 107-119.

Bielajew, C. and Shizgal, P. (1986). Evidence implicating descending fibers in self-stimulation of the medial forebrain bundle. *Journal of Neuroscience*, **6**, 919-929.

Bielajew, C., Thrasher, A., and Fouriezos, G. (1987). Self-stimulation sites in the lateral hypothalamic and lateral preoptic areas are functionally connected. *Canadian Psychology Abstracts*, **28**, 2a.

Bishop, M. P., Elder, S. T., and Heath, R. G. (1963). Intracranial self-stimulation in man. *Science*, **140**, 394-396.

Blander, A. and Wise, R. A. (1989). Anatomical mapping of brain stimulation reward sites in the anterior hypothalamic area: special attention to the stria medullaris. *Brain Research*, **48**, 12-16.

Boke-Kuhn, K., Danneberg, P., Kuhn, F. J., and Lehr, E. (1986). Antiemotional and anticonvulsant activity of brotizolam and its effects on motor performance in animals. *Drug Research*, **36**, 528-531.

Bower, G. H. and Miller, N. E. (1958). Rewarding and punishing effects from stimulating the same place in the rat's brain. *Journal of Comparative and Physiological Psychology*, **51**, 669-674.

Boyd, E. S., and Gardner L. C. (1962). Positive and negative reinforcement from intracranial stimulation of a teleost. *Science*, **136**, 648-649.

Cagguila, A. R. and Hoebel, B. G. (1966). "Copulation-reward site" in the posterior hypothalamus. *Science*, **153**, 1284-1285.

Clavier, R. M. and Gerfen, C. R. (1982). Intracranial self-stimulation in the thalamus of the rat. *Brain Research Bulletin*, **8**, 353-358.

Cooper, R. and Taylor, L. (1967). Thalamic reticular system and central gray: self-stimulation. *Science*, **156**, 102-103.

Corbett, D., Fox, E., and Milner, P. M. (1982). Fiber pathways associated with cerebellar self-stimulation in the rat: a retrograde and anterograde tracing study. *Behavioural Brain Research*, **6**, 167-184.

Corbett, D., Laferriere, A., and Milner, P. M. (1982). Elimination of medial prefrontal cortex self-stimulation following transection of efferents to the sulcal cortex in the rat. *Physiology and Behaviour*, **29**, 425-431.

Corbett, D., Skelton, R. W., and Wise, R. A. (1977). Dorsal bundle lesions fail to disrupt self-stimulation from the region of the locus coeruleus. *Brain Research*, **133**, 37-44.

Durivage, A. and Miliaressis, E. (1987). Anatomical dissociation of the substrates of medial forebrain bundle self-stimulation and exploration. *Behavioral Neuroscience*, **101**, 57-61.

Edmonds, D. E. and Gallistel, C. R. (1974). Parametric analysis of brain stimulation reward in the rat: III. Effect of performance variables on the reward summation function. *Journal of Comparative and Physiological Psychology*, **87**, 876-883.

Edmonds, D. E. and Gallistel, C. R. (1977). Reward versus performance in self-stimulation: electrode-specific effects of ∝-methyl-p-tyrosine on reward in the rat. *Journal of Comparative and Physiological Psychology*, **91**, 962-974.

Edmonds, D. E., Stellar, J. R., and Gallistel, C. R. (1974). Parametric analysis of brain stimulation reward in the rat: II. Temporal summation in the reward system. *Journal of Comparative and Physiological Psychology*, **87**, 860-869.

Ferssiwi, A., Cardo, B., and Velley, L. (1987). Electrical self-stimulation in the parabrachial area is depressed after ibotenic acid lesion of the lateral hypothalamus. *Behavioural Brain Research*, **25**, 109-116.

Fouriezos, G., Bielajew, C., and Pagotto, W. (1990). Task difficulty increases thresholds of rewarding brain stimulation. *Behavioural Brain Research*, **37**, 1-7.

Fouriezos, G., Walker, S., Rick, J., and Bielajew, C. (1987). Refractoriness of neurons mediating intracranial self-stimulation in the anterior basal forebrain. *Behavioural Brain Research*, **24**, 73-80.

Gallistel, C. R. (1978). Self-stimulation in the rat: Quantitative characteristics of the reward pathway. *Journal of Comparative and Physiological Psychology*, **92**, 977-998.

Gallistel, C. R., Gomita, Y., Yadin, E., and Campbell, K. A. (1985). Forebrain origins and terminations of the medial forebrain bundle metabolically activated by rewarding stimulation or by reward-blocking doses of pimozide. *The Journal of Neuroscience*, **5**, 1246-1261.

Gallistel, C. R., Shizgal, P., and Yeomans, J. S. (1981). A portrait of the substrate for self-stimulation. *Psychological Review*, **88**, 228-273.

Glimcher, P. W. and Gallistel, C. R. (1988). Small lesions in the anterior ventral tegmental area (VTA) attenuate the rewarding efficacy of lateral hypothalamic (LH) self-stimulation. *Society for Neuroscience Abstracts*, **14**, 1101.

Gratton, A. and Wise, R. A. (1988). Comparisons of refractory periods for medial forebrain bundle fibers subserving stimulation-induced feeding and brain stimulation reward: a psychophysical study. *Brain Research*, **438**, 256-263.

Gratton, A. and Wise, R. A. (1988). Comparisons of connectivity and conduction velocities for medial forebrain bundle fibers subserving stimulation-induced feeding and brain stimulation reward. *Brain Research*, **438**, 264-270.

Haefely, W. E. (1987). Structure and function of the benzodiazepine receptor. *Chimia*, **41**, 389-396.

Haefely, W. E. (1990). The GABA-benzodiazepine interaction fifteen years later. *Neurochemical Research*, **15**, 169-174.

Harris, T. and Bielajew, C. (1988). *An examination of current/frequency tradeoffs of rewarding brain stimulation along the medial forebrain bundle*. presented at the Milner Reward and Reinforcement Conference. Montreal, Quebec.

Hoebel, B. G. and Teitelbaum, P. (1962). Hypothalamic control of feeding and self-stimulation. *Science*, **135**, 375-377.

Huston, J. P. and Borbely, A. A. (1973). Operant conditioning in forebrain ablated rats by use of rewarding hypothalamic stimulation. *Brain Research*, **50**, 467-472.

Huston, J. P. and Borbely, A. A. (1974). The thalamic rat: General behavior, operant learning with rewarding hypothalamic stimulation, and effects of amphetamine. *Physiology and Behavior*, **12**, 433-448.

Huston, J. P., Kiefer, S., Buscher, W., and Munoz, C. (1987). Lateralized functional relationship between the preoptic area and lateral hypothalamic reinforcement. *Brain Research*, **436**, 1-8.

Janas, J. D. and Stellar, J. R. (1987). Effects of knife-cut lesions of the medial forebrain bundle in self-stimulating rats. *Behavioral Neuroscience*, **101**, 832-845.

MacMillan, C. J., Simantirakis, P., and Shizgal, P. (1985). Self-stimulation of the lateral hypothalamus and ventrolateral tegmentum: Excitability characteristics of the directly stimulated substrates. *Physiology and Behavior*, **35**, 711-723.

McClelland, R. C., Sarfaty, T., Hernandez, L., and Hoebel, B. G. (1989). The appetite suppressant, d-fenfluramine, decreases self-stimulation at a feeding site in the lateral hypothalamus. *Pharmacology, Biochemistry and Behavior*, **32**, 411-414.

McGregor, J. S. and Atrens, D. M. (1991). Prefrontal cortex self-stimulation and energy balance. *Neuroscience*, **105**, 870-883.

Mendelson, J. (1967). Lateral hypothalamic stimulation in satiated rats: the rewarding effects of self-induced drinking. *Science*, **157**, 1077-1079.

Miliaressis, E. (1981). A miniature, moveable electrode for brain stimulation in small animals. *Brain Research Bulletin*, **7**, 715-718.

Miliaressis, E. and Malette, J. (1987). Summation and saturation properties in the rewarding effect of brain stimulation. *Physiology and Behaviour*, **41**, 595-604.

Miliaressis, E. and Rompre, P.-P. (1980). Self-stimulation and circling: differentiation of the neural substrata by behavioral measurement with the use of a double pulse technique. *Physiology and Behavior*, **25**, 939-943.

Miliaressis, E., and Rompre, P.-P. (1987). Effects of concomitant motor reactions on the measurement of rewarding efficacy of brain stimulation. *Behavioral Neuroscience*, **101**, 827-831.

Miliaressis, E., Rompre, P.-P., and Durivage, A. (1982). A psychophysical method for mapping behavioral substrates using a moveable electrode. *Brain Research Bulletin*, **8**, 693-701.

Miliaressis, E., Rompre, P.-P., Laviolette, P., Philippe, L., and Coulombe, D. (1986). The curve-shift paradigm in self-stimulation. *Physiology and Behavior*, **37**, 85-91.

Mundl, W. J. (1980). A constant-current stimulator. *Physiology and Behavior*, **24**, 991-993.

Munoz, C., Keller, I., and Huston, J. P. (1985). Evidence for a role of the preoptic area in lateral hypothalamic self-stimulation. *Brain Research*, **358**, 85-95.

Murray, B. and Shizgal, P. (1991). Anterolateral lesions of the medial forebrain bundle increase the frequency threshold for self-stimulation of the lateral hypothalamus and ventral tegmental area in the rat. *Psychobiology*, **19**, 135-146.

Nieuwenhuys, R., Geeraedts, L. M. G., and Veening, J. G. (1982). The medial forebrain bundle of the rat. I. General introduction. *The Journal of Comparative Neurology*, **206**, 49-81.

Olds, J. and Milner, P. (1954). Positive reinforcement produced by electrical stimulation of septal area and other regions of the rat brain. *Journal of Comparative and Physiological Psychology*, **47**, 419-427.

Paxinos, G. and Watson, C. (1986). *The Rat Brain in Stereotaxic Coordinates Second Edition*. New York: Academic Press.

Perkins, M. N. and Whitehead, S. A. (1978). Responses and pharmacological properties of preoptic/anterior hypothalamic neurones following medial forebrain bundle stimulation. *Journal of Physiology*, **279**, 347-360.

Phillipson, O. T. (1979). Afferent projections to the ventral tegmental area of tsai and interfascicular nucleus: a horseradish peroxidase study in the rat. *The Journal of Comparative Neurology*, **187**, 117-144.

Racine, R. (1975). Modification of seizure activity by electrical stimulation: Cortical areas. *Electroencephalography and Clinical Neurophysiology*, **38**, 1-12.

Robertson, A., Laferriere, A., and Milner, P. (1982). Development of brain stimulation reward in the medial prefrontal cortex: facilitation by prior electrical stimulation of the sulcal prefrontal cortex. *Physiology and Behavior*, **28**, 869-872.

Rolls, E.T. (1974). The neural basis of brain-stimulation reward. *Progress in Neurobiology*, **3**, 71-160.

Rompre, P.-P. and Boye, S. (1989). Localization of reward-relevant neurons in the pontine tegmentum: a moveable electrode mapping study. *Brain Research*, **496**, 295-302.

Rompre, P.-P. and Miliaressis, E. T. (1980). A comparison of the excitability cycles of the hypothalamic fibers involved in self-stimulation and exploration. *Physiology and Behavior*, **24**, 995-998.

Rompre, P.-P. and Miliaressis, E. T. (1985). Pontine and mesencephalic substrates of self-stimulation. *Brain Research*, **1985**, 359, 246-259.

Rompre, P.-P. and Shizgal, P. (1986). Electrophysiological characteristics of neurons in forebrain regions implicated in self-stimulation of the medial forebrain bundle in the rat. *Brain Research*, **364**, 338-349.

Saper, C. B., Swanson, L. W., and Cowan, W. M. (1979). An autoradiographic study of the efferent connections of the lateral hypothalamic area in the rat. *Journal of Comparative Neurology*, **183**, 689-706.

Schenk, S. and Shizgal, P. (1982). The substrates for lateral hypothalamic and medial prefrontal cortex self-stimulation have different refractory periods and show poor spatial summation. *Physiology and Behavior*, **28**, 133-138.

Schindler, D. C. (1983). *Spatial and temporal integration in the substrate for self-stimulation of the lateral hypothalamus in the rat*. Unpublished master's thesis, Concordia University, Montreal, Quebec, Canada.

Shizgal, P. (1989). Toward a cellular analysis of intracranial self-stimulation: Contributions of collision studies. *Neuroscience and Biobehavioural Reviews*, **13**, 81-90.

Shizgal, P., Bielajew, C., Corbett, D., Skelton, R., and Yeomans, J. (1980). Behavioral methods for inferring anatomical linkage between rewarding brain stimulation sites. *Journal of Comparative and Physiological Psychology*, **94**, 227-237.

Shizgal, P., Schindler, D., and Rompre, P.-P. (1989). Forebrain neurons driven by rewarding stimulation of the medial forebrain bundle in the rat: comparison of psychophysical and electrophysiological estimates of refractory periods. *Brain Research*, **499**, 234-248.

Sprick, U., Munoz, C., and Huston, J. P. (1985). Lateral hypothalamic self-stimulation persists in rats after destruction of lateral hypothalamic neurons by kainic acid or ibotenic acid. *Neuroscience Letters*, **56**, 211-216.

Stellar, J. R., Illes, J., and Mills, L. E. (1982). Role of ipsilateral forebrain in lateral hypothalamic stimulation reward in rats. *Physiology and Behavior*, **29**, 1089-1097.

Stellar, J. R. and Stellar, E. (1985). *The neurobiology of motivation and reward*. New York: Springer-Verlag.

Swanson, L. W. (1976). An autoradiographic study of the efferent connections of the preoptic region in the rat. *The Journal of Comparative Neurology*, **167**, 227-256.

Trzcinska, M. and Bielajew, C. (1992). Behaviourally derived estimates of excitability in striatal and medial prefrontal cortical self-stimulation sites. *Behavioural Brain Research*, **48**, 1-8.

Umemoto, M. (1968). Self-stimulation of the lateral hypothalamus after electrolytic injury of the medial forebrain bundle in the cat. *Brain Research*, **11**, 325-335.

Ungerstedt, U. (1971). Sterotaxic mapping of the monoamine pathways in the rat brain. *Acta Physiologiae Scandinavica*, **367** (suppl.), 1-48.

Valenstein, E. S. (1964). Problems of measurement and interpretation with reinforcing brain stimulation. *Psychological Review*, **71**, 415-436.

Valenstein, E. S., Cox, V. C. , and Kakolewski, J. W. (1968). Modification of motivated behavior elicited by electrical stimulation of the hypothalamus. *Science*, **159**, 1119-1121.

Veening, J. G., Lie, S. T., Posthuma, P., Geeraedts, M. G., and Nieuwenhuys, R. (1987). A topographical analysis of the origin of some efferent projections from the lateral hypothalamic area in the rat. *Neuroscience*, **22**, 537-551.

Veening, J. G., Swanson, L. W., Cowan, W. M., Nieuwenhuys, R., and Geeraedts, L. M. G. (1982). The medial forebrain bundle of the rat. II. An autoradiographic study of the topography of the major descending and ascending components. *The Journal of Comparative Neurology*, **206**, 82-108.

Velley, L. (1986). Effects of ibotenic acid lesion in the basal forebrain on electrical self-stimulation in the middle part of the lateral hypothalamus. *Behavioural Brain Research*, **20**, 303-311.

Velley, L. (1986). The role of intrinsic neurons in lateral hypothalamic self-stimulation. *Behavioural Brain Research*, **22**, 141-152.

Waraczynski, M. A. (1988). Basal forebrain knife cuts and medial forebrain bundle self-stimulation. *Brain Research*, **438**, 8-22.

Waraczynski, M. and Kaplan, J. M. (1990). Frequency-response characteristics provide a functional separation between stimulation-bound feeding and self-stimulation. *Physiology and Behavior*, **47**, 843-851.

Weber, K. H., Kuhn, F. J., Boke-Kuhn, K., Lehr, E., Danneberg, P. B., Hommer, D., Paul, S. M., and Skolnick, P. (1985). Pharmacological and neurochemical properties of 1,4-diazepines with two annelated heterocycles ('hetrazepines'). *European Journal of Pharmacology*, **109**, 19-31.

Wise, R. A. (1974). Lateral hypothalamic electrical stimulation: Does it make animals "hungry"? *Brain Research*, **67**, 187-209.

Yadin, E., Guarini, V., and Gallistel, C. R. (1983). Unilaterally activated systems in rats self-stimulating at sites in the medial forebrain bundle, medial prefrontal cortex, or locus coeruleus. *Brain Research*, **266**, 39-50.

Yeomans, J. S. (1975). Quantitative measurement of neural post-stimulation excitability with behavioral methods. *Physiology and Behavior*, **15**, 593-602.

Yeomans, J. S. (1979). The absolute refractory periods of self-stimulation neurons. *Physiology and Behavior*, **22**, 911-919.

Yeomans, J. S. (1990). *Principles of brain stimulation*. Oxford University Press, New York.

Yeomans, J. S. and Buckenham, K. E. (1992). Electrically evoked turning: Asymmetric and symmetric collision between anteromedial cortex and striatum. *Brain Research*, **570**, 279-292.

Yeomans, J. S., Matthews, G. G., Hawkins, R. D., Bellman, K., and Doppelt, H. (1979). Characterization of self-stimulation neurons by their local potential summation properties. *Physiology and Behavior*, **22**, 921-929.

Yeomans, J. S., Pearce, R., Wen, D., and Hawkins, R. D. (1984). Mapping midbrain sites for circling using current-frequency trade-off data. *Physiology and Behaviour*, **32**, 287-294.

APPENDIX

ANOVA Source Tables for Subjects in Collision Study

* $p < .05$

A) Subject TH27, site 1

Source	df	MS	F	p
C-T Interval (C-T)	4	.057	3.340	.022*
Order of Presentation of Pulses (AP/PA)	1	.107	6.247	.018*
C-T X AP/PA	4	.003	.189	.942

B) Subject TH27, site 2

Source	df	MS	F	p
C-T Interval (C-T)	4	.011	.531	.714
Order of Presentation of Pulses (AP/PA)	1	.169	8.389	.009*
C-T X AP/PA	4	.006	.283	.886

C) Subject TH21, site 1

Source	df	MS	F	p
C-T Interval (C-T)	9	.013	1.233	.303
Order of Presentation of Pulses (AP/PA)	1	.008	.828	.368
C-T X AP/PA	9	.005	.461	.892

D) Subject TH21, site 2

Source	df	MS	F	p
C-T Interval (C-T)	10	.019	1.868	.070
Order of Presentation of Pulses (AP/PA)	1	.105	10.129	.002*
C-T X AP/PA	10	.005	.508	.877

E) Subject TH21, site 3

Source	df	MS	F	p
C-T Interval (C-T)	8	.040	4.164	.001*
Order of Presentation of Pulses (AP/PA)	1	.019	1.956	.170
C-T X AP/PA	8	.015	1.569	.169

F) Subject TH21, site 4

Source	df	MS	F	p
C-T Interval (C-T)	10	.019	1.685	.115
Order of Presentation of Pulses (AP/PA)	1	.371	32.411	<.001*
C-T X AP/PA	10	.018	1.566	.149

G) Subject TH21, site 5

Source	df	MS	F	p
C-T Interval (C-T)	10	.017	1.107	.379
Order of Presentation of Pulses (AP/PA)	1	.005	.326	.571
C-T X AP/PA	10	.005	.326	.969

H) Subject TH21, site 6

Source	df	MS	F	p
C-T Interval (C-T)	10	.026	1.701	.111
Order of Presentation of Pulses (AP/PA)	1	.047	3.105	.085
C-T X AP/PA	10	.009	.619	.790

I) Subject TH21, site 7

Source	df	MS	F	p
C-T Interval (C-T)	10	.016	1.709	.109
Order of Presentation of Pulses (AP/PA)	1	.061	6.597	.014*
C-T X AP/PA	10	.013	1.362	.230

J) Subject TH34, site 1

Source	df	MS	F	p
C-T Interval (C-T)	6	.041	1.052	.406
Order of Presentation of Pulses (AP/PA)	1	.045	1.148	.290
C-T X AP/PA	6	.014	.361	.899

K) Subject TH36, site 1

Source	df	MS	F	p
C-T Interval (C-T)	6	.021	.731	.627
Order of Presentation of Pulses (AP/PA)	1	.366	12.591	.001*
C-T X AP/PA	6	.008	.273	.947

L) Subject TH36, site 2

Source	df	MS	F	p
C-T Interval (C-T)	6	.061	2.343	.048
Order of Presentation of Pulses (AP/PA)	1	.172	6.564	.014*
C-T X AP/PA	6	.011	.421	.861

M) Subject TH36, site 3

Source	df	MS	F	p
C-T Interval (C-T)	6	.028	.751	.611
Order of Presentation of Pulses (AP/PA)	1	.035	.927	.340
C-T X AP/PA	6	.032	.851	.537

N) Subject TH36, site 4

Source	df	MS	F	p
C-T Interval (C-T)	6	.038	2.066	.078
Order of Presentation of Pulses (AP/PA)	1	.007	.365	.549
C-T X AP/PA	6	.014	.747	.615

O) Subject TH36, site 5

Source	df	MS	F	p
C-T Interval (C-T)	6	.007	.399	.875
Order of Presentation of Pulses (AP/PA)	1	.005	.263	.611
C-T X AP/PA	6	.010	.557	.762

P) Subject TH33, site 1

Source	df	MS	F	p
C-T Interval (C-T)	6	.036	2.818	.020*
Order of Presentation of Pulses (AP/PA)	1	.125	9.730	.003*
C-T X AP/PA	6	.014	1.078	.388

Q) Subject TH33, site 2

Source	df	MS	F	p
C-T Interval (C-T)	6	.026	2.652	.028*
Order of Presentation of Pulses (AP/PA)	1	.038	3.843	.057
C-T X AP/PA	6	.008	.784	.587

R) Subject TH29, site 1

Source	df	MS	F	p
C-T Interval (C-T)	4	.027	2.150	.112
Order of Presentation of Pulses (AP/PA)	1	.217	17.340	<.001*
C-T X AP/PA	4	.010	.785	.549

S) Subject TH29, site 2

Source	df	MS	F	p
C-T Interval (C-T)	6	.108	6.044	<.001*
Order of Presentation of Pulses (AP/PA)	1	.293	16.407	<.001*
C-T X AP/PA	6	.012	.696	.654

T) Subject TH29, site 3

Source	df	MS	F	p
C-T Interval (C-T)	7	.064	2.162	.048
Order of Presentation of Pulses (AP/PA)	1	.098	3.317	.073
C-T X AP/PA	7	.012	.396	.902

U) Subject TH29, site 4

Source	df	MS	F	p
C-T Interval (C-T)	7	.090	4.612	<.001*
Order of Presentation of Pulses (AP/PA)	1	.004	.212	.647
C-T X AP/PA	7	.027	1.391	.224

V) Subject TH29, site 5

Source	df	MS	F	p
C-T Interval (C-T)	7	.044	1.289	.272
Order of Presentation of Pulses (AP/PA)	1	.118	3.481	.067
C-T X AP/PA	7	.031	.902	.511

W) Subject TH29, site 6

Source	df	MS	F	p
C-T Interval (C-T)	7	.039	1.619	.149
Order of Presentation of Pulses (AP/PA)	1	.062	2.544	.116
C-T X AP/PA	7	.014	.583	.767

X) Subject TH29, site 7

Source	df	MS	F	p
C-T Interval (C-T)	6	.058	2.559	.029*
Order of Presentation of Pulses (AP/PA)	1	.020	.861	.357
C-T X AP/PA	6	.030	1.313	.266

Y) Subject TH29, site 8

Source	df	MS	F	p
C-T Interval (C-T)	6	.022	.868	.527
Order of Presentation of Pulses (AP/PA)	1	.000	.014	.907
C-T X AP/PA	6	.021	.818	.562

Z) Subject TH30, site 1

Source	df	MS	F	p
C-T Interval (C-T)	6	.062	5.328	<.001*
Order of Presentation of Pulses (AP/PA)	1	.020	1.725	.196
C-T X AP/PA	6	.018	1.570	.180

AA) Subject TH30, site 2

Source	df	MS	F	p
C-T Interval (C-T)	7	.027	2.651	.019*
Order of Presentation of Pulses (AP/PA)	1	.026	2.527	.117
C-T X AP/PA	7	.014	1.355	.241

BB) Subject TH30, site 3

Source	df	MS	F	p
C-T Interval (C-T)	6	.078	4.884	.001*
Order of Presentation of Pulses (AP/PA)	1	.009	.530	.470
C-T X AP/PA	6	.007	.461	.833

CC) Subject TH30, site 4

Source	df	MS	F	p
C-T Interval (C-T)	6	.009	.680	.667
Order of Presentation of Pulses (AP/PA)	1	.001	.082	.776
C-T X AP/PA	6	.005	.404	.872

DD) Subject TH30, site 5

Source	df	MS	F	p
C-T Interval (C-T)	6	.059	5.735	<.001*
Order of Presentation of Pulses (AP/PA)	1	.000	.000	.990
C-T X AP/PA	6	.049	4.759	.001*

EE) Subject TH30, site 6

Source	df	MS	F	p
C-T Interval (C-T)	6	.039	2.498	.033*
Order of Presentation of Pulses (AP/PA)	1	.019	1.201	.278
C-T X AP/PA	6	.010	.605	.725

FF) Subject TH30, site 7

Source	df	MS	F	p
C-T Interval (C-T)	6	.039	1.451	.219
Order of Presentation of Pulses (AP/PA)	1	.034	1.274	.265
C-T X AP/PA	6	.006	.233	.963

GG) Subject TH30, site 8

Source	df	MS	F	p
C-T Interval (C-T)	6	.074	.466	.829
Order of Presentation of Pulses (AP/PA)	1	.451	2.837	.100
C-T X AP/PA	6	.125	.789	.584

HH) Subject TH19, site 1

Source	df	MS	F	p
C-T Interval (C-T)	8	.027	2.465	.031*
Order of Presentation of Pulses (AP/PA)	1	.012	1.055	.311
C-T X AP/PA	8	.005	.452	.881

II) Subject TH19, site 2

Source	df	MS	F	p
C-T Interval (C-T)	10	.031	1.033	.426
Order of Presentation of Pulses (AP/PA)	1	.026	.887	.350
C-T X AP/PA	10	.019	.633	.780

JJ) Subject TH19, site 3

Source	df	MS	F	p
C-T Interval (C-T)	10	.039	1.949	.064
Order of Presentation of Pulses (AP/PA)	1	.037	1.846	.181
C-T X AP/PA	10	.026	1.291	.265

KK) Subject TH19, site 4

Source	df	MS	F	p
C-T Interval (C-T)	10	.073	2.548	.009*
Order of Presentation of Pulses (AP/PA)	1	.170	5.940	.017*
C-T X AP/PA	10	.024	.841	.590

LL) Subject TH19, site 5

Source	df	MS	F	p
C-T Interval (C-T)	10	.032	1.058	.407
Order of Presentation of Pulses (AP/PA)	1	.067	2.190	.144
C-T X AP/PA	10	.034	1.102	.374

MM) Subject TH19, site 6

Source	df	MS	F	p
C-T Interval (C-T)	10	.031	1.283	.280
Order of Presentation of Pulses (AP/PA)	1	.050	2.086	.158
C-T X AP/PA	10	.047	1.951	.073

NN) Subject TH19, site 7

Source	df	MS	F	p
C-T Interval (C-T)	10	.028	1.366	.228
Order of Presentation of Pulses (AP/PA)	1	.193	9.575	.003*
C-T X AP/PA	10	.020	1.007	.453

OO) Subject TH20, site 1

Source	df	MS	F	p
C-T Interval (C-T)	8	.018	.939	.493
Order of Presentation of Pulses (AP/PA)	1	.000	.014	.905
C-T X AP/PA	8	.040	2.081	.054

PP) Subject TH20, site 2

Source	df	MS	F	p
C-T Interval (C-T)	8	.017	.900	.527
Order of Presentation of Pulses (AP/PA)	1	.572	29.707	<.001*
C-T X AP/PA	8	.014	.707	.683

QQ) Subject TH20, site 3

Source	df	MS	F	p
C-T Interval (C-T)	9	.016	.623	.772
Order of Presentation of Pulses (AP/PA)	1	.237	9.519	.003*
C-T X AP/PA	9	.014	.551	.831

RR) Subject TH20, site 4

Source	df	MS	F	p
C-T Interval (C-T)	10	.011	.386	.948
Order of Presentation of Pulses (AP/PA)	1	1.217	43.215	<.001*
C-T X AP/PA	10	.026	.915	.525